

Robust Principal Components by Casewise and Cellwise Weighting

Fabio Centofanti¹, Mia Hubert², and Peter J. Rousseeuw²

¹*Department of Industrial Engineering, University of Naples Federico II, Naples, Italy*

²*Section of Statistics and Data Science, Department of Mathematics, KU Leuven, Belgium*

August 24, 2024

Abstract

Principal component analysis (PCA) is a fundamental tool for analyzing multivariate data. Here the focus is on dimension reduction to the principal subspace, characterized by its projection matrix. The classical principal subspace can be strongly affected by the presence of outliers. Traditional robust approaches consider casewise outliers, that is, cases generated by an unspecified outlier distribution that differs from that of the clean cases. But there may also be cellwise outliers, which are suspicious entries that can occur anywhere in the data matrix. Another common issue is that some cells may be missing. This paper proposes a new robust PCA method, called cellPCA, that can simultaneously deal with casewise outliers, cellwise outliers, and missing cells. Its single objective function combines two robust loss functions, that together mitigate the effect of casewise and cellwise outliers. The objective function is minimized by an iteratively reweighted least squares (IRLS) algorithm. Residual cellmaps and enhanced outlier maps are proposed for outlier detection. The casewise and cellwise influence functions of the principal subspace are derived, and its asymptotic distribution is obtained. Extensive simulations and two real data examples illustrate the performance of cellPCA.

Keywords: Cellwise outliers; Iteratively reweighted least squares; Missing values; Principal subspace; Rowwise outliers.

1 Introduction

The prevalence of ever larger datasets poses substantial challenges for statistical analysis. A common issue is the presence of outliers and missing data, caused by a variety of factors such as measurement errors, sensor malfunctions, or rare and unexpected events. Robust methods construct a fit that is affected little by outliers, after which the outliers can be detected by their deviation from the robust fit. To date research was mainly focused on *casewise outliers*, that is, cases not generated by the distribution underlying the clean data. They are also called *rowwise* outliers, due to the statistical convention of storing multivariate data in a matrix where the rows are cases and the columns are variables. However, recently *cellwise outliers* have come in the spotlight. These are deviating entries (cells) that can occur anywhere in the data matrix (Alqallaf et al., 2009). They are especially common in high dimensional data, where one does not wish to downweight an entire row due to one or a few outlying cells, because the other cells in that row still contain valuable information.

The most popular dimension reduction method is principal component analysis (PCA), but its classical version is strongly affected by both rowwise and cellwise outliers because it is a least squares method. Several rowwise robust PCA methods have been proposed, such as Locantore et al. (1999) and Hubert et al. (2005), and also a few cellwise robust PCA methods (De La Torre and Black, 2003; Maronna and Yohai, 2008; Candès et al., 2011). Kiers (1997) developed a PCA method that can handle incomplete data, but is not robust to outliers. Serneels and Verdonck (2008) constructed a rowwise robust method that can also cope with missing values. The more recent MacroPCA method (Hubert et al., 2019) was the first to address the three issues of rowwise outliers, cellwise outliers, and missing values simultaneously. However, it is a combination of elements from earlier methods, and lacks a unifying underlying principle.

In this paper we propose the cellPCA method which also deals with all three issues, and is the first method to do so by minimizing a single objective function. It combines two robust losses that effectively mitigate the effect of rowwise and cellwise outliers, while discarding missing cells. The focus is on estimating the principal subspace, characterized by its projection matrix. Section 2 presents the cellPCA objective and its iteratively

reweighted least squares (IRLS) algorithm. Section 3 describes the enhanced residual map and the outlier map. Section 4 derives the casewise and cellwise influence functions of the projection matrix, as well as its asymptotic distribution. Section 5 applies cellPCA out of sample. The performance of cellPCA is assessed by Monte Carlo in Section 6, and Section 7 illustrates it on real data. Section 8 concludes.

2 Methodology

2.1 The objective function

The p coordinates of the n cases are stored in an $n \times p$ data matrix \mathbf{X} . In the absence of outliers and missing values, the goal is to represent the data in a lower dimensional space, that is

$$\mathbf{X} = \mathbf{X}^0 + \mathbf{1}_n \boldsymbol{\mu}^T + \mathbf{E} \quad (1)$$

where \mathbf{X}^0 is an $n \times p$ matrix of rank $q < p$, $\mathbf{1}_n$ is a column vector with all n components equal to 1, the center $\boldsymbol{\mu} = (\mu_1, \dots, \mu_p)^T$ is a column vector of size p , and \mathbf{E} is the error term. We can also write this as

$$\mathbf{X} = \mathbf{X}^0 \mathbf{P} + \mathbf{1}_n \boldsymbol{\mu}^T + \mathbf{E} \quad (2)$$

where \mathbf{P} is a $p \times p$ orthogonal projection matrix of rank q , that is, $\mathbf{P}^T = \mathbf{P}$, $\mathbf{P}^2 = \mathbf{P}$ and $\text{rank}(\mathbf{P}) = q$, which projects \mathbf{X}^0 on itself, i.e. $\mathbf{X}^0 \mathbf{P} = \mathbf{X}^0$. We denote the rows of \mathbf{X}^0 as \mathbf{x}_i^0 . The image of \mathbf{P} is a q -dimensional linear subspace $\boldsymbol{\Pi}_0$ through the origin. The predicted datapoints $\widehat{\mathbf{x}}_i = \mathbf{x}_i^0 + \boldsymbol{\mu}$ lie on the affine subspace $\boldsymbol{\Pi} = \boldsymbol{\Pi}_0 + \boldsymbol{\mu}$, which is called the *principal subspace*. Note that any q -dimensional linear subspace $\boldsymbol{\Pi}_0$ determines a unique \mathbf{P} satisfying the constraints $\text{rank}(\mathbf{P}) = q$, $\mathbf{P}^T = \mathbf{P}$ and $\mathbf{P}^2 = \mathbf{P}$, and that any such \mathbf{P} determines a unique subspace $\boldsymbol{\Pi}_0$.

Classical PCA approximates \mathbf{X} by $\widehat{\mathbf{X}} = \mathbf{X}^0 \mathbf{P} + \mathbf{1}_n \boldsymbol{\mu}^T$ which minimizes

$$\|\mathbf{X} - \mathbf{X}^0 \mathbf{P} - \mathbf{1}_n \boldsymbol{\mu}^T\|_F^2 \quad (3)$$

under the same constraints on \mathbf{X}^0 and \mathbf{P} , where $\|\cdot\|_F$ is the Frobenius norm. Note that (3) estimates the principal subspace $\boldsymbol{\Pi}$ determined by \mathbf{P} and $\boldsymbol{\mu}$, and not (yet) any principal

directions inside $\mathbf{\Pi}$. Minimizing (3) is equivalent to minimizing

$$\sum_{i=1}^n \sum_{j=1}^p (x_{ij} - \hat{x}_{ij})^2 = \sum_{i=1}^n \sum_{j=1}^p r_{ij}^2 \quad (4)$$

with $\hat{x}_{ij} := \mathbf{p}_j^T \mathbf{x}_i^0 + \mu_j$, where $\mathbf{p}_1, \dots, \mathbf{p}_p$ are the columns of \mathbf{P} , and $r_{ij} := x_{ij} - \hat{x}_{ij}$. The solution is easily obtained. First carry out a singular value decomposition (SVD) of rank q as $\mathbf{X} - \mathbf{1}_n \bar{\mathbf{x}}^T \approx \mathbf{U}_q \mathbf{D}_q \mathbf{V}_q^T$ where $\bar{\mathbf{x}}$ is the sample mean, the $q \times q$ diagonal matrix \mathbf{D}_q contains the q leading singular values, and the columns of \mathbf{V}_q are the right singular vectors. Then the solution is $\mathbf{P} = \mathbf{V}_q \mathbf{V}_q^T$, $\mathbf{X}^0 = \mathbf{U}_q \mathbf{D}_q \mathbf{V}_q^T$, and $\boldsymbol{\mu} = \bar{\mathbf{x}} - \mathbf{P} \bar{\mathbf{x}}$. But the quadratic loss function in (4) makes this a least squares fit, which is very sensitive to rowwise as well as cellwise outliers. Moreover, the data matrix may not be fully observed, that is, some x_{ij} may be missing.

To deal with rowwise and cellwise outliers and missing cells, we propose the cellPCA method which approximates \mathbf{X} by $\widehat{\mathbf{X}} = \mathbf{X}^0 + \mathbf{1}_n \boldsymbol{\mu}^T$ obtained by minimizing

$$L_{\rho_1, \rho_2}(\mathbf{X}, \mathbf{P}, \mathbf{X}^0, \boldsymbol{\mu}) := \frac{\hat{\sigma}_2^2}{m} \sum_{i=1}^n m_i \rho_2 \left(\frac{1}{\hat{\sigma}_2} \sqrt{\frac{1}{m_i} \sum_{j=1}^p m_{ij} \hat{\sigma}_{1,j}^2 \rho_1 \left(\frac{x_{ij} - \hat{x}_{ij}}{\hat{\sigma}_{1,j}} \right)} \right) \quad (5)$$

with respect to $(\mathbf{P}, \mathbf{X}^0, \boldsymbol{\mu})$, under the same constraints $\mathbf{P}^T = \mathbf{P}$, $\mathbf{P}^2 = \mathbf{P}$, $\text{rank}(\mathbf{P}) = q$, and $\mathbf{X}^0 \mathbf{P} = \mathbf{X}^0$. Here m_{ij} is 0 if x_{ij} is missing and 1 otherwise, $m_i = \sum_{j=1}^p m_{ij}$, and $m = \sum_{i=1}^n m_i$.

The scale estimates $\hat{\sigma}_{1,j}$ and $\hat{\sigma}_2$ will be computed in the next subsection. The scales $\hat{\sigma}_{1,j}$ standardize the *cellwise residuals*

$$r_{ij} := x_{ij} - \hat{x}_{ij} \quad (6)$$

of variable j . The scale $\hat{\sigma}_2$ standardizes the *rowwise total deviation* defined as

$$t_i := \sqrt{\frac{1}{m_i} \sum_{j=1}^p m_{ij} \hat{\sigma}_{1,j}^2 \rho_1 \left(\frac{r_{ij}}{\hat{\sigma}_{1,j}} \right)}. \quad (7)$$

For $\rho_1(z) = \rho_2(z) = z^2$ the objective (5) becomes the objective (4) of classical PCA. But here the functions ρ_1 and ρ_2 are bounded. The combination of ρ_1 and ρ_2 in (5) allows the cellPCA estimates to be robust against both cellwise and rowwise outliers. Indeed, a cellwise outlier in the cell (i, j) yields a cellwise residual r_{ij} with a large absolute value, but the boundedness of ρ_1 reduces its effect on the estimates. Similarly, a rowwise outlier

results in a large rowwise total deviation t_i but its effect is reduced by ρ_2 . Note that in the computation of t_i the effect of cellwise outliers is tempered by the presence of ρ_1 . This avoids that a single cellwise outlier would always give its row a large t_i .

In our implementation, ρ_1 and ρ_2 are of the hyperbolic tangent (*tanh*) form $\rho_{b,c}$ (Hampel et al., 1981), which is defined piecewise by

$$\rho_{b,c}(z) = \begin{cases} z^2/2 & \text{if } 0 \leq |z| \leq b \\ d - (q_1/q_2) \ln(\cosh(q_2(c - |z|))) & \text{if } b \leq |z| \leq c \\ d & \text{if } c \leq |z| \end{cases}$$

where $d = (b^2/2) + (q_1/q_2) \ln(\cosh(q_2(c - b)))$. Its first derivative $\psi_{b,c} = \rho'_{b,c}$ has been used as the *wrapping function* (Raymaekers and Rousseeuw, 2021) and equals

$$\psi_{b,c}(z) = \begin{cases} z & \text{if } 0 \leq |z| \leq b \\ q_1 \tanh(q_2(c - |z|)) \text{sign}(z) & \text{if } b \leq |z| \leq c \\ 0 & \text{if } c \leq |z|. \end{cases}$$

The function $\psi_{b,c}$ satisfies an optimality property (Hampel et al., 1981) and is continuous, which implies certain constraints on q_1 and q_2 . We use the default wrapping function shown in Figure 1, which has $b = 1.5$ and $c = 4$ with $q_1 = 1.540793$ and $q_2 = 0.8622731$.

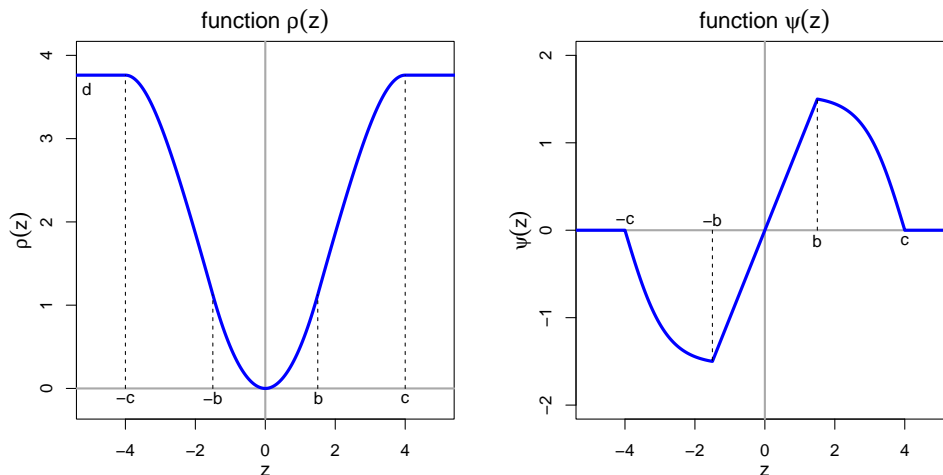


Figure 1: The function $\rho_{b,c}$ with $b = 1.5$ and $c = 4$ (left) and its derivative $\psi_{b,c}$ (right).

2.2 Setup of the algorithm

Principal component analysis is a dimension reduction method which approximates p -variate data by points in a principal subspace $\mathbf{\Pi}$ of lower dimension $q \ll p$. The principal subspace is $\mathbf{\Pi} = \mathbf{\Pi}_0 + \boldsymbol{\mu}$ where $\mathbf{\Pi}_0$ is a linear subspace, which is fully characterized by its projection matrix \mathbf{P} . But in actual computations, it is unwieldy to work with this huge constrained matrix \mathbf{P} that may not fit in memory. Therefore we parametrize \mathbf{P} more economically. We take an orthonormal basis of $\mathbf{\Pi}_0$ and form a $p \times q$ matrix $\mathbf{V} = \{v_{j\ell}\} = [\mathbf{v}^1, \dots, \mathbf{v}^q] = [\mathbf{v}_1, \dots, \mathbf{v}_p]^T$ whose columns are the basis vectors. Therefore \mathbf{V} is orthonormal too, that is, $\mathbf{V}^T \mathbf{V} = \mathbf{I}_q$. We can then write $\mathbf{P} = \mathbf{V} \mathbf{V}^T$. We call \mathbf{V} a loadings matrix, and define the corresponding scores matrix as $\mathbf{U} := \mathbf{X}^0 \mathbf{V} = \{u_{i\ell}\} = [\mathbf{u}^1, \dots, \mathbf{u}^q] = [\mathbf{u}_1, \dots, \mathbf{u}_n]^T$ which is $n \times q$. This way we can carry out the computations with the smaller matrices \mathbf{V} and \mathbf{U} instead of \mathbf{P} and \mathbf{X}^0 .

The only disadvantage of working with \mathbf{V} is that it is not unique, whereas \mathbf{P} is. We could take a different orthonormal basis of $\mathbf{\Pi}_0$ corresponding to a matrix $\tilde{\mathbf{V}}$, so that $\tilde{\mathbf{V}} \tilde{\mathbf{V}}^T = \mathbf{P}$ as well. As shown in Section A of the Supplementary Material there then exists a $q \times q$ orthogonal matrix \mathbf{O} such that $\tilde{\mathbf{V}} = \mathbf{V} \mathbf{O}$, so \mathbf{V} is only determined up to right multiplication by an orthogonal matrix. However, we will see that whichever parametrization \mathbf{V} is chosen, the final algorithmic and theoretical results on \mathbf{P} are the same.

The algorithm needs to start from an initial estimate $(\mathbf{V}_{(0)}, \mathbf{U}_{(0)}, \boldsymbol{\mu}_{(0)})$ that is already fairly robust against cellwise and rowwise outliers. For this we employ the MacroPCA method (Hubert et al., 2019), which is robust against both cellwise and rowwise outliers and can deal with NA's. It starts by imputing the NA's by the DDC algorithm (Rousseeuw and Van den Bossche, 2018). MacroPCA yields an initial fit $\widehat{\mathbf{X}}_{(0)} = \mathbf{U}_{(0)} \mathbf{V}_{(0)}^T + \mathbf{1}_n \boldsymbol{\mu}_{(0)}^T$ from which we compute cellwise residuals $r_{ij}^{(0)}$ as in (6). For every coordinate $j = 1, \dots, p$ we then compute $\widehat{\sigma}_{1,j}$ as an M-estimate of scale of the cellwise residuals $r_{ij}^{(0)}$. A scale M-estimator of a univariate sample (z_1, \dots, z_n) is the solution $\widehat{\sigma}$ of the equation

$$\frac{1}{n} \sum_{i=1}^n \rho\left(\frac{z_i}{\sigma}\right) = \delta \quad (8)$$

for some δ . In our implementation we chose ρ to be Tukey's biweight function

$$\rho_a(z) = \begin{cases} 1 - \left(1 - \frac{z^2}{a^2}\right)^3 & |z| \leq a \\ 1 & |z| > a \end{cases} \quad (9)$$

with tuning parameter $a = 1.548$ and $\delta = \mathbb{E}[\rho_a(z)] = 0.5$ for $z \sim N(0, 1)$, so the M-scale is consistent at the Gaussian model and attains a 50% breakdown value. We then construct rowwise total deviations $t_i^{(0)}$ by (7). Next, we compute $\widehat{\sigma}_2$ as the M-scale of those $t_i^{(0)}$. The scale estimates $\widehat{\sigma}_{1,j}$ and $\widehat{\sigma}_2$ are used in the next steps.

2.3 The concentration step

We now address the minimization of our objective (5). Because L_{ρ_1, ρ_2} is continuously differentiable, its solution must satisfy the first-order necessary conditions for optimality. These are derived in Section B of the Supplementary Material. For instance, the first one is obtained by setting the gradients of L_{ρ_1, ρ_2} with respect to $\mathbf{v}_1, \dots, \mathbf{v}_p$ to zero. The second and third one use the gradients with respect to $\mathbf{u}_1, \dots, \mathbf{u}_n$ and to $\boldsymbol{\mu}$, yielding

$$(\mathbf{U}^T \mathbf{W}^j \mathbf{U}) \mathbf{v}_j = \mathbf{U}^T \mathbf{W}^j (\mathbf{x}^j - \mu_j \mathbf{1}_n), \quad j = 1, \dots, p \quad (10)$$

$$(\mathbf{V}^T \mathbf{W}_i \mathbf{V}) \mathbf{u}_i = \mathbf{V}^T \mathbf{W}_i (\mathbf{x}_i - \boldsymbol{\mu}), \quad i = 1, \dots, n \quad (11)$$

$$\sum_{i=1}^n \mathbf{W}_i \mathbf{V} \mathbf{u}_i = \sum_{i=1}^n \mathbf{W}_i (\mathbf{x}_i - \boldsymbol{\mu}) \quad (12)$$

where $\mathbf{x}_1^T, \dots, \mathbf{x}_n^T$ and $\mathbf{x}^1, \dots, \mathbf{x}^p$ are the rows and columns of \mathbf{X} . Here \mathbf{W}_i is a $p \times p$ diagonal matrix, whose diagonal entries are equal to the i th row of the $n \times p$ weight matrix

$$\mathbf{W} = \{w_{ij}\} = \widetilde{\mathbf{W}}_c \odot \widetilde{\mathbf{W}}_r \odot \mathbf{M} \quad (13)$$

where the Hadamard product \odot multiplies matrices entry by entry. Analogously, \mathbf{W}^j is an $n \times n$ diagonal matrix, whose diagonal entries are the j th column of the matrix \mathbf{W} . In expression (13) for \mathbf{W} , the $n \times p$ matrix $\widetilde{\mathbf{W}}_c = \{w_{ij}^c\}$ contains the *cellwise weights*

$$w_{ij}^c = \psi_1 \left(\frac{r_{ij}}{\widehat{\sigma}_{1,j}} \right) / \frac{r_{ij}}{\widehat{\sigma}_{1,j}}, \quad i = 1, \dots, n, \quad j = 1, \dots, p \quad (14)$$

where $\psi_1 = \rho'_1$ with the convention $w_{ij}^c(0) = 1$. The $n \times p$ matrix $\widetilde{\mathbf{W}}_r$ has constant rows, where each entry of row i is the *rowwise weight* w_i^r given by

$$w_i^r = \psi_2 \left(\frac{t_i}{\widehat{\sigma}_2} \right) / \frac{t_i}{\widehat{\sigma}_2}, \quad i = 1, \dots, n \quad (15)$$

with $\psi_2 = \rho'_2$, and the $n \times p$ matrix \mathbf{M} contains the missingness indicators m_{ij} .

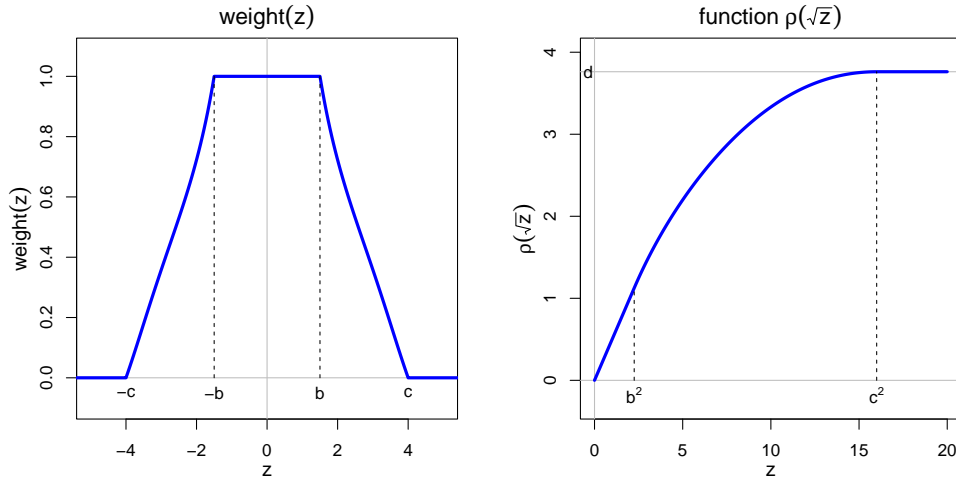


Figure 2: The weight function $w(z)$ used in (14) and (15) (left), and the function $\rho(\sqrt{z})$ (right).

The left panel of Figure 2 shows the weight function $w(z)$ used in (14) and (15). Note that the weight is exactly 1 in the central part due to the form of $\psi = \rho'$. Therefore inlying cells will not be modified, which is an advantage over other ρ functions that could be used.

To address (10)–(12) we look at a different objective function, given by

$$\sum_{i=1}^n \sum_{j=1}^p w_{ij} (x_{ij} - \mu_j - (\mathbf{UV}^T)_{ij})^2 \quad (16)$$

where $(\mathbf{UV}^T)_{ij} = \mathbf{u}_i^T \mathbf{v}_j = \sum_{\ell=1}^q u_{i\ell} v_{j\ell}$ and the weight matrix \mathbf{W} is assumed fixed for now. What does this have to do with the objective (5) we are trying to minimize? Well, it is shown in Section B of the Supplementary Material that the first order conditions on the weighted PCA of (16) are exactly the same as the first order conditions (10)–(12) on the original objective (5).

The system of equations (10)–(12) is nonlinear because the weight matrices depend on the estimates, and the estimates depend on the weight matrices. The optimization of (16) can be performed by alternating least squares (Gabriel, 1978). The IRLS algorithm starts from our initial estimate $(\mathbf{V}_{(0)}, \mathbf{U}_{(0)}, \boldsymbol{\mu}_{(0)})$ and the corresponding $\mathbf{W}_{(0)}$ obtained from (13), (14), and (15). Then, for each $k = 0, 1, 2, \dots$, we obtain $(\mathbf{V}_{(k+1)}, \mathbf{U}_{(k+1)}, \boldsymbol{\mu}_{(k+1)})$ from $(\mathbf{V}_{(k)}, \mathbf{U}_{(k)}, \boldsymbol{\mu}_{(k)})$ by the following four-step procedure, which is described in more detail in Section C of the Supplementary Material.

(a) Minimize (16) with respect to \mathbf{V} by applying (10) with $\mathbf{U}_{(k)}$, $\boldsymbol{\mu}_{(k)}$, and $\mathbf{W}_{(k)}$. This

is done by computing

$$(\mathbf{v}_{(k+1)})_j = (\mathbf{U}_{(k)}^T \mathbf{W}_{(k)}^j \mathbf{U}_{(k)})^\dagger \mathbf{U}_{(k)}^T \mathbf{W}_{(k)}^j (\mathbf{x}^j - (\boldsymbol{\mu}_{(k)})_j \mathbf{1}_n) \quad j = 1, \dots, p \quad (17)$$

where \dagger denotes the generalized inverse of a matrix. It is proved that starting from a different parametrization of the initial $\mathbf{P}_{(0)}$ by $\tilde{\mathbf{V}}_{(0)} = \mathbf{V}_{(0)} \mathbf{O}$ with corresponding $\tilde{\mathbf{U}}_{(0)} = \mathbf{U}_{(0)} \mathbf{O}$ yields $\tilde{\mathbf{V}}_{(k+1)} = \mathbf{V}_{(k+1)} \mathbf{O}$ and hence the same $\mathbf{P}_{(k+1)}$.

(b) To obtain a new \mathbf{U} from the new $\mathbf{V}_{(k+1)}$ and the old $\boldsymbol{\mu}_{(k)}$ and $\mathbf{W}_{(k)}$ we apply

$$(\mathbf{V}^T \tilde{\mathbf{W}}_i \mathbf{V}) \mathbf{u}_i = \mathbf{V}^T \tilde{\mathbf{W}}_i (\mathbf{x}_i - \boldsymbol{\mu}), \quad i = 1, \dots, n \quad (18)$$

where $\tilde{\mathbf{W}}_i$ is a diagonal matrix whose diagonal is the i -th row of $\tilde{\mathbf{W}}_c \odot \mathbf{M}$. This implies (11) because each case i has a constant row weight w_i^r . We compute

$$(\mathbf{u}_{(k+1)})_i = (\mathbf{V}_{(k+1)}^T (\tilde{\mathbf{W}}_{(k)})_i \mathbf{V}_{(k+1)})^\dagger \mathbf{V}_{(k+1)}^T (\tilde{\mathbf{W}}_{(k)})_i (\mathbf{x}_i - \boldsymbol{\mu}_{(k)}) \quad i = 1, \dots, n. \quad (19)$$

It is proved that this minimizes (16), and that starting from the alternative parametrization yields $\tilde{\mathbf{U}}_{(k+1)} = \mathbf{U}_{(k+1)} \mathbf{O}$ and therefore the same $\mathbf{X}_{(k+1)}^0 = \mathbf{U}_{(k+1)} \mathbf{V}_{(k+1)}^T$.

(c) Minimize (16) with respect to $\boldsymbol{\mu}$ by applying (12) with the new $\mathbf{V}_{(k+1)}$ and $\mathbf{U}_{(k+1)}$ and the old $\mathbf{W}_{(k)}$ by setting

$$\boldsymbol{\mu}_{(k+1)} = \left(\sum_{i=1}^n (\mathbf{W}_{(k)})_i \right)^{-1} \sum_{i=1}^n (\mathbf{W}_{(k)})_i (\mathbf{x}_i - \mathbf{V}_{(k+1)} (\mathbf{u}_{(k+1)})_i). \quad (20)$$

(d) Update $\mathbf{W}_{(k)}$ according to (13), (14), and (15) with the new $\mathbf{V}_{(k+1)}$, $\mathbf{U}_{(k+1)}$ and $\boldsymbol{\mu}_{(k+1)}$.

Proposition 1. *Each iteration step of the algorithm decreases the objective function (5), that is, $L_{\rho_1, \rho_2}(\mathbf{X}, \mathbf{P}_{(k+1)}, \mathbf{X}_{(k+1)}^0, \boldsymbol{\mu}_{(k+1)}) \leq L_{\rho_1, \rho_2}(\mathbf{X}, \mathbf{P}_{(k)}, \mathbf{X}_{(k)}^0, \boldsymbol{\mu}_{(k)})$.*

This monotonicity result says that going from $(\mathbf{P}_{(k)}, \mathbf{X}_{(k)}^0, \boldsymbol{\mu}_{(k)})$ to $(\mathbf{P}_{(k+1)}, \mathbf{X}_{(k+1)}^0, \boldsymbol{\mu}_{(k+1)})$ reduces the variability around the PCA subspace. Therefore it is a *concentration step* in the terminology of Rousseeuw and Van Driessen (1999). The proof is given in Section D of the Supplementary Material, and uses the fact that for $z \geq 0$ the functions $z \rightarrow \rho_1(\sqrt{z})$ and $z \rightarrow \rho_2(\sqrt{z})$ are differentiable and concave, as we can see in Figure 2. Since the objective function is decreasing and it has a lower bound of zero, the algorithm must converge.

2.4 Selecting the rank q

The rank q of the PCA model (1) is rarely given in advance, one typically needs to select it based on the data. In classical PCA one defines the proportion of explained variance, given by $1 - \nu_s/\nu_0$ where $\nu_s := \|\mathbf{X} - \widehat{\mathbf{X}}_s\|_F^2$ in which $\widehat{\mathbf{X}}_s$ is the best approximation of \mathbf{X} of rank s . In particular $\nu_0 = \|\mathbf{X} - \mathbf{1}_n \bar{\mathbf{x}}^T\|_F^2$ where $\bar{\mathbf{x}}$ is the sample mean. This ν_s is computed for a range of s values. The rank q may be selected as the first s which brings the explained variance over a given threshold, say 80% or 90%, or by looking where the plot of ν_s versus s has an ‘elbow’ (Jolliffe, 2011).

Here we define ν_s as the objective (5) of the cellPCA fit of rank s . For ν_0 we compute (5) on the cellwise residuals $x_{ij} - \text{median}_{\ell=1}^n(x_{\ell j})$. Afterward we can again take the first s for which $1 - \nu_s/\nu_0$ exceeds a threshold, or look for an elbow in the plot of ν_s .

2.5 Imputation

When one or more cells of \mathbf{x}_i have weights below 1, it would be good to obtain an imputed version $\mathbf{x}_i^{\text{imp}}$ whose cells are $x_{ij}^{\text{imp}} = x_{ij}$ for all j with $w_{ij} = 1$, and with different cells x_{ij}^{imp} where $w_{ij} < 1$. The modified cells should be such that $\mathbf{x}_i^{\text{imp}}$ is shrunk toward the PCA subspace, and that the orthogonal projection of $\mathbf{x}_i^{\text{imp}}$ coincides with the fitted $\widehat{\mathbf{x}}_i$.

We do this as follows. From (18) and $\widehat{\mathbf{x}}_i = \mathbf{V}\mathbf{u}_i + \boldsymbol{\mu}$ we know that $(\widetilde{\mathbf{W}}_i(\mathbf{x}_i - \widehat{\mathbf{x}}_i))^\top \mathbf{V} = \mathbf{0}$, so $\widetilde{\mathbf{W}}_i(\mathbf{x}_i - \widehat{\mathbf{x}}_i)$ is orthogonal to the PCA subspace. We then construct the imputed point

$$\mathbf{x}_i^{\text{imp}} := \widehat{\mathbf{x}}_i + \widetilde{\mathbf{W}}_i(\mathbf{x}_i - \widehat{\mathbf{x}}_i) \quad (21)$$

so that its orthogonal projection on the PCA subspace equals $\widehat{\mathbf{x}}_i$. Note that every imputed cell x_{ij}^{imp} lies between the original cell x_{ij} and the cell \widehat{x}_{ij} of the fitted point.

Figure 3 illustrates the imputation for a 1-dimensional principal subspace in 3-dimensional space. Most points are projected orthogonally on the fitted subspace, but the first cell of point a is imputed before projecting it, and the second cell of b , and the third cell of c . Note that neither of these three cells stand out enough to be marginal outliers.

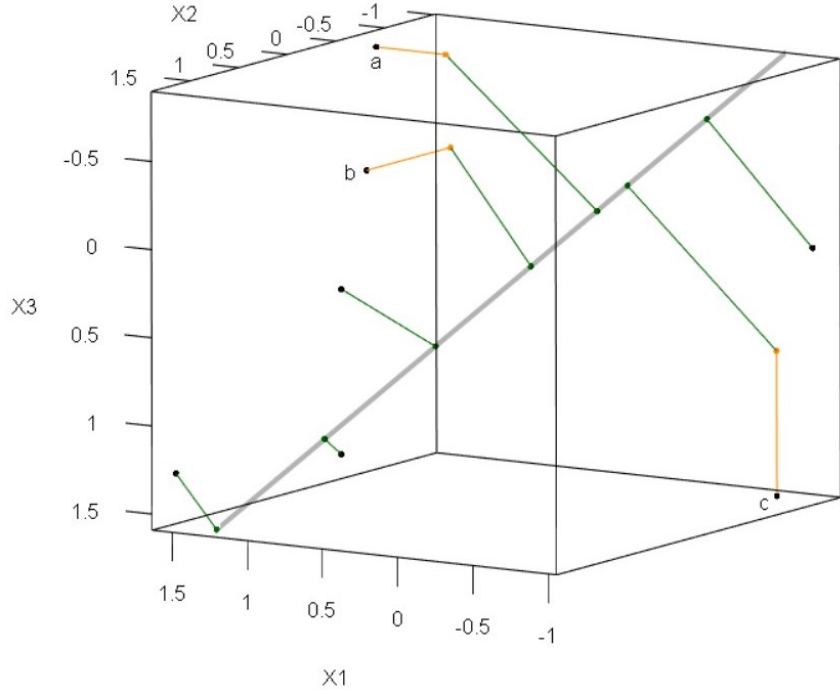


Figure 3: Illustration of imputation for $p = 3$ and $q = 1$. The first cell of point a was imputed before projecting it on the principal subspace, the second cell of b , and the third cell of c .

2.6 Estimating a center and principal directions

So far our estimation targets were the principal subspace Π and the fit $\widehat{\mathbf{X}}$. This is often sufficient, e.g. for face recognition, computer vision, signal processing, and data compression (Vaswani et al., 2018). However, in many other applications one may wish to obtain major directions in the principal subspace, as well as a good estimate of the center of the fitted data. These may facilitate interpretation of the PCA scores in \mathbf{U} .

Note that the matrix \mathbf{V} obtained by the algorithm in Section 2.3 need not have orthonormal columns. But this can be fixed by carrying out an SVD of \mathbf{V} and putting its right singular vectors in the new $p \times q$ matrix $\widetilde{\mathbf{V}}$. From this we also immediately obtain a set of q -variate scores $\widetilde{\mathbf{U}} = \mathbf{U}\mathbf{V}^T\widetilde{\mathbf{V}}$, and we denote $\widetilde{\boldsymbol{\mu}} := \boldsymbol{\mu}$.

This initial parametrization $(\widetilde{\mathbf{V}}, \widetilde{\mathbf{U}}, \widetilde{\boldsymbol{\mu}})$ is not yet satisfactory, because the columns of $\widetilde{\mathbf{V}}$ do not reflect the shape of the point cloud, and $\widetilde{\boldsymbol{\mu}}$ does not have to lie in its center. In order to obtain principal axes in the PCA subspace, the algorithm carries out an additional step which estimates a center and a scatter matrix of the scores in $\widetilde{\mathbf{U}}$. This needs to be done by a robust estimation method to avoid that outlying score vectors have a large effect on

the result, as illustrated in Appendix A.1 of Hubert et al. (2019). For this estimation we use the fast and robust deterministic algorithm DetMCD of Hubert et al. (2012), yielding $\hat{\boldsymbol{\mu}}_{\tilde{U}}$ and $\hat{\boldsymbol{\Sigma}}_{\tilde{U}}$. The spectral decomposition of $\hat{\boldsymbol{\Sigma}}_{\tilde{U}}$ yields a $q \times q$ loading matrix $\hat{\mathbf{V}}_{\tilde{U}}$ and eigenvalues $\hat{\lambda}_1 \geq \hat{\lambda}_2 \geq \dots \geq \hat{\lambda}_q$. We set the final parameter estimates to $\hat{\boldsymbol{\mu}} := \tilde{\boldsymbol{\mu}} + \hat{\mathbf{V}}_{\tilde{U}} \hat{\boldsymbol{\mu}}_{\tilde{U}}$, $\hat{\mathbf{V}} := \tilde{\mathbf{V}} \hat{\mathbf{V}}_{\tilde{U}}$, and $\hat{U} := (\tilde{U} - \mathbf{1}_n \hat{\boldsymbol{\mu}}_{\tilde{U}}^T) \hat{\mathbf{V}}_{\tilde{U}}$.

3 Outlier Detection

The `ionosphere` dataset in the R package `rrcov` (Todorov and Filzmoser, 2009) contains $n = 351$ cases with $p = 32$ numerical variables. The data were collected by the Space Physics Group of Johns Hopkins as described by Sigillito et al. (1989). The dataset contains two classes, and we restrict attention to the 225 cases labeled “good”. We applied cellPCA with $q = 2$, which explains 84% of the variability according to Section 2.4.

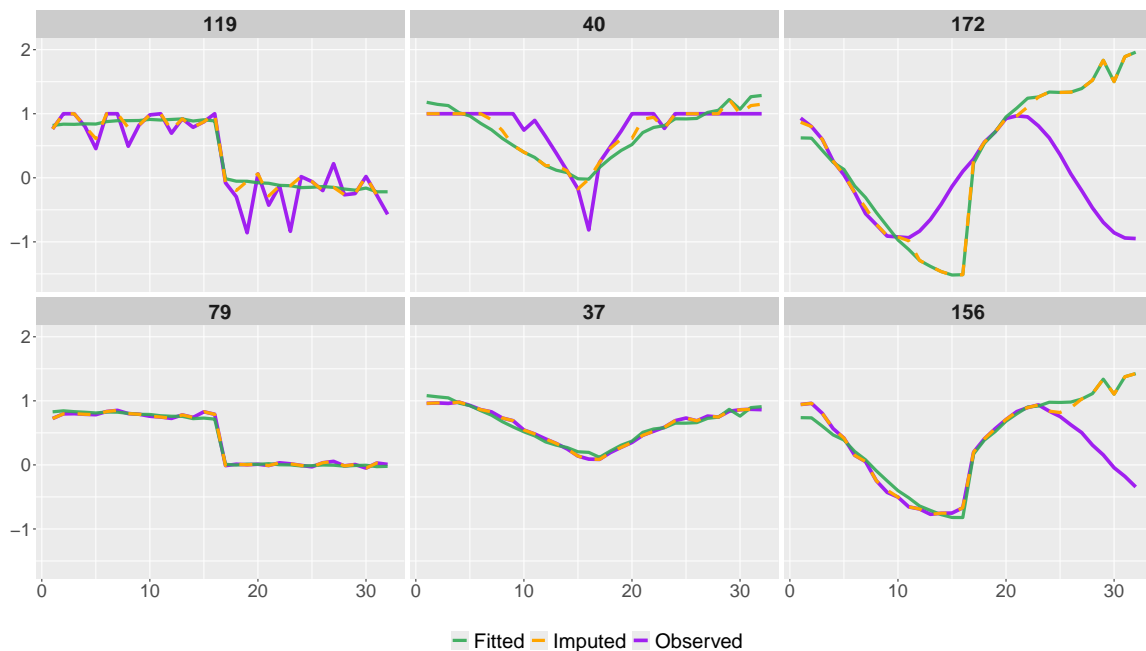


Figure 4: Observed (purple), fitted (green) and imputed (orange dashed) curves of six cases in the ionosphere data.

Figure 4 shows six cases (purple curves) together with their fitted (green) and imputed (dashed orange) curves. The bottom row shows cases that received a large rowwise weight ($w_{79}^r = w_{37}^r = 1$ and $w_{156}^r = 0.74$) whereas the top row plots curves with low ($w_{119}^r = 0.45$)

and zero rowwise weight ($w_{40}^r = w_{172}^r = 0$). The fitted values of the latter differ strongly from their observed values in most cells. According to (21) the imputed values agree with the observed ones in cells with cell weight $w_{ij}^c = 1$, whereas they align with the fitted values when $w_{ij}^c = 0$. Cell weights between 0 and 1 yield intermediate imputed values. Supplementary Material H illustrates this interpolation in detail.

In the final residual matrix $\mathbf{R} = \mathbf{X} - \widehat{\mathbf{X}} = \mathbf{X} - (\widehat{\mathbf{U}}\widehat{\mathbf{V}}^T + \mathbf{1}_n\hat{\boldsymbol{\mu}}^T)$ we estimate the scale of each column by the M-estimator (8) with (9). Dividing each column of \mathbf{R} by its scale yields the standardized residuals $\widetilde{\mathbf{R}} = \{\tilde{r}_{ij}\} = [\tilde{\mathbf{r}}_1, \dots, \tilde{\mathbf{r}}_n]^T$. We can then visualize $\widetilde{\mathbf{R}}$, or some of its rows and columns, by a *residual cellmap* as in Hubert et al. (2019). The residual cellmap of the 6 cases in Figure 4 is shown in Figure 5. Cells with $|\tilde{r}_{ij}| < \sqrt{\chi_{1,0.99}^2} = 2.57$ are considered regular and colored yellow, whereas any missing values would be white. Outlying positive residuals receive a color which ranges from light orange to dark red (here, when $\tilde{r}_{ij} > 6$) and outlying negative residuals from light purple to dark blue (when $\tilde{r}_{ij} < -6$).

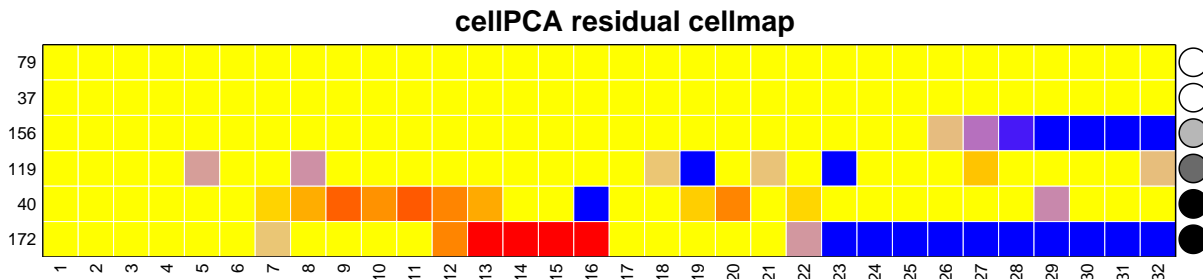


Figure 5: cellPCA residual cellmap of the six cases in Figure 4.

We see at a glance that cases 79 and 37 have no outlying cells, and that the last cells of case 156 have much lower values than expected. The cases at the bottom have cells with unexpectedly high values as well as cells with unexpectedly low values. To this residual cellmap we add information about rowwise (casewise) outlyingness, by coloring a circle to the right of each row according to its rowwise weight w_i^r . The color is black when $w_i^r = 0$, white when $w_i^r = 1$, with gray interpolated in between.

To focus more on the rowwise outlyingness we propose an *enhanced outlier map*, inspired by the outlier map of Hubert et al. (2019). This plot displays for each observation the norm of its standardized residual $\|\tilde{\mathbf{r}}_i\|$ versus its score distance SD_i which is defined as the norm of $(\widehat{\mathbf{V}}^T(\mathbf{x}_i - \hat{\boldsymbol{\mu}})) \odot [1/\sqrt{\hat{\lambda}_1}, \dots, 1/\sqrt{\hat{\lambda}_q}]^T$. Figure 6 shows the enhanced outlier map obtained by applying cellPCA to the ionosphere data. The vertical dotted line indicates

the cutoff $c_{\text{SD}} = \sqrt{\chi_{q,0.99}^2}$ and the horizontal dotted line is at the cutoff c_r , the 0.99-quantile of the distribution of $\|\tilde{\mathbf{r}}\|$ simulated at uncontaminated data. Regular cases have a small $\text{SD}_i \leq c_{\text{SD}}$ and a small $\|\tilde{\mathbf{r}}_i\| \leq c_r$. Cases with large SD_i and small $\|\tilde{\mathbf{r}}_i\|$ are called good leverage points. The cases with large $\|\tilde{\mathbf{r}}_i\|$ can be divided into orthogonal outliers when their SD_i is small, and bad leverage points when their SD_i is large.

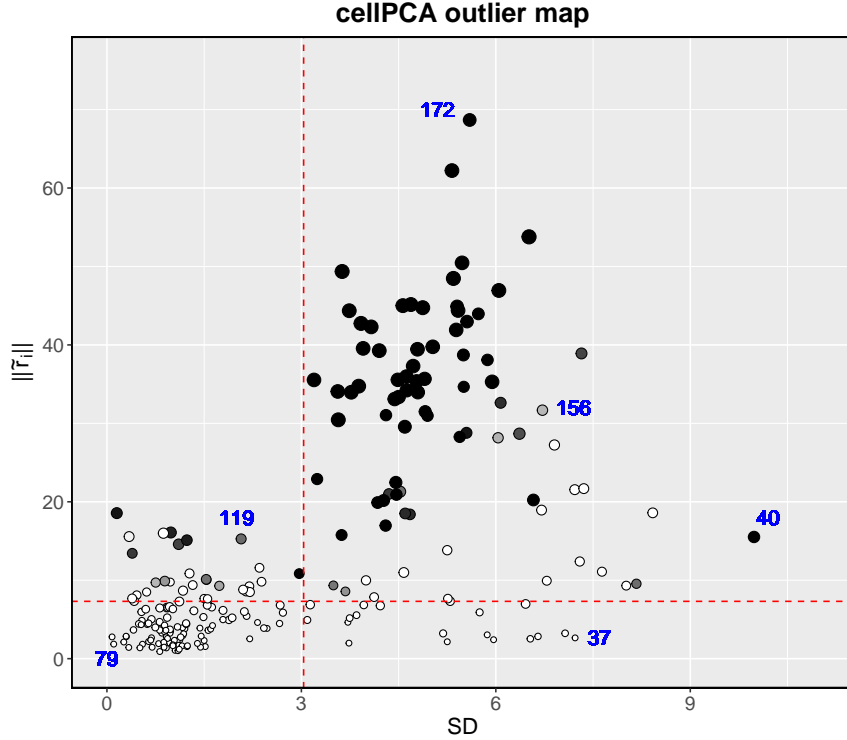


Figure 6: Enhanced outlier map of the ionosphere data.

The size of each point i in Figure 6 is proportional to one minus the average of its cellwise weights, i.e. $1 - \bar{w}_i^c = 1 - \frac{1}{p} \sum_{j=1}^p m_{ij} w_{ij}^c$. Larger points thus correspond to cases with many outlying cells. Finally, points are colored based on their rowwise weight, as in the residual cellmap. This enhanced outlier map thus combines information about the cellwise and rowwise weights of observations, and their position with respect to and within the fitted subspace. The curves in Figure 4 occupy different positions in this outlier map.

4 Large-sample properties

In the following, the influence function and asymptotic normality of cellPCA are presented. All the proofs are provided in Section E of the Supplementary Material.

We start by remarks about equivariance. Translation equivariance means that if we shift the data set \mathbf{X} by a vector \mathbf{a} yielding $\mathbf{X}_n + \mathbf{1}_n \mathbf{a}^T$, then the fitted $\widehat{\mathbf{X}}$ is transformed in the same way to $\widehat{\mathbf{X}}_n + \mathbf{1}_n \mathbf{a}^T$. This is true for the initial estimator, and $\widehat{\sigma}_{1,j}$ and $\widehat{\sigma}_2$ do not change. Therefore also cellPCA is translation equivariant, as can be seen from its objective. On the other hand cellPCA is not orthogonally equivariant because the objective does change when we rotate the data. This is typical for cellwise robust methods, also when estimating a covariance matrix (Raymaekers and Rousseeuw, 2023).

We now focus on types of outliers (contamination). Consider a p -variate random variable \mathbf{X} with distribution H_0 . We then contaminate it as in Alqallaf et al. (2009), yielding

$$\mathbf{X}_\varepsilon = (\mathbf{I}_p - \mathbf{B})\mathbf{X} + \mathbf{B}\mathbf{z} \quad (22)$$

where $\mathbf{z} = (z_1, \dots, z_p)^T$ is a fixed p -variate vector. The diagonal matrix \mathbf{B} equals $\text{diag}(B_1, B_2, \dots, B_p)$ where (B_1, B_2, \dots, B_p) follows the p -variate distribution G_ε . Its marginals B_1, \dots, B_p are Bernoulli random variables, and (B_1, B_2, \dots, B_p) and \mathbf{X} are independent. We denote the distribution of \mathbf{X}_ε as $H(G_\varepsilon, \mathbf{z})$.

The *fully dependent contamination model* (FDCM) assumes that $P(B_1 = \dots = B_p) = 1$. In that situation the distribution of \mathbf{X}_ε simplifies to $(1 - \varepsilon)H_0 + \varepsilon\Delta_{\mathbf{z}}$ where $\Delta_{\mathbf{z}}$ is the distribution which puts all of its mass in the point \mathbf{z} . The *fully independent contamination model* (FICM) instead assumes that B_1, \dots, B_p are independent. We denote G_ε as G_ε^D in the dependent model, and as G_ε^I in the independent model.

The influence function (IF) is a key robustness tool. It reveals how an estimating functional, i.e., a mapping from a space of probability measures to a parameter space, changes due to an infinitesimal amount of contamination. The usual IF uses casewise contamination, but Alqallaf et al. (2009) proposed a cellwise version as well. For a functional \mathbf{T} with values in \mathbb{R}^p , the cellwise influence function $\text{IF}_{FICM}(\mathbf{z}, \mathbf{T}, H_0)$ is defined as

$$\text{IF}_{FICM}(\mathbf{z}, \mathbf{T}, H_0) = \left. \frac{\partial}{\partial \varepsilon} \mathbf{T}(H(G_\varepsilon^I, \mathbf{z})) \right|_{\varepsilon=0} = \lim_{\varepsilon \downarrow 0} \frac{\mathbf{T}(H(G_\varepsilon^I, \mathbf{z})) - \mathbf{T}(H_0)}{\varepsilon} \quad (23)$$

whereas the usual rowwise influence function is defined as

$$\text{IF}_{FDCM}(\mathbf{z}, \mathbf{T}, H_0) = \left. \frac{\partial}{\partial \varepsilon} \mathbf{T}(H(G_\varepsilon^D, \mathbf{z})) \right|_{\varepsilon=0} = \lim_{\varepsilon \downarrow 0} \frac{\mathbf{T}(H(G_\varepsilon^D, \mathbf{z})) - \mathbf{T}(H_0)}{\varepsilon}. \quad (24)$$

So far influence functions of principal components have only been computed under the FDCM and for rowwise robust PCA methods (Debruyne and Hubert, 2009; Croux et al.,

2017). In the following, we derive the rowwise and cellwise IF of cellPCA. We aim to study the robustness properties of $\mathbf{\Pi}$ characterized by \mathbf{P} . When there are no missing values we can write the functional version $(\mathbf{P}(H), \boldsymbol{\mu}(H))$ of the minimizer of (5) as

$$\begin{aligned} (\mathbf{P}(H), \boldsymbol{\mu}(H)) &= \underset{\mathbf{P}, \boldsymbol{\mu}}{\operatorname{argmin}} \mathbb{E}_H \left[\rho_2 \left(\frac{1}{\sigma_2(H)} \sqrt{\frac{1}{p} \sum_{j=1}^p \sigma_{1,j}^2(H) \rho_1 \left(\frac{x_j - \mu_j - \mathbf{p}_j^T \mathbf{x}^0}{\sigma_{1,j}(H)} \right)} \right) \right] \\ \text{such that } \mathbf{x}^0 &= \underset{\mathbf{x}^0}{\operatorname{argmin}} \rho_2 \left(\frac{1}{\sigma_2(H)} \sqrt{\frac{1}{p} \sum_{j=1}^p \sigma_{1,j}^2(H) \rho_1 \left(\frac{x_j - \mu_j - \mathbf{p}_j^T \mathbf{x}^0}{\sigma_{1,j}(H)} \right)} \right) \end{aligned} \quad (25)$$

where $\mathbf{x}^0 = (x_1^0, \dots, x_p^0)^T$ and \mathbf{P} satisfy the usual constraints and $\mathbf{x} = (x_1, \dots, x_p)^T \sim H$ with H a distribution on \mathbb{R}^p , \mathbf{p}_j and μ_j stay as before, and $\sigma_{1,j}(H)$ and $\sigma_2(H)$ are the initial scale estimators of $r_j := x_j - \mu_j - \mathbf{p}_j^T \mathbf{x}^0$ and $t := \sqrt{\frac{1}{p} \sum_{j=1}^p \sigma_{1,j}^2(H) \rho_1(r_j / \sigma_{1,j}(H))}$. If we parametrize \mathbf{P} by an orthonormal matrix \mathbf{V} with $\mathbf{V}\mathbf{V}^T = \mathbf{P}$ and set the corresponding $\mathbf{U} = \mathbf{X}^0 \mathbf{V}$, the functional versions of the first-order conditions (10)–(12) must hold:

$$\mathbb{E}_G [\mathbf{W}_x \mathbf{V} \mathbf{u}_x \mathbf{u}_x^T] = \mathbb{E}_G [\mathbf{W}_x (\mathbf{x} - \boldsymbol{\mu}) \mathbf{u}_x^T] \quad (26)$$

$$(\mathbf{V}^T \mathbf{W}_x \mathbf{V}) \mathbf{u}_x = \mathbf{V}^T \mathbf{W}_x (\mathbf{x} - \boldsymbol{\mu}) \quad (27)$$

$$\mathbb{E}_G [\mathbf{W}_x \mathbf{V} \mathbf{u}_x] = \mathbb{E}_G [\mathbf{W}_x (\mathbf{x} - \boldsymbol{\mu})] . \quad (28)$$

Here $\mathbf{W}_x = \operatorname{diag}(\mathbf{w}_x)$ for $\mathbf{w}_x = (w_1, \dots, w_p)^T$. The components of \mathbf{w}_x are $w_j = w_j^c w^r$ with $w_j^c = \psi_1 \left(\frac{r_j}{\sigma_{1,j}} \right) / \frac{r_j}{\sigma_{1,j}}$ and $w^r = \psi_2 \left(\frac{t}{\sigma_2} \right) / \frac{t}{\sigma_2}$. For simplicity we will assume that $\boldsymbol{\mu} = \mathbf{0}$.

Proposition 2. *The influence functions of \mathbf{P} under FDCM and FICM are*

$$\operatorname{IF}_{FDCM}(\mathbf{z}, \mathbf{P}, H_0) = -\mathbf{D} \left(\mathbf{S} \operatorname{IF}_{FDCM}(\mathbf{z}, \boldsymbol{\sigma}, H_0) + \mathbf{g}(\Delta_{\mathbf{z}}, \mathbf{V}_0, \boldsymbol{\sigma}_0) \right) \quad (29)$$

and

$$\operatorname{IF}_{FICM}(\mathbf{z}, \mathbf{P}, H_0) = -\mathbf{D} \left(\mathbf{S} \operatorname{IF}_{FICM}(\mathbf{z}, \boldsymbol{\sigma}, H_0) + p \sum_{j=1}^p \mathbf{g}(H(G_1^j, \mathbf{z}), \mathbf{V}_0, \boldsymbol{\sigma}_0) \right) \quad (30)$$

with $\boldsymbol{\sigma}(H) = (\sigma_{1,1}(H), \dots, \sigma_{1,p}(H), \sigma_2(H))^T$, $\mathbf{P}(H_0) = \mathbf{V}_0 \mathbf{V}_0^T$, $\boldsymbol{\sigma}_0 = \boldsymbol{\sigma}(H_0)$ and

$$\mathbf{g}(H, \mathbf{V}, \boldsymbol{\sigma}) = \operatorname{vec} \left(\mathbb{E}_H [\mathbf{W}_x (\mathbf{V} \mathbf{u}_x - \mathbf{x}) \mathbf{u}_x^T] \right) \quad (31)$$

where $\operatorname{vec}(\cdot)$ is the vectorization operator that converts a matrix to a vector by stacking its columns on top of each other. The matrices \mathbf{D} and \mathbf{S} are computed in Sections E and F

of the Supplementary Material, and $\text{IF}_{\text{FDCM}}(\mathbf{z}, \boldsymbol{\sigma})$ and $\text{IF}_{\text{FICM}}(\mathbf{z}, \boldsymbol{\sigma})$ are the rowwise and cellwise influence functions of $\boldsymbol{\sigma}$. The G_1^j in (30) puts all its mass in $(0, \dots, 1, \dots, 0)$ with the single 1 in position j . Moreover, choosing a different parametrization \mathbf{V}_0 of $\mathbf{P}(H_0)$ yields the same $\text{IF}_{\text{FDCM}}(\mathbf{z}, \mathbf{P})$ and $\text{IF}_{\text{FICM}}(\mathbf{z}, \mathbf{P})$.

Note that (31) expresses one of the first order conditions, but the other first-order condition $(\mathbf{V}^T \mathbf{W}_x \mathbf{V}) \mathbf{u}_x = \mathbf{V}^T \mathbf{W}_x (\mathbf{x} - \boldsymbol{\mu})$ must hold as well, and acts as a constraint. Moreover, \mathbf{g} depends on $\boldsymbol{\sigma}$ through \mathbf{W}_x and \mathbf{u}_x . Also note that $H(G_1^j, \mathbf{z})$ in (30) is the distribution of $\mathbf{X} \sim H_0$ but with its j -th component fixed at the constant z_j . It is thus a degenerate distribution concentrated on the hyperplane $X_j = z_j$.

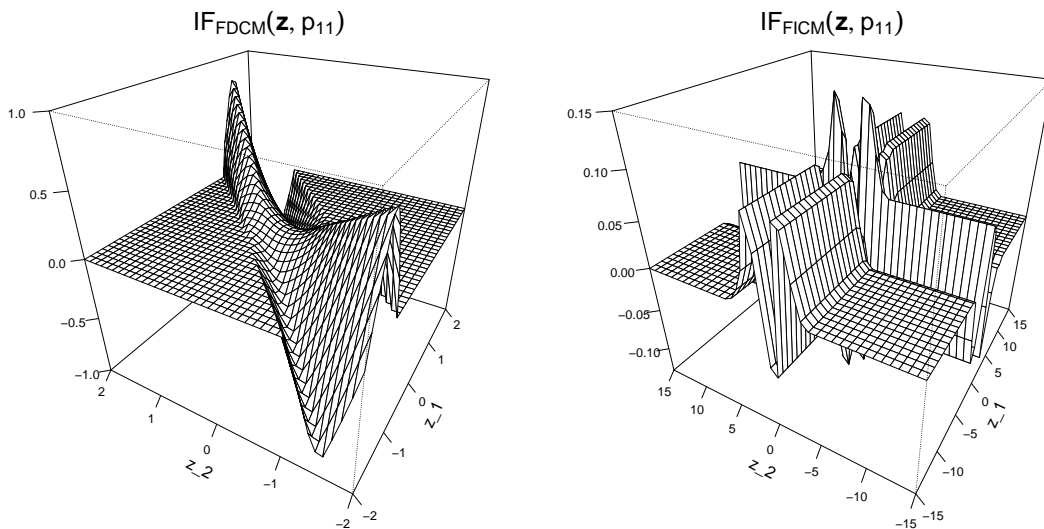


Figure 7: $\text{IF}(\mathbf{z}, p_{11})$ for bivariate normal H_0 under FDCM (left) and under FICM (right).

Let us look at a simple setting in order to get a feel for these results. The data are bivariate normal with $H_0 = N\left(\mathbf{0}, \begin{bmatrix} 1 & 0.9 \\ 0.9 & 1 \end{bmatrix}\right)$ and we want to fit a one-dimensional PCA subspace ($q = 1$). The PCA subspace of the population is thus the 45° line $x_2 = x_1$. The left panel of Figure 7 shows the rowwise influence function of the entry p_{11} of the estimated projection matrix \mathbf{P} . If we look along the line $z_2 = -z_1$ we see the shape of the ψ -function in the right panel of Figure 1 which is bounded and redescending, from which we conclude that cellPCA is rather insensitive to outliers orthogonal to the fitted subspace. Along lines of the type $z_2 = z_1 + \text{constant}$ with small nonzero constant, the IF is unbounded. This is harmless because those (z_1, z_2) are so-called good leverage points, which are closely aligned with the fitted subspace. The same effect is well-known for robust regression methods. For

the bad leverage points, i.e. with large constant, the IF is zero. Also note that \mathbf{P} itself is always bounded, since any rank- q projection matrix has Frobenius norm $\|\mathbf{P}\|_F = \sqrt{q}$.

The right panel of Figure 8 shows the cellwise IF in the same setting, which looks quite different. As a function of z_1 for a large fixed z_2 it again has the shape of the ψ -function, and for large $|z_1|$ the cellwise weight becomes zero. The situation is the same in the other direction. Also note that this IF is bounded. The exact same behavior was found by Alqallaf et al. (2009) for a redescending M-estimator of a bivariate location vector $[\mu_1 \mu_2]^T$.

It is harder to visualize the IF of the entire matrix \mathbf{P} , since it is an $p \times p$ matrix. Figure 8 shows the norm of the rowwise and cellwise IF of \mathbf{P} , in the same setting as in Figure 7. The shape is similar to before, bearing in mind that the norm is nonnegative.

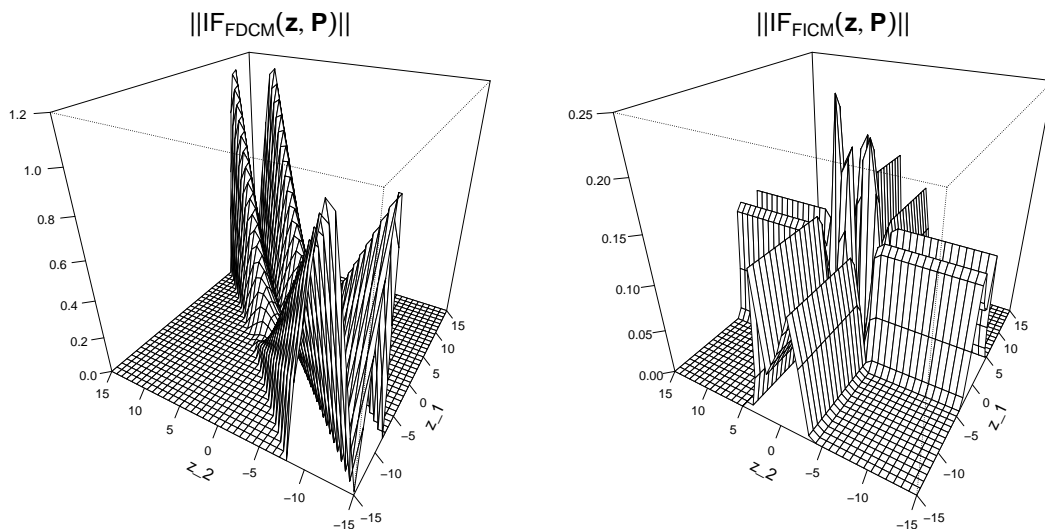


Figure 8: Norm of $\text{IF}(\mathbf{z}, \mathbf{P})$ for bivariate normal H_0 under FDCM (left) and under FICM (right).

Let us now look at the asymptotic distribution of cellPCA. Suppose we obtain i.i.d. observations $\mathbf{x}_1, \mathbf{x}_2, \dots$ from H_0 . For simplicity we assume that $\boldsymbol{\mu} = \mathbf{0}$ and that $\hat{\sigma}_{1,j}$ and $\hat{\sigma}_2$ are fixed at $\sigma_{1,j}(H)$ and $\sigma_2(H)$. We use a fixed initial estimate $\mathbf{P}_{(0)}$ obtained as in Section 2.2. We then choose an orthonormal basis in the principal subspace, that is, a $p \times q$ matrix $\mathbf{V}_{(0)}$ with orthonormal columns such that $\mathbf{V}_{(0)}\mathbf{V}_{(0)}^T = \mathbf{P}_{(0)}$. We start the algorithm from $\mathbf{V}_{(0)}$, yielding a $\hat{\mathbf{V}}_n$ for each sample $\{\mathbf{x}_1, \mathbf{x}_2, \dots, \mathbf{x}_n\}$. We know that $\mathbf{V}_{(0)}$ is not unique, but it is shown in Section C that the resulting estimates $\hat{\mathbf{P}}_n$ are the same no matter which $\mathbf{V}_{(0)}$ was chosen. Let us assume that $\hat{\mathbf{V}}_n$ converges in probability to the population version

$\widehat{\mathbf{V}}(H)$. We now denote

$$\widehat{\Lambda}_n(\mathbf{V}) := \frac{1}{n} \sum_{i=1}^n \Psi(\mathbf{x}_i, \mathbf{V}) \quad \text{and} \quad \Lambda(\mathbf{V}) := \mathbb{E}_H \Psi(\mathbf{x}, \mathbf{V})$$

where $\Psi(\mathbf{x}_i, \mathbf{V}) = (\Psi_1(\mathbf{x}_i, \mathbf{V}), \dots, \Psi_{pq}(\mathbf{x}_i, \mathbf{V}))^T = \text{vec}(\mathbf{W}_i(\mathbf{x}_i - \mathbf{V}\mathbf{u}_i)\mathbf{u}_i^T)$, $\mathbf{u}_i = \mathbf{V}^T \mathbf{x}_i^0$, and \mathbf{x}_i^0 satisfies $(\mathbf{P}\mathbf{W}_i\mathbf{P})\mathbf{x}_i^0 = \mathbf{P}\mathbf{W}_i\mathbf{x}_i^0$. Then $\widehat{\mathbf{V}}_n$ and $\mathbf{V}(H)$ satisfy $\widehat{\Lambda}_n(\widehat{\mathbf{V}}_n) = \mathbf{0}$ and $\Lambda(\mathbf{V}(H)) = \mathbf{0}$.

Proposition 3. *Assume that Ψ is twice differentiable with respect to \mathbf{V} with bounded second derivatives, and that $\dot{\Psi}_k = \frac{\partial \Psi_k}{\partial \text{vec}(\mathbf{V})}$ exists and satisfies*

$$\left| \dot{\Psi}_k(\mathbf{x}, \mathbf{V}) \right| \leq K(\mathbf{x}) \quad \text{with} \quad \mathbb{E}_H[K(\mathbf{x})] < \infty$$

for any $k = 1, \dots, pq$, \mathbf{V} and \mathbf{x} . Then $\widehat{\mathbf{P}}_n \rightarrow \mathbf{P}(H)$ in probability, and

$$\sqrt{n} \text{vec} \left(\widehat{\mathbf{P}}_n - \mathbf{P}(H) \right) \rightarrow N_{p^2}(\mathbf{0}, \Theta) \quad (32)$$

in distribution, where $\Theta = \mathbb{E}_H [\text{IF}_{FDCM}(\mathbf{x}, \mathbf{P}) \text{IF}_{FDCM}(\mathbf{x}, \mathbf{P})^T]$. The right hand side of (32) does not depend on the parametrization of \mathbf{P} .

5 Predicting new data

The cellPCA estimation in Section 2 can be seen as the training stage. There can also be an out-of-sample stage, where a new datapoint \mathbf{x}_* arrives and we wish to predict its $\widehat{\mathbf{x}}_*$. This task is not trivial, since \mathbf{x}_* can also contain cellwise outliers and NA's. To fit \mathbf{x}_* we will first predict its \mathbf{u}_* for the given \mathbf{V} and $\boldsymbol{\mu}$. For this purpose we minimize the inner part of the objective (5) for a single $\mathbf{x}_i = \mathbf{x}_*$. That is, we minimize

$$\sum_{j=1}^p m_j \widehat{\sigma}_{1,j}^2 \rho_1 \left(\frac{(\mathbf{x}_*)_j - \mu_j - \mathbf{v}_j^T \tilde{\mathbf{u}}}{\widehat{\sigma}_{1,j}} \right) \quad (33)$$

where \mathbf{V} and $\boldsymbol{\mu}$ are now known and x_{ij} was replaced by $(\mathbf{x}_*)_j$ and m_{ij} by m_j . When all m_j are zero we set \mathbf{u}_* and $\widehat{\mathbf{x}}_*$ to NA. If not, this becomes a sum over $J = \{j ; m_j = 1\}$ so

$$\mathbf{u}_* = \underset{\tilde{\mathbf{u}}}{\text{argmin}} \sum_{j \in J} \widehat{\sigma}_{1,j}^2 \rho_1 \left(\frac{\tilde{x}_j - \mathbf{v}_j^T \tilde{\mathbf{u}}}{\widehat{\sigma}_{1,j}} \right) \quad (34)$$

where $\tilde{x}_j := (\mathbf{x}_*)_j - \mu_j$. So \mathbf{u}_* is the slope vector of a robust regression without intercept of the column vector $\tilde{\mathbf{x}}_J = (\tilde{x}_j ; j \in J)$ on the matrix $V_J = [\mathbf{v}_j^T ; j \in J]$. Note that V_J has no outliers since all $|v_{j\ell}| \leq 1$. The IRLS algorithm uses the first order condition (18) and alternates updating \mathbf{u}_* according to (19) with updating the cellwise weights (14) by

$$(\mathbf{w}_*)_j = \psi_1\left(\frac{r_j}{\hat{\sigma}_{1,j}}\right) / \frac{r_j}{\hat{\sigma}_{1,j}} \quad \text{for } j \text{ in } J \quad (35)$$

and $(\mathbf{w}_*)_j = 0$ for j not in J . (Should all $(\mathbf{w}_*)_j$ become zero we set \mathbf{u}_* and $\hat{\mathbf{x}}_*$ to NA.) Lastly we compute $\mathbf{x}_*^{\text{imp}}$ by (21).

6 Simulation study

We study the performance of cellPCA by Monte Carlo, with setup similar to (Hubert et al., 2019). The clean data are generated from a multivariate Gaussian with $\boldsymbol{\mu} = \mathbf{0}$ and covariance matrix $\boldsymbol{\Sigma}$. The first $\boldsymbol{\Sigma}$ we consider is called A09, with entries $\Sigma_{jk} = (-0.9)^{|j-k|}$. We generate $n = 100$ data points in dimension $p = 20$ so that $n > p$, and in dimension $p = 200$ for which $n < p$. Since in both dimensions the first two eigenvectors together explain 90% of the variance and the third one adds little, we set $q = 2$.

Three contamination types are considered. In the cellwise outlier scenario we randomly select 20% of the cells x_{ij} and add γ_c to them, where γ_c varies from 0 to 6. In the rowwise outlier setting 20% of the rows are generated from $N(\gamma_r(\mathbf{e}_1 + \mathbf{e}_3), \boldsymbol{\Sigma}/1.5)$, where \mathbf{e}_1 and \mathbf{e}_3 are the first and third eigenvectors of $\boldsymbol{\Sigma}$, and γ_r varies from 0 to 9 when $p = 20$, and from 0 to 24 when $p = 200$. In the third scenario, the data is contaminated by 10% of cellwise outliers as well as 10% of rowwise outliers. Here $\gamma_r = 1.5\gamma_c$ when $p = 20$ and $\gamma_r = 4\gamma_c$ when $p = 200$, where γ_c again varies from 0 to 6. Note that the data are clean when $\gamma_c = \gamma_r = 0$.

We compare cellPCA with several competing approaches that are robust to either cellwise outliers, rowwise outliers, or both. We run the cellwise robust PCA method of Candès et al. (2011), called CANDÉS, the special case of cellPCA with $\rho_2(z) = z^2$ denoted as Only-cell, the rowwise robust method of Hubert et al. (2005) called ROBPCA, and the special case of cellPCA with $\rho_1(z) = z^2$, called Only-row. We also run the MacroPCA method (Hubert et al., 2019), and include classical PCA (CPCA) for comparison.

We measure performance by the angle between the estimated principal subspace and the true principal subspace. This angle is computed by the function `subspace()` of the R

package `pracma` (Borchers, 2022). We also compute the mean squared error given by

$$\text{MSE} = \frac{1}{|\mathcal{U}|} \sum_{(i,j) \in \mathcal{U}} (x_{ij} - \hat{x}_{ij})^2 \quad (36)$$

where \mathcal{U} is the set of uncontaminated cells in uncontaminated rows, and \hat{x}_{ij} is the prediction of x_{ij} . We report the median angle and MSE over 1000 replications.

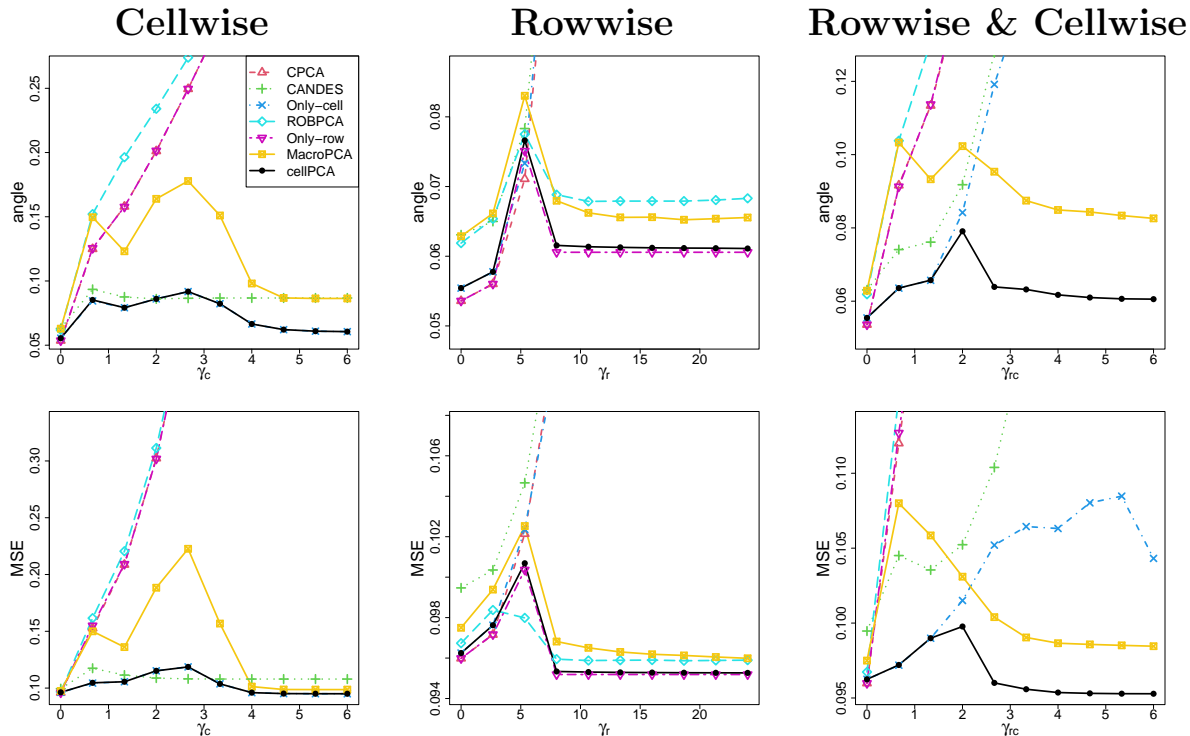


Figure 9: Median angle (top) and MSE (bottom) attained by CPCA, CANDES, Only-cell, ROBPCA, Only-row, MacroPCA, and cellPCA in the presence of either cellwise outliers, rowwise outliers, or both. The covariance model was A09 with $n = 100$ and $p = 200$, without NA's.

Figure 9 shows the median angle and MSE in the presence of either cellwise outliers, rowwise outliers, or both, for $p = 200$. The plots for $p = 20$ are very similar, see Section G of the Supplementary material. As expected, CPCA did best on clean data ($\gamma = 0$), but outperformed cellPCA by a small margin only. The results with outliers are more interesting. When there are only cellwise outliers, CPCA, ROBPCA, and Only-row break down, because they were not designed for cellwise outliers. CANDES did well in this setting. Here cellPCA did best, and Only-cell almost coincided with it.

In the presence of rowwise outliers, CPCA, CANDES and Only-cell break down, because

they were not created for that situation. Also here cellPCA does well, only slightly outperformed by Only-row. Note that cellPCA also outperforms the rowwise robust method ROBPCA, as well as MacroPCA, but the latter do not break down.

When cellwise outliers and rowwise outliers are combined, cellPCA outperforms overall. It naturally beats the methods that are not robust to cellwise outliers (CPCA, Only-row, ROBPCA) or not robust to rowwise outliers (CPCA, CANDES, Only-cell).

In all three settings cellPCA outperforms its predecessor MacroPCA, because it minimizes an objective function in which the cellwise and rowwise weights adapt to the data.

To assess the performance in the presence of missing data, we repeated the three scenarios but also randomly set 20% of the cells to NA. In this situation we cannot run CANDES or ROBPCA which are unable to deal with missing data, and for CPCA we use the ICPCA method of Kiers (1997) that can. The resulting Figure 10 looks quite similar to Figure 9. Again cellPCA performs best overall, and outperforms MacroPCA. The remaining methods break down under the combination of cellwise outliers, rowwise outliers and NA's.

Section G of the Supplementary material repeats the entire simulation where the covariance matrix A09 is replaced by more diverse random covariance matrices based on Agostinelli et al. (2015). The results are very similar to those shown here, with the same conclusions.

7 Real data example

Campi Flegrei is an active volcanic field partly underlying the city of Naples, Italy. It is monitored from six permanent ground stations, one of which is located at the Vesuvius crater (Sansivero and Vilardo, 2022). They record thermal infrared (TIR) images to investigate volcanic plumes and gases, lava flows, lava lakes, and fumaroles, which are vents of hot gas. The goal is to track surface thermal anomalies that may reveal a renewal of eruptive activity (Vilardo et al., 2015). The Solfatara data are part of a huge dataset of TIR frames available at <https://doi.org/10.13127/vd/tirnet>. They consist of TIR images of 200×200 pixels acquired from May to November 2022 by the remote station of Solfatara 1. Vectorizing each frame yields an ultra-high dimensional data matrix with $n = 205$ and $p = 40000$. We have applied cellPCA with $q = 2$.

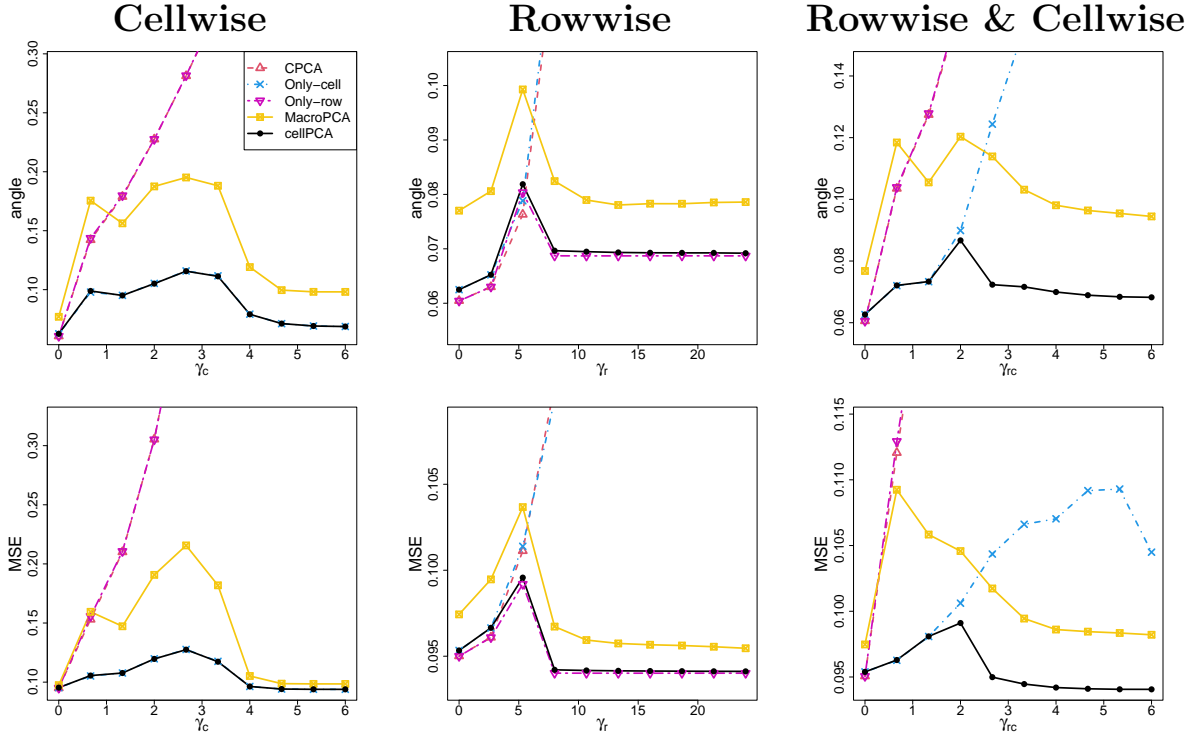


Figure 10: Median angle (top) and MSE (bottom) attained by CPCA, Only-cell, Only-row, MacroPCA, and cellPCA in the presence of either cellwise outliers, rowwise outliers, or both. The covariance model was A09 with $n = 100$ and $p = 200$, and 20% of randomly selected cells were set to NA.

Figure 11 shows the resulting enhanced outlier map. We see that many residuals have $\|\tilde{r}_i\|$ far above the horizontal cutoff line, and there are quite a few rowwise outliers (black points). The size of these points indicates that many of their cells have low weight. By way of illustration we look at one of them, case 14.

Figure 12 shows some results for frame 14. The top left panel is the observed frame, with cooler regions in blue and warmer regions in yellow to red. The predicted frame is slightly different, and overall a bit less cool. The standardized residuals are shown in the bottom panel. This is the part of the residual cellmap of the Solfatara data belonging to frame 14. The entire residual cellmap is much bigger, and has a row with 40000 cells for case 14. These cells are more easily visualized in this 200 by 200 square form corresponding to frame 14 itself. The blue region in the cellmap indicates where the observed temperature was lower than expected. It points to the condensation of hot water vapor in plumes from

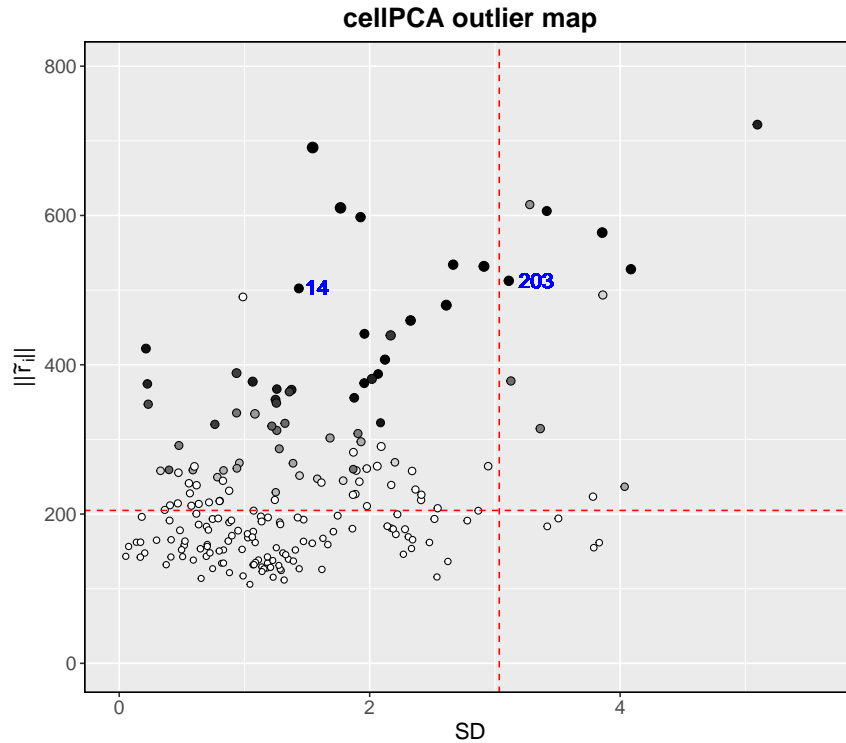


Figure 11: Enhanced outlier map of the Solfatara data.

the volcanic fumaroles, which partly hides the heat underneath. This behavior is not visible in the raw observed frame, but it deviates from the overall linear relations described by the principal subspace.

The outlier map of Figure 11 shows where case 14 is located, and the results for case 203 are shown in section I of the Supplementary Material. Inspection showed that the rowwise outliers in the outlier map were mainly among the first 23 and the last 65 cases, that correspond to TIR frames acquired in May, October, and November. By visually examining the frames we observed that the majority of the anomalous images exhibit temperature patterns distinctly different from those of the regular frames. As in frame 14 the residual frames often show extensive blurred regions, which have been attributed to the condensation of water vapor. This effect is most pronounced during the winter season, due to higher air humidity levels.

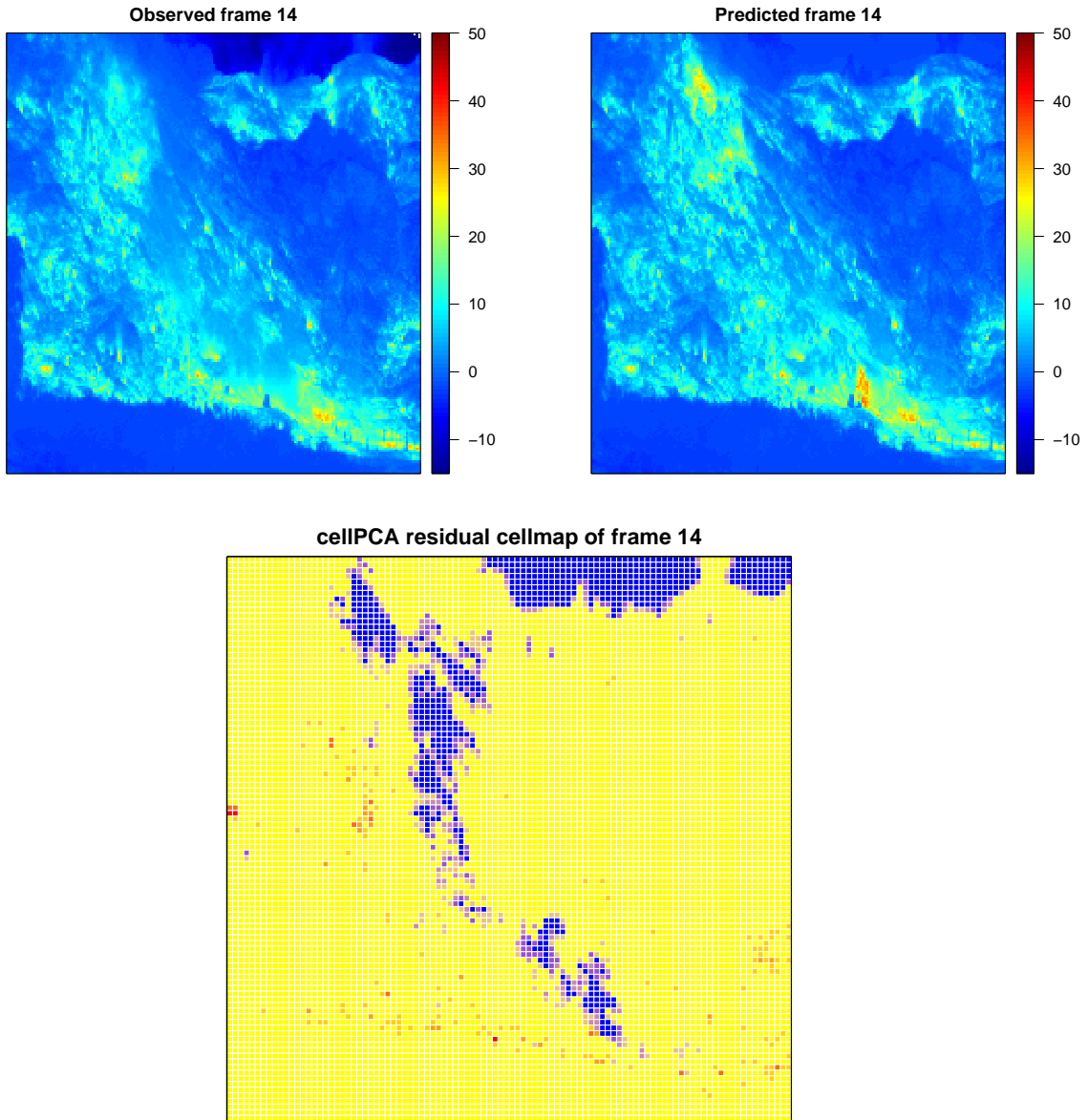


Figure 12: Solfatara data: (top left) observed frame 14, (top left) its prediction, and (bottom) its residual cellmap.

8 Conclusions

We have proposed the cellPCA method which is able to simultaneously handle missing values, cellwise outliers, and rowwise outliers. The main novelty of this method is that it minimizes a single objective function. Its algorithm assigns a weight to each cell in the data, as well as to each row (case). The unifying objective function allowed us to derive both the cellwise and the rowwise influence function of the projection matrix, as well as the

asymptotic distribution of the latter. The cellwise and rowwise weights made it possible to create more informative residual cellmaps and outlier maps to visualize outliers. The method also provides imputations that can be used in further analyses. The performance of cellPCA was showcased in a simulation study, and the method was illustrated on interesting datasets.

Software availability. R code for the proposed method and a script that reproduces the examples is available at <https://wis.kuleuven.be/statdatascience/robust>. The rather large Solfatara dataset that was analyzed in Section 7 can be downloaded from <https://figshare.com/s/82bcfb64d5130712aeef>.

Funding Details. The research activity of F. Centofanti was carried out within the MICS (Made in Italy – Circular and Sustainable) Extended Partnership and received funding from the European Union Next-GenerationEU (PIANO NAZIONALE DI RIPRESA E RESILIENZA (PNRR) – MISSIONE 4 COMPONENTE 2, INVESTIMENTO 1.3 – D.D. 1551.11-10-2022, PE00000004).

References

- Agostinelli, C., A. Leung, V. J. Yohai, and R. H. Zamar (2015). Robust estimation of multivariate location and scatter in the presence of cellwise and casewise contamination. *Test* 24, 441–461.
- Alqallaf, F., S. Van Aelst, V. J. Yohai, and R. H. Zamar (2009). Propagation of outliers in multivariate data. *The Annals of Statistics* 37, 311–331.
- Borchers, H. W. (2022). *pracma: Practical Numerical Math Functions*. CRAN. R package version 2.4.2.
- Candès, E. J., X. Li, Y. Ma, and J. Wright (2011). Robust principal component analysis? *Journal of the ACM* 58(3), 1–37.
- Croux, C., L. García-Escudero, A. Gordaliza, C. Ruwet, and R. S. Martín (2017). Robust

- principal component analysis based on trimming around affine subspaces. *Statistica Sinica* 27, 1437–1459.
- De La Torre, F. and M. J. Black (2003). A framework for robust subspace learning. *International Journal of Computer Vision* 54, 117–142.
- Debruyne, M. and M. Hubert (2009). The influence function of the Stahel–Donoho covariance estimator of smallest outlyingness. *Statistics & Probability Letters* 79(3), 275–282.
- Gabriel, K. R. (1978). Least squares approximation of matrices by additive and multiplicative models. *Journal of the Royal Statistical Society Series B* 40(2), 186–196.
- Hampel, F. R., E. M. Ronchetti, and P. J. Rousseeuw (1981). The Change-of-Variance Curve and Optimal Redescending M-Estimators. *Journal of the American Statistical Association* 76, 643–648.
- Hubert, M., P. J. Rousseeuw, and W. Van den Bossche (2019). MacroPCA: an all-in-one PCA method allowing for missing values as well as cellwise and rowwise outliers. *Technometrics* 61(4), 459–473.
- Hubert, M., P. J. Rousseeuw, and K. Vanden Branden (2005). ROBPCA: a new approach to robust principal component analysis. *Technometrics* 47, 64–79.
- Hubert, M., P. J. Rousseeuw, and T. Verdonck (2012). A deterministic algorithm for robust location and scatter. *Journal of Computational and Graphical Statistics* 21(3), 618–637.
- Jolliffe, I. (2011). *Principal Component Analysis*. Springer.
- Kiers, H. A. (1997). Weighted least squares fitting using ordinary least squares algorithms. *Psychometrika* 62, 251–266.
- Locantore, N., J. Marron, D. Simpson, N. Tripoli, J. Zhang, K. Cohen, G. Boente, R. Fraiman, B. Brumback, C. Croux, et al. (1999). Robust principal component analysis for functional data. *Test* 8(1), 1–73.
- Maronna, R. A. and V. J. Yohai (2008). Robust low-rank approximation of data matrices with elementwise contamination. *Technometrics* 50(3), 295–304.

- Raymaekers, J. and P. J. Rousseeuw (2021). Fast robust correlation for high-dimensional data. *Technometrics* 63, 184–198.
- Raymaekers, J. and P. J. Rousseeuw (2023). The cellwise minimum covariance determinant estimator. *Journal of the American Statistical Association*, appeared online.
- Rousseeuw, P. J. and W. Van den Bossche (2018). Detecting deviating data cells. *Technometrics* 60(2), 135–145.
- Rousseeuw, P. J. and K. Van Driessen (1999). A Fast Algorithm for the Minimum Covariance Determinant Estimator. *Technometrics* 41, 212–223.
- Sansivero, F. and G. Vilardo (2022). *Ground-based thermal/IR images acquired by TIRNet permanent volcanic surveillance network*. Istituto Nazionale di Geofisica e Vulcanologia (INGV).
- Serneels, S. and T. Verdonck (2008). Principal component analysis for data containing outliers and missing elements. *Computational Statistics & Data Analysis* 52(3), 1712–1727.
- Sigillito, V. G., S. P. Wing, L. V. Hutton, and K. B. Baker (1989). Classification of radar returns from the ionosphere using neural networks. *Johns Hopkins APL Technical Digest* 10(3), 262–266.
- Todorov, V. and P. Filzmoser (2009). An object-oriented framework for robust multivariate analysis. *Journal of Statistical Software* 32(3), 1–47.
- Vaswani, N., T. Bouwmans, S. Javed, and P. Narayanamurthy (2018). Robust subspace learning: Robust PCA, robust subspace tracking, and robust subspace recovery. *IEEE Signal Processing* 35(4), 32–55.
- Vilardo, G., F. Sansivero, and G. Chiodini (2015). Long-term TIR imagery processing for spatiotemporal monitoring of surface thermal features in volcanic environment: A case study in the Campi Flegrei (Southern Italy). *Journal of Geophysical Research: Solid Earth* 120(2), 812–826.

Supplementary Material to: Robust Principal Components

by Rowwise and Cellwise Weighting

Fabio Centofanti, Mia Hubert, and Peter J. Rousseeuw

A Equivalent parametrizations of \mathbf{V}

The principal subspace is of the form $\mathbf{\Pi} = \mathbf{\Pi}_0 + \boldsymbol{\mu}$ where \mathbf{P}_0 is a linear subspace of dimension q which is characterized by the $p \times p$ projection matrix \mathbf{P} . We saw in Section 2.2 that \mathbf{P} can be written as $\mathbf{P} = \mathbf{V}\mathbf{V}^T$ where the $p \times q$ matrix \mathbf{V} has orthonormal columns, which form an orthonormal basis of $\mathbf{\Pi}_0$. We could also take a different orthonormal basis of $\mathbf{\Pi}_0$ corresponding to a matrix $\tilde{\mathbf{V}}$, so that $\tilde{\mathbf{V}}\tilde{\mathbf{V}}^T = \mathbf{P}$ as well. But then there must be a nonsingular $q \times q$ matrix \mathbf{A} such that $\tilde{\mathbf{V}} = \mathbf{V}\mathbf{A}$. Left multiplying by \mathbf{V}^T yields $\mathbf{V}^T\tilde{\mathbf{V}} = \mathbf{V}^T\mathbf{V}\mathbf{A} = \mathbf{A}$. We can also go in the opposite direction by $\mathbf{V} = \tilde{\mathbf{V}}\mathbf{A}^{-1}$ and then left multiply by $\tilde{\mathbf{V}}^T$ yielding $\tilde{\mathbf{V}}^T\mathbf{V} = \tilde{\mathbf{V}}^T\tilde{\mathbf{V}}\mathbf{A}^{-1} = \mathbf{A}^{-1}$. Then $\mathbf{A}^{-1} = \tilde{\mathbf{V}}^T\mathbf{V} = (\mathbf{V}^T\tilde{\mathbf{V}})^T = \mathbf{A}^T$ so \mathbf{A} is an orthogonal matrix. Therefore we can write $\tilde{\mathbf{V}} = \mathbf{V}\mathbf{O}$ where $\mathbf{O} = \mathbf{A}$ is an orthogonal $q \times q$ matrix. This shows that \mathbf{V} is only determined up to right multiplication by an orthogonal matrix.

B First-order Conditions

In the following, the derivation of the first-order necessary conditions from (5) is presented.

The objective function was given by

$$L_{\rho_1, \rho_2}(\mathbf{X}, \mathbf{V}, \mathbf{U}, \boldsymbol{\mu}) := \frac{\hat{\sigma}_2^2}{m} \sum_{i=1}^n m_i \rho_2 \left(\frac{1}{\hat{\sigma}_2} \sqrt{\frac{1}{m_i} \sum_{j=1}^p m_{ij} \hat{\sigma}_{1,j}^2 \rho_1 \left(\frac{x_{ij} - \hat{x}_{ij}}{\hat{\sigma}_{1,j}} \right)} \right).$$

We start with the gradient of L_{ρ_1, ρ_2} with respect to \mathbf{v}_j which is

$$\begin{aligned}
\mathbf{0} &= \frac{\partial}{\partial \mathbf{v}_j} L_{\rho_1, \rho_2} = \frac{\widehat{\sigma}_2^2}{m} \sum_{i=1}^n m_i \rho_2'(t_i/\widehat{\sigma}_2) \frac{1}{\widehat{\sigma}_2} \frac{\partial}{\partial \mathbf{v}_j} \sqrt{\frac{1}{m_i} \sum_{j=1}^p m_{ij} \widehat{\sigma}_{1,j}^2 \rho_1 \left(\frac{x_{ij} - \widehat{x}_{ij}}{\widehat{\sigma}_{1,j}} \right)} \\
&= \frac{1}{m} \sum_{i=1}^n m_i \frac{\psi_2(t_i/\widehat{\sigma}_2)}{t_i/\widehat{\sigma}_2} \frac{1}{2m_i} \frac{\partial}{\partial \mathbf{v}_j} \left(\sum_{j=1}^p m_{ij} \widehat{\sigma}_{1,j}^2 \rho_1 \left(\frac{x_{ij} - \widehat{x}_{ij}}{\widehat{\sigma}_{1,j}} \right) \right) \\
&= \frac{1}{2m} \sum_{i=1}^n w_i^r \widehat{\sigma}_{1,j}^2 \psi_1(r_{ij}/\widehat{\sigma}_{1,j}) \frac{m_{ij}}{\widehat{\sigma}_{1,j}} \frac{\partial}{\partial \mathbf{v}_j} (x_{ij} - \mu_j - \mathbf{u}_i^T \mathbf{v}_j) \\
&= \frac{-1}{2m} \sum_{i=1}^n w_i^r \widehat{\sigma}_{1,j} \frac{\psi_1(r_{ij}/\widehat{\sigma}_{1,j})}{r_{ij}/\widehat{\sigma}_{1,j}} \frac{m_{ij}}{\widehat{\sigma}_{1,j}} r_{ij} \mathbf{u}_i \\
&= \frac{-1}{2m} \sum_{i=1}^n \mathbf{u}_i w_i^r w_{ij}^c m_{ij} (x_{ij} - \mu_j - \mathbf{u}_i^T \mathbf{v}_j) \\
&= \frac{-1}{2m} \sum_{i=1}^n \mathbf{u}_i w_{ij} (x_{ij} - \mu_j - \mathbf{u}_i^T \mathbf{v}_j) \\
&= \frac{-1}{2m} (\mathbf{U}^T \mathbf{W}^j (\mathbf{x}^j - \mu_j \mathbf{1}_n) - \mathbf{U}^T \mathbf{W}^j \mathbf{U} \mathbf{v}_j).
\end{aligned}$$

The gradient of L_{ρ_1, ρ_2} with respect to \mathbf{u}_i is

$$\begin{aligned}
\mathbf{0} &= \frac{\partial}{\partial \mathbf{u}_i} L_{\rho_1, \rho_2} = \frac{\widehat{\sigma}_2^2}{m} m_i \rho_2'(t_i/\widehat{\sigma}_2) \frac{1}{\widehat{\sigma}_2} \frac{\partial}{\partial \mathbf{u}_i} \sqrt{\frac{1}{m_i} \sum_{j=1}^p m_{ij} \widehat{\sigma}_{1,j}^2 \rho_1 \left(\frac{x_{ij} - \widehat{x}_{ij}}{\widehat{\sigma}_{1,j}} \right)} \\
&= \frac{1}{2m} \frac{\psi_2(t_i/\widehat{\sigma}_2)}{t_i/\widehat{\sigma}_2} \frac{\partial}{\partial \mathbf{u}_i} \left(\sum_{j=1}^p m_{ij} \widehat{\sigma}_{1,j}^2 \rho_1 \left(\frac{x_{ij} - \widehat{x}_{ij}}{\widehat{\sigma}_{1,j}} \right) \right) \\
&= \frac{1}{2m} \sum_{j=1}^p w_i^r \widehat{\sigma}_{1,j}^2 \psi_1(r_{ij}/\widehat{\sigma}_{1,j}) \frac{m_{ij}}{\widehat{\sigma}_{1,j}} \frac{\partial}{\partial \mathbf{v}_j} (x_{ij} - \mu_j - \mathbf{v}_j^T \mathbf{u}_i) \\
&= \frac{-1}{2m} \sum_{j=1}^p \mathbf{v}_j w_i^r \widehat{\sigma}_{1,j} \frac{\psi_1(r_{ij}/\widehat{\sigma}_{1,j})}{r_{ij} \widehat{\sigma}_{1,j}} \frac{m_{ij}}{\widehat{\sigma}_{1,j}} r_{ij} \\
&= \frac{-1}{2m} \sum_{j=1}^p \mathbf{v}_j w_i^r w_{ij}^c m_{ij} (x_{ij} - \mu_j - \mathbf{v}_j^T \mathbf{u}_i) \\
&= \frac{-1}{2m} (\mathbf{V}^T \mathbf{W}_i (\mathbf{x}_i - \boldsymbol{\mu}) - \mathbf{V}^T \mathbf{W}_i \mathbf{V} \mathbf{u}_i).
\end{aligned}$$

Finally, the derivative of L_{ρ_1, ρ_2} with respect to μ_j is

$$\begin{aligned}
\frac{\partial}{\partial \mu_j} L_{\rho_1, \rho_2} &= \frac{\hat{\sigma}_2^2}{m} \sum_{i=1}^n m_i \rho_2'(t_i/\hat{\sigma}_2) \frac{1}{\hat{\sigma}_2} \frac{\partial}{\partial \mu_j} \sqrt{\frac{1}{m_i} \sum_{j=1}^p m_{ij} \hat{\sigma}_{1,j}^2 \rho_1\left(\frac{x_{ij} - \hat{x}_{ij}}{\hat{\sigma}_{1,j}}\right)} \\
&= \frac{1}{2m} \sum_{i=1}^n \frac{\psi_2(t_i/\hat{\sigma}_2)}{t_i/\hat{\sigma}_2} \frac{\partial}{\partial \mu_j} \left(\sum_{j=1}^p m_{ij} \hat{\sigma}_{1,j}^2 \rho_1\left(\frac{x_{ij} - \hat{x}_{ij}}{\hat{\sigma}_{1,j}}\right) \right) \\
&= \frac{1}{2m} \sum_{i=1}^n w_i^r \hat{\sigma}_{1,j}^2 \psi_1(r_{ij}/\hat{\sigma}_{1,j}) \frac{m_{ij}}{\hat{\sigma}_{1,j}} \frac{\partial}{\partial \mu_j} (x_{ij} - \mu_j - \mathbf{u}_i^T \mathbf{v}_j) \\
&= \frac{-1}{2m} \sum_{i=1}^n w_i^r \hat{\sigma}_{1,j} \frac{\psi_1(r_{ij}/\hat{\sigma}_{1,j})}{r_{ij}/\hat{\sigma}_{1,j}} \frac{m_{ij}}{\hat{\sigma}_{1,j}} r_{ij} \\
&= \frac{-1}{2m} \sum_{i=1}^n w_i^r w_{ij}^c m_{ij} (x_{ij} - \mu_j - \mathbf{u}_i^T \mathbf{v}_j)
\end{aligned}$$

so the gradient with respect to the vector $\boldsymbol{\mu}$ becomes

$$\mathbf{0} = \frac{\partial}{\partial \boldsymbol{\mu}} L_{\rho_1, \rho_2} = \frac{-1}{2m} \sum_{i=1}^n \mathbf{W}_i (\mathbf{x}_i - \boldsymbol{\mu} - \mathbf{V} \mathbf{u}_i).$$

We also derive the first order conditions of the weighted PCA objective function

$$\tilde{L} = \sum_{i=1}^n \sum_{j=1}^p w_{ij} (x_{ij} - \mu_j - \mathbf{u}_i^T \mathbf{v}_j)^2.$$

We start with the gradient of \tilde{L} with respect to \mathbf{v}_j which is

$$\begin{aligned}
\mathbf{0} = \frac{\partial}{\partial \mathbf{v}_j} \tilde{L} &= \sum_{i=1}^n w_{ij} \frac{\partial}{\partial \mathbf{v}_j} (x_{ij} - \mu_j - \mathbf{u}_i^T \mathbf{v}_j)^2 \\
&= -2 \sum_{i=1}^n \mathbf{u}_i w_{ij} (x_{ij} - \mu_j - \mathbf{u}_i^T \mathbf{v}_j) \\
&= -2 (\mathbf{U}^T \mathbf{W}^j (\mathbf{x}^j - \mu_j \mathbf{1}_n) - \mathbf{U}^T \mathbf{W}^j \mathbf{U} \mathbf{v}_j).
\end{aligned}$$

The gradient of \tilde{L} with respect to \mathbf{u}_i is

$$\begin{aligned}
\mathbf{0} = \frac{\partial}{\partial \mathbf{v}_j} \tilde{L} &= \sum_{j=1}^p w_{ij} \frac{\partial}{\partial \mathbf{v}_j} (x_{ij} - \mu_j - \mathbf{u}_i^T \mathbf{v}_j)^2 \\
&= -2 \sum_{j=1}^p \mathbf{v}_j w_{ij} (x_{ij} - \mu_j - \mathbf{v}_j^T \mathbf{u}_i) \\
&= -2 (\mathbf{V}^T \mathbf{W}_i (\mathbf{x}_i - \boldsymbol{\mu}) - \mathbf{V}^T \mathbf{W}_i \mathbf{V} \mathbf{u}_i).
\end{aligned}$$

Finally, the derivative of \tilde{L} with respect to μ_j is

$$\begin{aligned}\frac{\partial}{\partial \mu_j} \tilde{L} &= \sum_{i=1}^n w_{ij} \frac{\partial}{\partial \mu_j} (x_{ij} - \mu_j - \mathbf{u}_i^T \mathbf{v}_j)^2 \\ &= -2 \sum_{i=1}^n w_{ij} (x_{ij} - \mu_j - \mathbf{v}_j^T \mathbf{u}_i)\end{aligned}$$

so the gradient with respect to the vector $\boldsymbol{\mu}$ becomes

$$\mathbf{0} = \frac{\partial}{\partial \boldsymbol{\mu}} \tilde{L} = -2 \sum_{i=1}^n \mathbf{W}_i (\mathbf{x}_i - \boldsymbol{\mu} - \mathbf{V} \mathbf{u}_i).$$

C Description of the Algorithm

In each step of the algorithm we optimize the objective function of the weighted principal subspace objective (16) by adjusting the components \mathbf{V} , \mathbf{U} and $\boldsymbol{\mu}$ one after the other, by means of the first-order optimality conditions (10)–(12). This is all done for a fixed weight function. Afterward, the weight function is updated too.

The IRLS algorithm starts from our initial estimate $(\mathbf{V}_{(0)}, \mathbf{U}_{(0)}, \boldsymbol{\mu}_{(0)})$. Then, for each $k = 1, 2, \dots$, we obtain $(\mathbf{V}_{(k+1)}, \mathbf{U}_{(k+1)}, \boldsymbol{\mu}_{(k+1)})$ from $(\mathbf{V}_{(k)}, \mathbf{U}_{(k)}, \boldsymbol{\mu}_{(k)})$ by a four-step procedure.

(a) Minimize (16) with respect to \mathbf{V} by applying (10) with $\mathbf{U}_{(k)}$, $\boldsymbol{\mu}_{(k)}$, and $\mathbf{W}_{(k)}$, the weight matrix based on $(\mathbf{V}_{(k)}, \mathbf{U}_{(k)}, \boldsymbol{\mu}_{(k)})$. Condition (10) says

$$(\mathbf{U}_{(k)}^T \mathbf{W}_{(k)}^j \mathbf{U}_{(k)}) \mathbf{v}_j = \mathbf{U}_{(k)}^T \mathbf{W}_{(k)}^j (\mathbf{x}^j - (\boldsymbol{\mu}_{(k)})_j \mathbf{1}_n) \quad j = 1, \dots, p. \quad (\text{A.1})$$

For a fixed j we now want to find the best column vector \mathbf{v}_j in the sense of minimizing the objective function (16), in particular the term

$$\begin{aligned}\sum_{i=1}^n (\mathbf{W}_{(k)}^j)_{ii} (x_{ij} - (\boldsymbol{\mu}_{(k)})_j - \hat{x}_{ij})^2 &= \sum_{i=1}^n (\mathbf{W}_{(k)}^j)_{ii} (x_{ij} - (\boldsymbol{\mu}_{(k)})_j - (\mathbf{U}_{(k)} \mathbf{V}^T)_{ij})^2 \\ &= \left\| (\mathbf{W}_{(k)}^j)^{1/2} (\mathbf{x}^j - (\boldsymbol{\mu}_{(k)})_j \mathbf{1}_n) - (\mathbf{W}_{(k)}^j)^{1/2} \mathbf{U}_{(k)} \mathbf{v}_j \right\|^2\end{aligned} \quad (\text{A.2})$$

that depends on \mathbf{v}_j . This is the objective of the least squares regression of $(\mathbf{W}_{(k)}^j)^{1/2} (\mathbf{x}^j - (\boldsymbol{\mu}_{(k)})_j \mathbf{1}_n)$ on $(\mathbf{W}_{(k)}^j)^{1/2} \mathbf{U}_{(k)}$, so the optimum is reached at

$$\begin{aligned}\tilde{\mathbf{v}}_j &= \left([(\mathbf{W}_{(k)}^j)^{1/2} \mathbf{U}_{(k)}]^T (\mathbf{W}_{(k)}^j)^{1/2} \mathbf{U}_{(k)} \right)^\dagger [(\mathbf{W}_{(k)}^j)^{1/2} \mathbf{U}_{(k)}]^T (\mathbf{W}_{(k)}^j)^{1/2} (\mathbf{x}^j - (\boldsymbol{\mu}_{(k)})_j \mathbf{1}_n) \\ &= (\mathbf{U}_{(k)}^T \mathbf{W}_{(k)}^j \mathbf{U}_{(k)})^\dagger \mathbf{U}_{(k)}^T \mathbf{W}_{(k)}^j (\mathbf{x}^j - (\boldsymbol{\mu}_{(k)})_j \mathbf{1}_n)\end{aligned} \quad (\text{A.3})$$

where \dagger stands for the Moore-Penrose generalized inverse. Repeating this for all $j = 1, \dots, p$ yields a new matrix $\tilde{\mathbf{V}}_{(k+1)}$ with rows $\tilde{\mathbf{v}}_1, \dots, \tilde{\mathbf{v}}_p$, which attains the lowest objective when everything else remains fixed.

Note that the initial $\mathbf{V}_{(0)}$ that we started the algorithm from was not unique, and could be replaced by $\tilde{\mathbf{V}}_{(0)} = \mathbf{V}_{(0)}\mathbf{O}$ for any $q \times q$ orthogonal matrix \mathbf{O} . It may seem that the resulting $\mathbf{P}_{(1)}, \dots, \mathbf{P}_{(k+1)}, \dots$ need not be unique, but we will show that they are. We will show this by induction. For $k = 0$ we note that the score matrix $\mathbf{U}_{(0)}$ becomes $\tilde{\mathbf{U}}_{(0)} = \mathbf{U}_{(0)}\mathbf{V}_{(0)}^T\tilde{\mathbf{V}}_{(0)} = \mathbf{U}_{(0)}\mathbf{V}_{(0)}^T\mathbf{V}_{(0)}\mathbf{O} = \mathbf{U}_{(0)}\mathbf{O}$. The right-hand side of (A.3) then becomes

$$\begin{aligned} & (\mathbf{O}^T\mathbf{U}_{(0)}^T\mathbf{W}_{(0)}^j\mathbf{U}_{(0)}\mathbf{O})^\dagger\mathbf{O}^T\mathbf{U}_{(0)}^T\mathbf{W}_{(0)}^j(\mathbf{x}^j - (\boldsymbol{\mu}_{(0)})_j\mathbf{1}_n) \\ & = \mathbf{O}^T(\mathbf{U}_{(0)}^T\mathbf{W}_{(0)}^j\mathbf{U}_{(0)})^\dagger\mathbf{U}_{(0)}^T\mathbf{W}_{(0)}^j(\mathbf{x}^j - (\boldsymbol{\mu}_{(0)})_j\mathbf{1}_n) \end{aligned}$$

because \mathbf{O} has orthonormal columns and $\mathbf{O}^\dagger = \mathbf{O}^{-1} = \mathbf{O}^T$. So $\tilde{\mathbf{V}}_{(1)} = \mathbf{V}_{(1)}\mathbf{O}$. The step from $\mathbf{V}_{(k)}$ to $\mathbf{V}_{(k+1)}$ is analogous, so by induction we know that for all k it holds that $\tilde{\mathbf{V}}_{(k+1)} = \mathbf{V}_{(k+1)}\mathbf{O}$ and $\tilde{\mathbf{V}}_{(k+1)}(\tilde{\mathbf{V}}_{(k+1)})^T = \mathbf{V}_{(k+1)}(\mathbf{V}_{(k+1)})^T$ hence $\mathbf{P}_{(k+1)}^* = \mathbf{P}_{(k+1)}$.

(b) Minimize (16) with respect to \mathbf{U} by (11) with the new $\mathbf{P}_{(k+1)}$ and the old $\boldsymbol{\mu}_{(k)}$ and $\mathbf{W}_{(k)}$. For this we use the first order condition (11), which says

$$(\mathbf{V}_{(k+1)}^T(\mathbf{W}_{(k)})_i\mathbf{V}_{(k+1)})\mathbf{u}_i = \mathbf{V}_{(k+1)}^T(\mathbf{W}_{(k)})_i(\mathbf{x}_i - \boldsymbol{\mu}_{(k)}), \quad i = 1, \dots, n. \quad (\text{A.4})$$

For a fixed i our goal is find the \mathbf{u}_i that minimizes the corresponding term

$$\|(\mathbf{W}_{(k)})_i^{1/2}(\mathbf{x}_i - \boldsymbol{\mu}_{(k)}) - (\mathbf{W}_{(k)})_i^{1/2}\mathbf{V}_{(k+1)}\mathbf{u}_i\|^2 \quad (\text{A.5})$$

of the objective (16). We instead minimize

$$\|(\tilde{\mathbf{W}}_{(k)})_i^{1/2}(\mathbf{x}_i - \boldsymbol{\mu}_{(k)}) - (\tilde{\mathbf{W}}_{(k)})_i^{1/2}\mathbf{V}_{(k+1)}\mathbf{u}_i\|^2. \quad (\text{A.6})$$

This is the least squares regression of $(\tilde{\mathbf{W}}_{(k)})_i^{1/2}(\mathbf{x}_i - \boldsymbol{\mu}_{(k)})$ on $(\tilde{\mathbf{W}}_{(k)})_i^{1/2}\mathbf{V}_{(k+1)}$ with solution

$$\begin{aligned} (\mathbf{u}_{(k+1)})_i & = \left([(\tilde{\mathbf{W}}_{(k)})_i^{1/2}\mathbf{V}_{(k+1)}]^T(\tilde{\mathbf{W}}_{(k)})_i^{1/2}\mathbf{V}_{(k+1)} \right)^\dagger [(\tilde{\mathbf{W}}_{(k)})_i^{1/2}\mathbf{V}_{(k+1)}]^T(\tilde{\mathbf{W}}_{(k)})_i^{1/2}(\mathbf{x}_i - \boldsymbol{\mu}_{(k)}) \\ & = \left(\mathbf{V}_{(k+1)}^T(\tilde{\mathbf{W}}_{(k)})_i\mathbf{V}_{(k+1)} \right)^\dagger \mathbf{V}_{(k+1)}^T(\tilde{\mathbf{W}}_{(k)})_i(\mathbf{x}_i - \boldsymbol{\mu}_{(k)}). \end{aligned} \quad (\text{A.7})$$

Note that this solution also minimizes (A.5) which equals w_i^r times (A.6). When the rowwise weight w_i^r is strictly positive these minimizations are equivalent, and when $w_i^r = 0$ the norm (A.5) attains its lower bound of zero anyway. Repeating this for all i yields $\mathbf{U}_{(k+1)}$ and therefore $\mathbf{X}_{(k+1)}^0 := \mathbf{U}_{(k+1)}\mathbf{V}_{(k+1)}^T$.

As in step (a) we note that $\mathbf{V}_{(k+1)}$ is not unique so neither is $\mathbf{U}_{(k+1)}$, but their product $\mathbf{X}_{(k+1)}^0 := \mathbf{U}_{(k+1)} \mathbf{V}_{(k+1)}^T$ is unique. We show this as follows. Writing $\tilde{\mathbf{V}}_{(k+1)} = \mathbf{V}_{(k+1)} \mathbf{O}$ and $\tilde{\mathbf{U}}_{(k+1)} = \mathbf{U}_{(k+1)} \mathbf{O}$ the right-hand side of (A.7) becomes

$$\mathbf{O}^\dagger (\mathbf{V}_{(k+1)}^T (\mathbf{W}_{(k)})_i \mathbf{V}_{(k+1)})^\dagger \mathbf{V}_{(k+1)}^T (\mathbf{W}_{(k)})_i (\mathbf{x}_i - \boldsymbol{\mu}_{(k)}) \quad \text{so} \quad \tilde{\mathbf{U}}_{(k+1)} = \mathbf{U}_{(k+1)} \mathbf{O},$$

and $\tilde{\mathbf{X}}_{(k+1)}^0 = \tilde{\mathbf{U}}_{(k+1)} \tilde{\mathbf{V}}_{(k+1)}^T = \mathbf{U}_{(k+1)} \mathbf{O} \mathbf{O}^T \mathbf{V}_{(k+1)}^T = \mathbf{U}_{(k+1)} \mathbf{V}_{(k+1)}^T = \mathbf{X}_{(k+1)}^0$.

(c) Minimize (16) with respect to $\boldsymbol{\mu}$ with the new $\mathbf{P}_{(k+1)}$ and $\mathbf{X}_{(k+1)}^0$ and the old $\mathbf{W}_{(k)}$. For each $j = 1, \dots, p$ the term of the objective function (16) involving μ_j is the weighted sum of squares

$$\begin{aligned} & \left| \left| (\mathbf{W}_{(k)})_j^{1/2} (\mathbf{x}^j - (\boldsymbol{\mu}_{(k)})_j \mathbf{1}_n - (\mathbf{U}_{(k+1)} \mathbf{V}_{(k+1)}^T)^j) \right| \right|^2 \\ &= \sum_{i=1}^n (\mathbf{W}_{(k)})_{ij} \left(x_{ij} - \mu_j - (\mathbf{U}_{(k+1)} \mathbf{V}_{(k+1)}^T)_{ij} \right)^2 \end{aligned} \quad (\text{A.8})$$

where \mathbf{x}^j is the j th column of \mathbf{X} , which is minimized by the weighted mean

$$(\boldsymbol{\mu}_{(k+1)})_j = \frac{\sum_{i=1}^n (\mathbf{W}_{(k)})_{ij} (x_{ij} - (\mathbf{U}_{(k+1)} \mathbf{V}_{(k+1)}^T)_{ij})}{\sum_{i=1}^n (\mathbf{W}_{(k)})_{ij}}. \quad (\text{A.9})$$

Repeating this for all j yields the column vector $\boldsymbol{\mu}_{(k+1)}$.

(d) Update $\mathbf{W}_{(k)}$ according to (13), (14), and (15) with the new $\mathbf{P}_{(k+1)}$, $\mathbf{X}_{(k+1)}^0$ and $\boldsymbol{\mu}_{(k+1)}$.

The use of the generalized inverse in steps (a) and (b) of the algorithm deserves some explanation. In (A.3) it could happen that the matrix $\mathbf{U}_{(k)}^T \mathbf{W}_{(k)}^j \mathbf{U}_{(k)}$ is singular, especially when q is not much smaller than n . In that case we cannot invert $\mathbf{U}_{(k)}^T \mathbf{W}_{(k)}^j \mathbf{U}_{(k)}$, but its generalized inverse still exists. The matrix $\mathbf{V}_{(k+1)}^T (\mathbf{W}_{(k)})_i \mathbf{V}_{(k+1)}$ in (A.7) can also be singular. This occurs for instance when \mathbf{x}_i is considered as a rowwise outlier so $w_i^r = 0$. Then the matrix $(\mathbf{W}_{(k)})_i$ becomes zero so that $(\mathbf{V}_{(k+1)}^T (\mathbf{W}_{(k)})_i \mathbf{V}_{(k+1)})^\dagger$ is zero too, yielding $(\mathbf{u}_{(k+1)})_i = \mathbf{0}$ so $\mathbf{x}_i^0 = \mathbf{0}$ hence $\hat{\mathbf{x}}_i = \boldsymbol{\mu}_{(k+1)}$. During the course of the algorithm we monitor the fraction of zero weights in each variable j . We do not want this fraction to be too high, because this could make it hard to identify the robust correlation between variables, making the estimation of \mathbf{P} imprecise or even impossible. So we impose a maximal fraction of zero weights per column, which is 25% by default. In case this fraction is exceeded, the iteration stops and the code returns the results of the previous iteration step, together with a warning that it may be better to remove that variable.

The update formula (A.9) does not compute the generalized inverse of $\sum_{i=1}^n (w_{(k)})_{ij}$ because it is strictly positive under the same condition. If $\sum_{i=1}^n (w_{(k)})_{ij}$ were zero this would mean all cells x_{ij} of variable j received zero weight.

D Proof of Proposition 1

In this section Proposition 1 is proved, which ensures that each step of the algorithm decreases the objective function (5). In order to prove Proposition 1 we need three lemmas.

Lemma 1. *For a given weight matrix $\mathbf{W}_{(k)}$, each of the update steps (a), (b), and (c) of the algorithm in Section B decreases the weighted PCA objective function (16).*

Proof. The objective function (16) we want to minimize is

$$\sum_{i=1}^n \sum_{j=1}^p w_{ij} (x_{ij} - \mu_j - (\mathbf{U}\mathbf{V}^T)_{ij})^2 \quad (\text{A.10})$$

where $x_{ij} = W_{(k)ij}$ is fixed. We start from the triplet $(\mathbf{V}_{(k)}, \mathbf{U}_{(k)}, \boldsymbol{\mu}_{(k)})$ with objective

$$\sum_{i=1}^n \sum_{j=1}^p w_{ij} (x_{ij} - (\boldsymbol{\mu}_{(k)})_j - (\mathbf{U}_{(k)} \mathbf{V}_{(k)}^T)_{ij})^2. \quad (\text{A.11})$$

Step (a) minimizes the squared norm (A.2), which after summing over $j = 1, \dots, p$ becomes the objective (16) in the new triplet $(\mathbf{V}_{(k+1)}, \mathbf{U}_{(k)}, \boldsymbol{\mu}_{(k)})$.

Next, step (b) minimizes the squared norm (A.5), which after summing over $i = 1, \dots, n$ becomes the objective (16) in the new triplet $(\mathbf{V}_{(k+1)}, \mathbf{U}_{(k+1)}, \boldsymbol{\mu}_{(k)})$.

Finally, step (c) minimizes the squared norm (A.8), whose sum over $j = 1, \dots, p$ is the objective (16) in the new triplet $(\mathbf{V}_{(k+1)}, \mathbf{U}_{(k+1)}, \boldsymbol{\mu}_{(k+1)})$. \square

We will denote a potential fit to (5) as $\boldsymbol{\theta} = \widehat{\mathbf{X}} = \mathbf{X}^0 \mathbf{P} + \boldsymbol{\mu}$ where the matrices have the appropriate dimensions. We introduce the notation $\mathbf{f}(\boldsymbol{\theta})$ for $\text{vec}((\mathbf{X} - \boldsymbol{\theta}) \odot (\mathbf{X} - \boldsymbol{\theta}))$ where $\text{vec}(\cdot)$ turns a matrix into a column vector. The vector $\mathbf{f}(\boldsymbol{\theta})$ has np entries, which are the values $(\mathbf{X}_{ij} - \boldsymbol{\theta}_{ij})^2$ for $i = 1, \dots, n$ and $j = 1, \dots, p$. We can then write the PCA objective function (5) as $L(\mathbf{f}(\boldsymbol{\theta})) := L_{\rho_1, \rho_2}(\mathbf{X}, \mathbf{V}, \mathbf{U}, \boldsymbol{\mu})$.

Lemma 2. *The function $\mathbf{f} \rightarrow L(\mathbf{f})$ is concave.*

Proof. We first show that the univariate function $h : \mathbb{R}_+ \rightarrow \mathbb{R}_+ : z \rightarrow \rho_{b,c}(\sqrt{z})$, in which $\rho_{b,c}$ is the wrapping ρ -function, is concave as suggested in Figure 2. Note that the derivative h' is continuous, and differentiable except in the points b^2 and c^2 . Its derivative $h''(z)$ is zero on the intervals $(0, b^2)$ and (c^2, ∞) , and on (b^2, c^2) we obtain

$$h''(z) = \frac{-z^{3/2}}{4} q_1 \tanh(q_2(c - \sqrt{z})) - \frac{q_1 q_2}{4z} \operatorname{sech}^2(q_2(c - \sqrt{z})) \leq 0.$$

Since the function $h'(z)$ is continuous and on each of the three open intervals its derivative $h''(z)$ is nonpositive, it is nonincreasing everywhere. Therefore h is concave.

By the definition of concavity of a multivariate function, we now need to prove that for any column vectors \mathbf{f}, \mathbf{g} in \mathbb{R}_+^{np} and any λ in $(0, 1)$ it holds that $L(\lambda \mathbf{f} + (1 - \lambda) \mathbf{g}) \geq \lambda L(\mathbf{f}) + (1 - \lambda) L(\mathbf{g})$. This works out as

$$\begin{aligned} L(\lambda \mathbf{f} + (1 - \lambda) \mathbf{g}) &= \\ \frac{\widehat{\sigma}_2^2}{m} \sum_{i=1}^n h_2 \left(\frac{1}{m_i \widehat{\sigma}_2^2} \sum_{j=1}^p m_{ij} \widehat{\sigma}_{1,j}^2 h_1 \left(\frac{\lambda f_{ij} + (1 - \lambda) g_{ij}}{\widehat{\sigma}_{1,j}^2} \right) \right) &\geq \\ \frac{\widehat{\sigma}_2^2}{m} \sum_{i=1}^n h_2 \left(\frac{1}{m_i \widehat{\sigma}_2^2} \sum_{j=1}^p m_{ij} \widehat{\sigma}_{1,j}^2 [\lambda h_1(f_{ij}/\widehat{\sigma}_{1,j}^2) + (1 - \lambda) h_1(g_{ij}/\widehat{\sigma}_{1,j}^2)] \right) &= \\ \frac{\widehat{\sigma}_2^2}{m} \sum_{i=1}^n h_2 \left(\lambda \frac{1}{m_i \widehat{\sigma}_2^2} \sum_{j=1}^p m_{ij} \widehat{\sigma}_{1,j}^2 h_1(f_{ij}/\widehat{\sigma}_{1,j}^2) + (1 - \lambda) \frac{1}{m_i \widehat{\sigma}_2^2} \sum_{j=1}^p m_{ij} \widehat{\sigma}_{1,j}^2 h_1(g_{ij}/\widehat{\sigma}_{1,j}^2) \right) &\geq \\ \frac{\widehat{\sigma}_2^2}{m} \sum_{i=1}^n \left[\lambda h_2 \left(\frac{1}{m_i \widehat{\sigma}_2^2} \sum_{j=1}^p m_{ij} \widehat{\sigma}_{1,j}^2 h_1(f_{ij}/\widehat{\sigma}_{1,j}^2) \right) \right. & \\ \left. + (1 - \lambda) h_2 \left(\frac{1}{m_i \widehat{\sigma}_2^2} \sum_{j=1}^p m_{ij} \widehat{\sigma}_{1,j}^2 h_1(g_{ij}/\widehat{\sigma}_{1,j}^2) \right) \right] &= \\ \lambda L(\mathbf{f}) + (1 - \lambda) L(\mathbf{g}). & \end{aligned}$$

The first inequality derives from the concavity of h_1 and the fact that h_2 is nondecreasing. The second inequality is due to the concavity of h_2 . Therefore L is a concave function. \square

We can also write the weighted PCA objective (16) as a function of \mathbf{f} . We will denote it as $L_{\mathbf{W}}(\mathbf{f}) := (\operatorname{vec}(\mathbf{W}))^T \mathbf{f}$, so \mathbf{W} was turned into a vector in the same way as was done to obtain the column vector \mathbf{f} . The next lemma makes a connection between the weighted PCA objective $L_{\mathbf{W}}$ and the original objective L .

Lemma 3. *If two column vectors \mathbf{f}, \mathbf{g} in \mathbb{R}_+^{np} satisfy $L_{\mathbf{W}}(\mathbf{f}) \leq L_{\mathbf{W}}(\mathbf{g})$, then $L(\mathbf{f}) \leq L(\mathbf{g})$.*

Proof. From Lemma 2 we know that $L(\mathbf{f})$ is concave as a function of \mathbf{f} , and it is also differentiable because h_1 and h_2 are. Therefore

$$L(\mathbf{f}) \leq L(\mathbf{g}) + (\nabla L(\mathbf{g}))^T(\mathbf{f} - \mathbf{g})$$

where the column vector $\nabla L(\mathbf{g})$ is the gradient of L in \mathbf{g} . But $\nabla L(\mathbf{g})$ is proportional to $\nabla L_{\mathbf{W}}(\mathbf{g})$ which equals $\text{vec}(\mathbf{W})$ by construction, so $(\nabla L(\mathbf{g}))^T(\mathbf{f} - \mathbf{g})$ is proportional to $L_{\mathbf{W}}(\mathbf{f}) - L_{\mathbf{W}}(\mathbf{g}) \leq 0$. Therefore $L(\mathbf{f}) \leq L(\mathbf{g})$. \square

With this preparation we can prove Proposition 1.

Proof of Proposition 1. When we go from $\boldsymbol{\theta}_{(k)}$ to $\boldsymbol{\theta}_{(k+1)}$, Lemma 1 ensures that $L_{\mathbf{W}_{(k)}}(\mathbf{f}(\boldsymbol{\theta}_{(k+1)})) \leq L_{\mathbf{W}_{(k)}}(\mathbf{f}(\boldsymbol{\theta}_{(k)}))$, so Lemma 3 implies $L(\mathbf{f}(\boldsymbol{\theta}_{(k+1)})) \leq L(\mathbf{f}(\boldsymbol{\theta}_{(k)}))$. \square

E Proofs of influence functions

We consider the contamination model of Alqallaf et al. (2009), given by

$$\mathbf{X}_\varepsilon = (\mathbf{I}_p - \mathbf{B})\mathbf{X} + \mathbf{B}\mathbf{z} \tag{A.12}$$

where $\mathbf{z} = (z_1, \dots, z_p)$ is a fixed p -variate vector. The diagonal matrix \mathbf{B} equals $\text{diag}(B_1, B_2, \dots, B_p)$ where (B_1, B_2, \dots, B_p) follows the p -variate distribution G_ε . Its marginals B_1, \dots, B_p are Bernoulli random variables with success parameter ε , and (B_1, B_2, \dots, B_p) and \mathbf{X} are independent.

Under both the dependent and independent contamination models it holds that G_ε satisfies (i) $P(B_i = 1) = \varepsilon$, $i = 1, \dots, p$, and (ii) for any sequence (j_1, j_2, \dots, j_p) of zeroes and ones with $p - k$ zeroes and k ones $P(B_1 = j_1, \dots, B_p = j_p)$ has the same value, denoted as $\delta_k(\varepsilon)$. Under the fully dependent contamination model (FDCM) $P(B_1 = \dots = B_p) = 1$, and then $\delta_0(\varepsilon) = (1 - \varepsilon)$, $\delta_1(\varepsilon) = \dots = \delta_{p-1}(\varepsilon) = 0$, and $\delta_p(\varepsilon) = \varepsilon$. In that situation the distribution of \mathbf{X}_ε simplifies to $(1 - \varepsilon)H_0 + \varepsilon\Delta_{\mathbf{z}}$ where $\Delta_{\mathbf{z}}$ is the distribution which puts all of its mass in the point \mathbf{z} . The fully independent contamination model (FICM) instead assumes that B_1, \dots, B_p are independent, hence

$$\delta_k(\varepsilon) = \binom{p}{k} (1 - \varepsilon)^{p-k} \varepsilon^k, \quad k = 0, 1, \dots, p.$$

G_ε is denoted as G_ε^D in the dependent model, and as G_ε^I in the independent model.

The proof of Proposition 2 is based on the implicit function theorem, see e.g. Rio Branco de Oliveira (2012):

Theorem 1 (Implicit Function Theorem). *Let $\mathbf{f}(x, \boldsymbol{\theta}) = (f_1, \dots, f_p)$ be a function from $\mathbb{R} \times \mathbb{R}^p$ to \mathbb{R}^p that is continuous in $(x_0, \tilde{\boldsymbol{\theta}}) \in \mathbb{R} \times \mathbb{R}^p$ with $\mathbf{f}(x_0, \tilde{\boldsymbol{\theta}}) = \mathbf{0}$. Suppose the derivative of \mathbf{f} exists in a neighbourhood N of $(x_0, \tilde{\boldsymbol{\theta}})$ and is continuous at $(x_0, \tilde{\boldsymbol{\theta}})$, and that the derivative matrix $\partial \mathbf{f} / \partial \boldsymbol{\theta}$ is nonsingular at $(x_0, \tilde{\boldsymbol{\theta}})$. Then there are neighbourhoods N_1 of x_0 and N_p of $\tilde{\boldsymbol{\theta}}$ with $N_1 \times N_p \subset N$, such that for every x in N_1 there is a unique $\boldsymbol{\theta} = \mathbf{T}(x)$ in N_p for which $\mathbf{f}(x, \mathbf{T}(x)) = \mathbf{0}$. In addition, \mathbf{T} is differentiable in x_0 with derivative matrix given by*

$$\left. \frac{\partial \mathbf{T}(x)}{\partial x} \right|_{x=x_0} = - \left(\left. \frac{\partial \mathbf{f}(x_0, \boldsymbol{\theta})}{\partial \boldsymbol{\theta}} \right|_{\boldsymbol{\theta}=\tilde{\boldsymbol{\theta}}} \right)^{-1} \left. \frac{\partial \mathbf{f}(x, \tilde{\boldsymbol{\theta}})}{\partial x} \right|_{x=x_0}.$$

Proof of Proposition 2. From (23), the IF of \mathbf{P} at a distribution H_0 is defined as

$$\text{IF}_H(\mathbf{z}, \mathbf{P}) = \text{vec} \left(\left. \frac{\partial}{\partial \varepsilon} \mathbf{P}(H(G_\varepsilon, \mathbf{z})) \right|_{\varepsilon=0} \right).$$

For $\varepsilon = 0$ we obtain $\mathbf{P}(H(G_0, \mathbf{z})) = \mathbf{P}(H_0) = \mathbf{P}_0$. We can then parametrize $\mathbf{P}_0 = \mathbf{V}_0 \mathbf{V}_0^T$ where \mathbf{V}_0 has orthonormal columns, corresponding to an orthonormal basis of the linear subspace $\boldsymbol{\Pi}_0$. Note that \mathbf{V}_0 is not unique, but we will see later that different choices lead to the same influence function of \mathbf{P} . When the distribution H_0 is contaminated by FDCM or FICM to $H(G_\varepsilon, \mathbf{z})$ we define $\mathbf{V}(H(G_\varepsilon, \mathbf{z}))$ as the result of the algorithm of Section C above, translated from finite samples to population distributions and starting from \mathbf{V}_0 . This construction makes $\mathbf{V}(H(G_\varepsilon, \mathbf{z}))$ unique, and it has to satisfy the first-order condition (26) saying

$$E_H[\mathbf{W}_x(\mathbf{V} \mathbf{u}_x - \mathbf{x}) \mathbf{u}_x^T] = \mathbf{0} \quad (\text{A.13})$$

hence

$$\mathbf{g}(H(G_\varepsilon, \mathbf{z}), \mathbf{T}(\varepsilon), \boldsymbol{\sigma}(H(G_\varepsilon, \mathbf{z}))) = \text{vec} \left(E_{H(G_\varepsilon, \mathbf{z})} [\mathbf{W}_x(\mathbf{V} \mathbf{u}_x - \mathbf{x}) \mathbf{u}_x^T] \right) = \mathbf{0} \quad (\text{A.14})$$

where the pq -variate column vector \mathbf{g} is written as a function of the pq -variate column vector $\mathbf{T}(\varepsilon) := \text{vec}(\mathbf{V}(H(G_\varepsilon, \mathbf{z})))$. In order to compute $\text{vec} \left(\left. \frac{\partial}{\partial \varepsilon} \mathbf{V}(H(G_\varepsilon, \mathbf{z})) \right|_{\varepsilon=0} \right)$ we would like to apply the implicit function theorem in the point $\varepsilon = 0$, but the contaminated distribution

$H(G_\varepsilon, \mathbf{z})$ is only defined for $\varepsilon > 0$. To circumvent this issue we extend the definition of \mathbf{g} to negative ε by defining a function \mathbf{f} from $\mathbb{R} \times \mathbb{R}^{pq}$ to \mathbb{R}^{pq} as

$$\mathbf{f}(\varepsilon, \boldsymbol{\theta}) = \begin{cases} \mathbf{g}(H(G_\varepsilon, \mathbf{z}), \boldsymbol{\theta}, \boldsymbol{\sigma}(H(G_\varepsilon, \mathbf{z}))) & \text{for } \varepsilon \geq 0 \\ 2\mathbf{g}(H_0, \boldsymbol{\theta}, \boldsymbol{\sigma}(H_0)) - \mathbf{g}(H(|\varepsilon|, \mathbf{z}), \boldsymbol{\theta}, \boldsymbol{\sigma}(H(|\varepsilon|, \mathbf{z}))) & \text{for } \varepsilon < 0. \end{cases}$$

We now put $\varepsilon_0 = 0$ and $\tilde{\boldsymbol{\theta}} = \mathbf{T}(0) = \text{vec}(\mathbf{V}_0)$. Then $\mathbf{f}(\varepsilon_0, \boldsymbol{\theta}) = \mathbf{f}(0, \mathbf{T}(0)) = \mathbf{0}$, and assuming that \mathbf{g} is sufficiently smooth for the differentiability requirements of the implicit function theorem, we can conclude that $\mathbf{T}(\varepsilon)$ is uniquely defined for small ε and that

$$\begin{aligned} \left. \frac{\partial \mathbf{T}(\varepsilon)}{\partial \varepsilon} \right|_{\varepsilon=0} &= - \left(\left. \frac{\partial \mathbf{f}(0, \mathbf{T})}{\partial \mathbf{T}} \right|_{\mathbf{T}=\mathbf{T}(0)} \right)^{-1} \left. \frac{\partial \mathbf{f}(\varepsilon, \mathbf{T}(0))}{\partial \varepsilon} \right|_{\varepsilon=0} \\ &= - \left(\left. \frac{\partial \mathbf{g}(0, \mathbf{T})}{\partial \mathbf{T}} \right|_{\mathbf{T}=\mathbf{T}(0)} \right)^{-1} \left. \frac{\partial \mathbf{g}(\varepsilon, \mathbf{T}(0))}{\partial \varepsilon} \right|_{\varepsilon=0}. \end{aligned}$$

Note that the left hand side is $\text{vec} \left(\left. \frac{\partial}{\partial \varepsilon} \mathbf{V}(H(G_\varepsilon, \mathbf{z})) \right|_{\varepsilon=0} \right)$. We now have to work out the right hand side. For the first factor we denote the matrix

$$\mathbf{B} := \left. \frac{\partial \mathbf{g}(H_0, \mathbf{T}, \boldsymbol{\sigma}_0)}{\partial \mathbf{T}} \right|_{\mathbf{T}=\text{vec}(\mathbf{V}_0)}$$

which does not depend on \mathbf{z} and will be computed numerically in Section F. For the second factor, from (A.14) we know that $\mathbf{g}(H(G_\varepsilon, \mathbf{z}), \boldsymbol{\theta}_\varepsilon, \boldsymbol{\sigma}_\varepsilon)$ is an expectation over the mixture distribution $H(G_\varepsilon, \mathbf{z})$, so we can write \mathbf{g} as a linear combination with coefficients $\delta_k(\varepsilon)$ for $k = 0, 1, \dots, p$. For the FDCM model we know that G_ε^D has $\delta_0(\varepsilon) = (1 - \varepsilon)$, $\delta_1(\varepsilon) = \dots = \delta_{p-1}(\varepsilon) = 0$ and $\delta_p(\varepsilon) = \varepsilon$, so \mathbf{g} can be written as

$$\begin{aligned} &\mathbf{g}(H(G_\varepsilon^D, \mathbf{z}), \text{vec}(\mathbf{V}_0), \boldsymbol{\sigma}(H(G_\varepsilon^D, \mathbf{z}))) \\ &= \delta_0(\varepsilon) \mathbf{g}(H_0, \text{vec}(\mathbf{V}_0), \boldsymbol{\sigma}(H(G_\varepsilon^D, \mathbf{z}))) + \delta_p(\varepsilon) \mathbf{g}(H(G_\varepsilon^D, \mathbf{z}), \text{vec}(\mathbf{V}_0), \boldsymbol{\sigma}(H(G_\varepsilon^D, \mathbf{z}))) \\ &= (1 - \varepsilon) \mathbf{g}(H_0, \text{vec}(\mathbf{V}_0), \boldsymbol{\sigma}_\varepsilon) + \varepsilon \mathbf{g}(\Delta_{\mathbf{z}}, \text{vec}(\mathbf{V}_0), \boldsymbol{\sigma}_\varepsilon) \end{aligned}$$

which yields the derivative

$$\begin{aligned} &-\mathbf{g}(H_0, \text{vec}(\mathbf{V}_0), \boldsymbol{\sigma}_0) + \left. \frac{\partial \mathbf{g}}{\partial \varepsilon} \mathbf{g}(H_0, \text{vec}(\mathbf{V}_0), \boldsymbol{\sigma}_\varepsilon) \right|_{\varepsilon=0} + \mathbf{g}(\Delta_{\mathbf{z}}, \text{vec}(\mathbf{V}_0), \boldsymbol{\sigma}_0) \\ &= \mathbf{0} + \left. \frac{\partial \mathbf{g}}{\partial \boldsymbol{\sigma}}(H_0, \text{vec}(\mathbf{V}_0), \boldsymbol{\sigma}) \right|_{\boldsymbol{\sigma}=\boldsymbol{\sigma}_0} \left. \frac{\partial \boldsymbol{\sigma}_\varepsilon}{\partial \varepsilon} \right|_{\varepsilon=0} + \mathbf{g}(\Delta_{\mathbf{z}}, \text{vec}(\mathbf{V}_0), \boldsymbol{\sigma}_0) \\ &= \mathbf{S} \text{IF}_{FDCM}(\mathbf{z}, \boldsymbol{\sigma}) + \mathbf{g}(\Delta_{\mathbf{z}}, \text{vec}(\mathbf{V}_0), \boldsymbol{\sigma}_0) \end{aligned} \tag{A.15}$$

where $\mathbf{S} := \left. \frac{\partial}{\partial \boldsymbol{\sigma}} \mathbf{g}(H_0, \text{vec}(\mathbf{V}_0), \boldsymbol{\sigma}) \right|_{\boldsymbol{\sigma}=\boldsymbol{\sigma}_0}$ and $\text{IF}_{FDCM}(\mathbf{z}, \boldsymbol{\sigma})$ is the influence function of $\boldsymbol{\sigma}$ under FDCM.

Under the FICM model the second factor is different. We have $\delta_0(\varepsilon) = (1 - \varepsilon)^p$, $\delta_0(0) = 1$, $\delta_1(\varepsilon) = p(1 - \varepsilon)^{p-1}\varepsilon$ so $\delta_1(0) = 0$ and $\delta'_1(0) = p$, and $\delta_i(0) = \delta'_i(0) = 0$ for $i \geq 2$. Therefore \mathbf{g} can be written as the sum

$$\begin{aligned} \mathbf{g}(H(G_\varepsilon^I, \mathbf{z}), \mathbf{V}_0, \boldsymbol{\sigma}(H(G_\varepsilon^I, \mathbf{z}))) \\ &= \delta_0(\varepsilon)\mathbf{g}(H_0, \mathbf{V}_0, \boldsymbol{\sigma}(H(G_\varepsilon^I, \mathbf{z}))) + \delta_1(\varepsilon)\mathbf{g}(H(G_\varepsilon^I, \mathbf{z}), \mathbf{V}_0, \boldsymbol{\sigma}(H(G_\varepsilon^I, \mathbf{z}))) \\ &= (1 - \varepsilon)^p\mathbf{g}(H_0, \mathbf{V}_0, \boldsymbol{\sigma}_\varepsilon) + p(1 - \varepsilon)^{p-1}\varepsilon\mathbf{g}(H(G_\varepsilon^I, \mathbf{z}), \mathbf{V}_0, \boldsymbol{\sigma}(H(G_\varepsilon^I, \mathbf{z}))) \\ &= (1 - \varepsilon)^p\mathbf{g}(H_0, \mathbf{V}_0, \boldsymbol{\sigma}_\varepsilon) + p(1 - \varepsilon)^{p-1}\varepsilon \sum_{j=1}^p \mathbf{g}(H(G_\varepsilon^j, \mathbf{z}), \mathbf{V}_0, \boldsymbol{\sigma}(G_\varepsilon^j, \mathbf{z}))) \end{aligned}$$

where G_ε^j is the distribution of $(0, \dots, B_j, \dots, 0)$ with only the j -th Bernoulli(ε) component and all other components zero. The derivative now becomes

$$\mathbf{S} \text{IF}_{FICM}(\mathbf{z}, \boldsymbol{\sigma}) + p \sum_{j=1}^p \mathbf{g}(H(G_1^j, \mathbf{z}), \mathbf{V}_0, \boldsymbol{\sigma}_0) \quad (\text{A.16})$$

where \mathbf{S} is the same as before but $\text{IF}_{FICM}(\mathbf{z}, \boldsymbol{\sigma})$ is now the cellwise influence function of $\boldsymbol{\sigma}$. Note that $H(G_1^j, \mathbf{z})$ is the distribution of $\mathbf{X} \sim H_0$ but with its j -th component fixed at the constant z_j . It is thus a degenerate distribution concentrated on the hyperplane $X_j = z_j$.

Now that we have an expression for $\frac{\partial}{\partial \varepsilon} \mathbf{V}(H(G_\varepsilon, \mathbf{z}))$ we can use it to derive the IF of \mathbf{P} . Note that the columns of \mathbf{V}_0 were orthonormal, but the columns of $\mathbf{V}(H(G_\varepsilon, \mathbf{z}))$ do not have to be. Therefore the projection matrix $\mathbf{P}(H(G_\varepsilon, \mathbf{z}))$ is given by

$$\mathbf{P}(H(G_\varepsilon, \mathbf{z})) = \mathbf{V}(H(G_\varepsilon, \mathbf{z}))(\mathbf{V}(H(G_\varepsilon, \mathbf{z}))^T \mathbf{V}(H(G_\varepsilon, \mathbf{z})))^{-1} \mathbf{V}(H(G_\varepsilon, \mathbf{z}))^T.$$

Differentiating yields

$$\begin{aligned} \frac{\partial}{\partial \varepsilon} \mathbf{P}(H(G_\varepsilon, \mathbf{z})) \Big|_{\varepsilon=0} &= \frac{\partial}{\partial \varepsilon} \mathbf{V}(H(G_\varepsilon, \mathbf{z}))(\mathbf{V}(H(G_\varepsilon, \mathbf{z}))^T \mathbf{V}(H(G_\varepsilon, \mathbf{z})))^{-1} \mathbf{V}(H(G_\varepsilon, \mathbf{z}))^T \Big|_{\varepsilon=0} \\ &= \frac{\partial}{\partial \varepsilon} \mathbf{V}(H(G_\varepsilon, \mathbf{z})) \Big|_{\varepsilon=0} (\mathbf{V}_0^T \mathbf{V}_0)^{-1} \mathbf{V}_0^T \\ &\quad - \mathbf{V}_0 (\mathbf{V}_0^T \mathbf{V}_0)^{-1} \frac{\partial}{\partial \varepsilon} \mathbf{V}(H(G_\varepsilon, \mathbf{z}))^T \Big|_{\varepsilon=0} \mathbf{V}_0 (\mathbf{V}_0^T \mathbf{V}_0)^{-1} \mathbf{V}_0^T \\ &\quad - \mathbf{V}_0 (\mathbf{V}_0^T \mathbf{V}_0)^{-1} \mathbf{V}_0^T \frac{\partial}{\partial \varepsilon} \mathbf{V}(H(G_\varepsilon, \mathbf{z})) \Big|_{\varepsilon=0} (\mathbf{V}_0^T \mathbf{V}_0)^{-1} \mathbf{V}_0^T \\ &\quad + \mathbf{V}_0 (\mathbf{V}_0^T \mathbf{V}_0)^{-1} \frac{\partial}{\partial \varepsilon} \mathbf{V}(H(G_\varepsilon, \mathbf{z}))^T \Big|_{\varepsilon=0} \end{aligned}$$

where the derivative of $(\mathbf{V}(H(G_\varepsilon, \mathbf{z}))^T \mathbf{V}(H(G_\varepsilon, \mathbf{z})))^{-1}$ comes from the identity $\frac{\partial \mathbf{Y}^{-1}}{\partial x} = -\mathbf{Y}^{-1} \frac{\partial \mathbf{Y}}{\partial x} \mathbf{Y}^{-1}$ (Magnus and Neudecker, 2019). Since $\mathbf{V}_0^T \mathbf{V}_0 = \mathbf{I}_q$ is the identity matrix and

$\mathbf{V}_0 \mathbf{V}_0^T = \mathbf{P}$, the expression simplifies to

$$\begin{aligned} \frac{\partial}{\partial \varepsilon} \mathbf{P}(H(G_\varepsilon, \mathbf{z})) \Big|_{\varepsilon=0} &= \frac{\partial}{\partial \varepsilon} \mathbf{V}(H(G_\varepsilon, \mathbf{z})) \Big|_{\varepsilon=0} \mathbf{V}_0^T - \mathbf{V}_0 \frac{\partial}{\partial \varepsilon} \mathbf{V}(H(G_\varepsilon, \mathbf{z}))^T \Big|_{\varepsilon=0} \mathbf{P}_0 \\ &\quad - \mathbf{P}_0 \frac{\partial}{\partial \varepsilon} \mathbf{V}(H(G_\varepsilon, \mathbf{z})) \Big|_{\varepsilon=0} \mathbf{V}_0^T + \mathbf{V}_0 \frac{\partial}{\partial \varepsilon} \mathbf{V}(H(G_\varepsilon, \mathbf{z}))^T \Big|_{\varepsilon=0} \\ &= (\mathbf{I}_p - \mathbf{P}_0) \frac{\partial}{\partial \varepsilon} \mathbf{V}(H(G_\varepsilon, \mathbf{z})) \Big|_{\varepsilon=0} \mathbf{V}_0^T + \mathbf{V}_0 \frac{\partial}{\partial \varepsilon} \mathbf{V}(H(G_\varepsilon, \mathbf{z}))^T \Big|_{\varepsilon=0} (\mathbf{I}_p - \mathbf{P}_0). \end{aligned} \quad (\text{A.17})$$

Since the second term is the transpose of the first we see that the derivative of $\mathbf{P}(H(G_\varepsilon, \mathbf{z}))$ is symmetric, as it should be.

Now suppose we had chosen a different orthonormal basis of $\mathbf{\Pi}_0$, corresponding to a matrix $\tilde{\mathbf{V}}_0$. We need to verify that this would yield the same result. First compute the $q \times q$ matrix $\mathbf{O} = (\tilde{\mathbf{V}}_0^{-1} \mathbf{V}_0)$. This matrix is orthogonal because $\mathbf{O}^T \mathbf{O} = \mathbf{V}_0^T (\tilde{\mathbf{V}}_0 \tilde{\mathbf{V}}_0^T)^{-1} \mathbf{V}_0 = \mathbf{V}_0^T \mathbf{V}_0 = \mathbf{I}_q$, and $\tilde{\mathbf{V}}_0 = \mathbf{V}_0 \mathbf{O}$. Then construct $\tilde{\mathbf{V}}(H(G_\varepsilon, \mathbf{z}))$ by running the algorithm starting from $\tilde{\mathbf{V}}_0$ instead of \mathbf{V}_0 . In Section C we saw that every step will have $\tilde{\mathbf{V}}_{(k+1)} = \mathbf{V}_{(k+1)} \mathbf{O}$, so this holds in the limit as well, hence $\tilde{\mathbf{V}}(H(G_\varepsilon, \mathbf{z})) = \mathbf{V}(H(G_\varepsilon, \mathbf{z})) \mathbf{O}$. Writing (A.17) with $\tilde{\mathbf{V}}(H(G_\varepsilon, \mathbf{z}))$ and $\tilde{\mathbf{V}}_0$ yields factors $\mathbf{O} \mathbf{O}^T$ that cancel, yielding (A.17) again.

Applying the vec operation to (A.17) gives the IF. Applying it to the first term yields

$$\text{vec} \left((\mathbf{I}_p - \mathbf{P}_0) \frac{\partial}{\partial \varepsilon} \mathbf{V}(H(G_\varepsilon, \mathbf{z})) \Big|_{\varepsilon=0} \mathbf{V}_0^T \right) = (\mathbf{V}_0 \otimes (\mathbf{I}_p - \mathbf{P}_0)) \text{vec} \left(\frac{\partial}{\partial \varepsilon} \mathbf{V}(H(G_\varepsilon, \mathbf{z})) \Big|_{\varepsilon=0} \right)$$

by the rule $\text{vec}(\mathbf{ABC}) = (\mathbf{C}^T \otimes \mathbf{A}) \text{vec}(\mathbf{B})$. For the second term we find

$$\text{vec} \left(\mathbf{V}_0 \frac{\partial}{\partial \varepsilon} \mathbf{V}(H(G_\varepsilon, \mathbf{z}))^T \Big|_{\varepsilon=0} (\mathbf{I}_p - \mathbf{P}_0) \right) = ((\mathbf{I}_p - \mathbf{P}_0) \otimes \mathbf{V}_0) \text{vec} \left(\left(\frac{\partial}{\partial \varepsilon} \mathbf{V}(H(G_\varepsilon, \mathbf{z})) \Big|_{\varepsilon=0} \right)^T \right)$$

by the same rule. The last factor is the vec of a transposed matrix, which can be written as

$$\text{vec} \left(\left(\frac{\partial}{\partial \varepsilon} \mathbf{V}(H(G_\varepsilon, \mathbf{z})) \Big|_{\varepsilon=0} \right)^T \right) = \mathbf{K}_{p,q} \text{vec} \left(\frac{\partial}{\partial \varepsilon} \mathbf{V}(H(G_\varepsilon, \mathbf{z})) \Big|_{\varepsilon=0} \right)$$

where $\mathbf{K}_{p,q}$ is a $pq \times pq$ permutation matrix that rearranges the entries of the column vector $\text{vec}(\frac{\partial}{\partial \varepsilon} \mathbf{V}(H(G_\varepsilon, \mathbf{z})) \Big|_{\varepsilon=0})$ to become those of $\text{vec}(\frac{\partial}{\partial \varepsilon} \mathbf{V}(H(G_\varepsilon, \mathbf{z}))^T \Big|_{\varepsilon=0})$. In all we can write

$$\text{vec} \left(\frac{\partial}{\partial \varepsilon} \mathbf{P}(H(G_\varepsilon, \mathbf{z})) \Big|_{\varepsilon=0} \right) = \mathbf{R}_0 \text{vec} \left(\frac{\partial}{\partial \varepsilon} \mathbf{V}(H(G_\varepsilon, \mathbf{z})) \Big|_{\varepsilon=0} \right) \quad (\text{A.18})$$

where \mathbf{R}_0 is the $p^2 \times pq$ matrix

$$\mathbf{R}_0 = \mathbf{V}_0 \otimes (\mathbf{I}_p - \mathbf{P}_0) + ((\mathbf{I}_p - \mathbf{P}_0) \otimes \mathbf{V}_0) \mathbf{K}_{(p,q)}. \quad (\text{A.19})$$

Combining (A.15) with $\mathbf{D} := \mathbf{R}_0 \mathbf{B}^{-1}$ yields (29), and left multiplying (A.16) by \mathbf{D} yields (30). \square

Proof of Proposition 3. For each $k = 1, \dots, pq$, call $\ddot{\Psi}_k = \frac{\partial^2 \Psi_k}{\partial \text{vec}(\mathbf{V}) \partial \text{vec}(\mathbf{V})}$ the matrix of second derivatives of Ψ_k with respect to the entries of \mathbf{V} , and $\mathbf{C}_n(\mathbf{x}, \mathbf{V})$ the matrix with k th row equal to $\text{vec}(\widehat{\mathbf{V}}_n - \mathbf{V}(H))^T \ddot{\Psi}_k(\mathbf{x}, \mathbf{V})$. A Taylor expansion yields

$$\mathbf{0} = \widehat{\Lambda}_n(\widehat{\mathbf{V}}_n) = \frac{1}{n} \sum_{i=1}^n \left\{ \Psi(\mathbf{x}_i, \mathbf{V}(H)) + \dot{\Psi}(\mathbf{x}_i, \mathbf{V}(H)) \text{vec}(\widehat{\mathbf{V}}_n - \mathbf{V}(H)) + \frac{1}{2} \mathbf{C}_n(\mathbf{x}_i, \mathbf{V}(H)) \text{vec}(\widehat{\mathbf{V}}_n - \mathbf{V}(H)) \right\}.$$

In other words

$$\mathbf{0} = \mathbf{A}_n + (\mathbf{B}_n + \overline{\mathbf{C}}_n) \text{vec}(\widehat{\mathbf{V}}_n - \mathbf{V}(H)) \quad (\text{A.20})$$

with

$$\mathbf{A}_n = \frac{1}{n} \sum_{i=1}^n \Psi(\mathbf{x}_i, \mathbf{V}(H)), \quad \mathbf{B}_n = \frac{1}{n} \sum_{i=1}^n \dot{\Psi}(\mathbf{x}_i, \mathbf{V}(H)), \quad \overline{\mathbf{C}}_n = \frac{1}{2n} \sum_{i=1}^n \mathbf{C}_n(\mathbf{x}_i, \mathbf{V}(H)).$$

The k th row of the matrix $\overline{\mathbf{C}}_n$ equals $\text{vec}(\widehat{\mathbf{V}}_n - \mathbf{V}(H))^T \overline{\ddot{\Psi}}_k$ where

$$\overline{\ddot{\Psi}}_k = \frac{1}{n} \sum_{i=1}^n \ddot{\Psi}_k(\mathbf{x}_i, \mathbf{V}(H))$$

which is bounded. Since $\widehat{\mathbf{V}}_n \rightarrow \mathbf{V}(H)$ in probability, this implies that $\overline{\mathbf{C}}_n \rightarrow \mathbf{0}$ in probability.

Note that for $i = 1, 2, \dots$ the vectors $\Psi(\mathbf{x}_i, \mathbf{V}(H))$ are i.i.d. with mean $\mathbf{0}$ (since $\Lambda(\mathbf{V}(H)) = \mathbf{0}$) and covariance matrix \mathbf{A} , where $\mathbf{A} = \text{E}_H[\Psi(\mathbf{x}, \mathbf{V}(H))\Psi(\mathbf{x}, \mathbf{V}(H))^T]$, and the matrices $\dot{\Psi}(\mathbf{x}_i, \mathbf{V}(H))$ are i.i.d. with mean \mathbf{B} , where $\mathbf{B} = \text{E}_H[\dot{\Psi}(\mathbf{x}, \mathbf{V}(H))]$. Hence when $n \rightarrow \infty$, the law of large numbers implies $\mathbf{B}_n \rightarrow \mathbf{B}$ in probability, which implies $\mathbf{B}_n + \overline{\mathbf{C}}_n \rightarrow \mathbf{B}$ in probability, and we assume that \mathbf{B} is nonsingular. The central limit theorem implies $\sqrt{n}\mathbf{A}_n \rightarrow N_p(\mathbf{0}, \mathbf{A})$ in distribution. Then from (A.20) and Slutsky's lemma we have that

$$\sqrt{n} \text{vec}(\widehat{\mathbf{V}}_n - \mathbf{V}(H)) \rightarrow_d N_{pq}(\mathbf{0}, \mathbf{B}^{-1} \mathbf{A} (\mathbf{B}^{-1})^T).$$

From $\widehat{\mathbf{V}}_n \rightarrow \mathbf{V}(H)$ in probability it follows that $\widehat{\mathbf{P}}_n \rightarrow \mathbf{P}(H)$ in probability. Consider the differentiable mapping $\mathbf{h}(\mathbf{M}) = \mathbf{M}(\mathbf{M}^T \mathbf{M})^{-1} \mathbf{M}^T$ on the set of $p \times q$ matrices \mathbf{M} of rank q . From the multivariate delta method, see e.g. Casella and Berger (2002), it follows that

$$\sqrt{n} \text{vec}(\mathbf{h}(\widehat{\mathbf{V}}_n) - \mathbf{h}(\mathbf{V}(H))) \rightarrow_d N_{p^2}(\mathbf{0}, \mathbf{R}_0 \mathbf{B}^{-1} \mathbf{A} \mathbf{B}^{-T} \mathbf{R}_0^T)$$

where $\mathbf{R}_0 = \frac{\partial \text{vec}(\mathbf{h}(\mathbf{V}))}{\partial \text{vec}(\mathbf{V})} \Big|_{\mathbf{V}=\text{vec}(\mathbf{V}(H))}$ was defined in (A.19). Moreover $\mathbf{R}_0 \mathbf{B}^{-1} \mathbf{A} \mathbf{B}^{-T} \mathbf{R}_0^T = \Theta$ because $\text{IF}_{FDCM}(\mathbf{x}, \mathbf{P}) = \mathbf{R}_0 \mathbf{B}^{-1} \Psi(\mathbf{x}, \mathbf{V}(H))$ by Proposition 2 with fixed $\boldsymbol{\sigma}$. Since $\text{IF}_{FDCM}(\mathbf{x}, \mathbf{P})$ does not depend on the parametrization of \mathbf{P} , neither does $\Theta = E_H[\text{IF}_{FDCM}(\mathbf{x}, \mathbf{P}) \text{IF}_{FDCM}(\mathbf{x}, \mathbf{P})^T]$. \square

F Derivation of \mathbf{B} and \mathbf{S}

We now compute the $pq \times pq$ matrix $\mathbf{B} = \frac{\partial}{\partial \text{vec}(\mathbf{V})} g(H_0, \text{vec}(\mathbf{V}), \boldsymbol{\sigma}_0) \Big|_{\text{vec}(\mathbf{V})=\text{vec}(\mathbf{V}(H))}$ and the $pq \times (p+1)$ matrix $\mathbf{S} = \frac{\partial}{\partial \boldsymbol{\sigma}} g(H_0, \text{vec}(\mathbf{V}(H)), \boldsymbol{\sigma}) \Big|_{\boldsymbol{\sigma}=\boldsymbol{\sigma}_0}$.

Recall that $\boldsymbol{\mu}$ is known and equal to $\mathbf{0}$. Then

$$w_j^c = \psi_1 \left(\frac{r_j}{\sigma_{1,j}} \right) / \frac{r_j}{\sigma_{1,j}} \quad r_j := x_j - \mathbf{v}_j^T \mathbf{u}_x \quad j = 1, \dots, p$$

and

$$w^r = \psi_2 \left(\frac{t}{\sigma_2} \right) / \frac{t}{\sigma_2} \quad t := \sqrt{\frac{1}{p} \sum_{j=1}^p \sigma_{1,j}^2 \rho_1 \left(\frac{r_j}{\sigma_{1,j}} \right)}.$$

For $j, l = 1, \dots, p$ and $k, m = 1, \dots, q$, we have that

$$-\frac{\partial}{\partial v_{lm}} E_{H_0} [w_j (x_j - \mathbf{v}_j^T \mathbf{u}_x) u_{x,k}] = -E_{H_0} \left[\frac{\partial w_j}{\partial v_{lm}} r_j u_{x,k} + w_j \frac{\partial r_j}{\partial v_{lm}} u_{x,k} + w_j r_j \frac{\partial u_{x,k}}{\partial v_{lm}} \right]$$

where

$$\frac{\partial r_j}{\partial v_{lm}} = - \left(\frac{\partial \mathbf{v}_j^T}{\partial v_{lm}} \mathbf{u}_x + \mathbf{v}_j^T \frac{\partial \mathbf{u}_x}{\partial v_{lm}} \right) = - \left(\delta_{j=l} u_{x,m} + \mathbf{v}_j^T \frac{\partial \mathbf{u}_x}{\partial v_{lm}} \right)$$

and $\delta_{j=l}$ is the Kronecker delta. Then

$$\begin{aligned} \frac{\partial w_j^c}{\partial v_{lm}} &= \left(\frac{\psi_1'(r_j/\sigma_{1,j})}{\sigma_{1,j}} \left(\frac{\partial r_j}{\partial v_{lm}} \right) \frac{r_j}{\sigma_{1,j}} - \frac{\psi_1(r_j/\sigma_{1,j})}{\sigma_{1,j}} \left(\frac{\partial r_j}{\partial v_{lm}} \right) \right) / \frac{r_j^2}{\sigma_{1,j}^2} \\ &= \frac{\psi_1'(r_j/\sigma_{1,j})}{r_j} \left(\frac{\partial r_j}{\partial v_{lm}} \right) - \frac{\sigma_{1,j} \psi_1(r_j/\sigma_{1,j})}{r_j^2} \left(\frac{\partial r_j}{\partial v_{lm}} \right) \\ &= w_j^c \left(\frac{\partial r_j}{\partial v_{lm}} \right) \end{aligned}$$

where $w_j^c = \psi_1'(r_j/\sigma_{1,j})/r_j - \sigma_{1,j} \psi_1(r_j/\sigma_{1,j})/r_j^2$. Moreover

$$\begin{aligned} \frac{\partial w^r}{\partial v_{lm}} &= \left(\frac{\psi_2'(t/\sigma_2)}{\sigma_2} \frac{\partial t}{\partial v_{lm}} \frac{t}{\sigma_2} - \frac{\psi_2(t/\sigma_2)}{\sigma_2} \frac{\partial t}{\partial v_{lm}} \right) / \frac{t^2}{\sigma_2^2} \\ &= \left(\frac{\psi_2'(t/\sigma_2)}{t} - \frac{\sigma_2 \psi_2(t/\sigma_2)}{t^2} \right) \frac{\partial t}{\partial v_{lm}} \\ &= w^r \frac{\partial t}{\partial v_{lm}} \end{aligned}$$

where $w^r = \psi'_2(t/\sigma_2)/r - \sigma_2\psi_2(t/\sigma_2)/t^2$ and

$$\begin{aligned}\frac{\partial t}{\partial v_{lm}} &= \frac{1}{2pt} \sum_{s=1}^p \sigma_{1,s} \psi_1(r_s/\sigma_{1,s}) \left(\frac{\partial r_s}{\partial v_{lm}} \right) \\ &= \frac{1}{2pt} \sum_{s=1}^p w_s^c r_s \left(\frac{\partial r_s}{\partial v_{lm}} \right).\end{aligned}$$

Then

$$\begin{aligned}\frac{\partial w_j}{\partial v_{lm}} &= \frac{\partial w_j^c}{\partial v_{lm}} w_r + w_j^c \frac{\partial w_r}{\partial v_{lm}} \\ &= w_r w_j^c \left(\frac{\partial r_j}{\partial v_{lm}} \right) + w_j^c w^r \frac{1}{2pt} \sum_{s=1}^p w_s^c r_s \left(\frac{\partial r_s}{\partial v_{lm}} \right) \\ &= \sum_{s=1}^p \left(\frac{w_j^c w^r w_s^c r_s}{2pt} + \delta_{s=j} w_r w_j^c \right) \left(\frac{\partial r_s}{\partial v_{lm}} \right).\end{aligned}$$

Then $\mathbf{B}(H_0, \text{vec}(\mathbf{V}(H)), \boldsymbol{\sigma}_0)$ is obtained from

$$\mathbf{B}(H_0, \text{vec}(\mathbf{V}(H)), \boldsymbol{\sigma}_0) = \{B_{\tilde{k}\tilde{m}}(H_0, \text{vec}(\mathbf{V}(H)), \boldsymbol{\sigma}_0)\},$$

where $B_{\tilde{k}\tilde{m}}(H_0, \text{vec}(\mathbf{V}(H)), \boldsymbol{\sigma}_0) = -\frac{\partial}{\partial v_{lm}} \mathbb{E}_{H_0} [w_j(x_j - \mathbf{v}_j^T \mathbf{u}_x) u_{x,k}] \Big|_{\text{vec}(\mathbf{V})=\text{vec}(\mathbf{V}(H))}$ with $\tilde{k} = (k-1)p + j$ and $\tilde{m} = (m-1)p + l$. Note that $\frac{\partial \mathbf{u}_x}{\partial v_{lm}}$ does not have a closed form, so it has to be computed numerically.

For $\mathbf{S}(H_0, \text{vec}(\mathbf{V}(H)), \boldsymbol{\sigma}_0)$ we compute

$$-\frac{\partial}{\partial \sigma_{1,j}} \mathbb{E}_{H_0} [w_j(x_j - \mathbf{v}_j^T \mathbf{u}_x) u_{x,k}] = -\mathbb{E}_{H_0} \left[\frac{\partial w_j}{\partial \sigma_{1,j}} r_j u_{x,k} + w_j \frac{\partial r_j}{\partial \sigma_{1,j}} u_{x,k} + w_j r_j \frac{\partial u_{x,k}}{\partial \sigma_{1,j}} \right]$$

where

$$\frac{\partial r_j}{\partial \sigma_{1,j}} = -\mathbf{v}_j^T \frac{\partial \mathbf{u}_x}{\partial \sigma_{1,j}}.$$

Then

$$\begin{aligned}\frac{\partial w_j^c}{\partial \sigma_{1,j}} &= \left(\psi'_1(r_j/\sigma_{1,j}) \frac{\partial r_j/\sigma_{1,j}}{\partial \sigma_{1,j}} \frac{r_j}{\sigma_{1,j}} - \psi_1(r_j/\sigma_{1,j}) \frac{\partial r_j/\sigma_{1,j}}{\partial \sigma_{1,j}} \right) / \frac{r_j^2}{\sigma_{1,j}^2} \\ &= \left(\frac{\psi'_1(r_j/\sigma_{1,j})}{r_j} \sigma_{1,j} \frac{\partial r_j/\sigma_{1,j}}{\partial \sigma_{1,j}} - \sigma_{1,j}^2 \frac{\psi_1(r_j/\sigma_{1,j})}{r_j^2} \frac{\partial r_j/\sigma_{1,j}}{\partial \sigma_{1,j}} \right) \\ &= \sigma_{1,j} w_j^c \frac{\partial r_j/\sigma_{1,j}}{\partial \sigma_{1,j}}.\end{aligned}$$

Moreover,

$$\begin{aligned}
\frac{\partial w^r}{\partial \sigma_{1,j}} &= \left(\frac{\psi_2'(t/\sigma_2)}{\sigma_2} \frac{\partial t}{\partial \sigma_{1,j}} \frac{t}{\sigma_2} - \frac{\psi_2(t/\sigma_2)}{\sigma_2} \frac{\partial t}{\partial \sigma_{1,j}} \right) / \frac{t^2}{\sigma_2^2} \\
&= \left(\frac{\psi_2'(t/\sigma_2)}{t} - \frac{\sigma_2 \psi_2(t/\sigma_2)}{t^2} \right) \frac{\partial t}{\partial \sigma_{1,j}} \\
&= w^r \frac{\partial t}{\partial \sigma_{1,j}}
\end{aligned}$$

where

$$\begin{aligned}
\frac{\partial t}{\partial \sigma_{1,j}} &= \frac{1}{2pt} \sum_{s=1}^p \left[\delta_{s=j} 2\sigma_{1,j} \rho_1 \left(\frac{r_j}{\sigma_{1,j}} \right) + \sigma_{1,s}^2 \psi_1 \left(\frac{r_s}{\sigma_{1,s}} \right) \frac{\partial r_s / \sigma_{1,s}}{\partial \sigma_{1,j}} \right] \\
&= \frac{1}{2pt} \sum_{s=1}^p \left[\delta_{s=j} 2\sigma_{1,j} \rho_1 \left(\frac{r_j}{\sigma_{1,j}} \right) + \sigma_{1,s} r_s w_s^c \frac{\partial r_s / \sigma_{1,s}}{\partial \sigma_{1,j}} \right],
\end{aligned}$$

and

$$\frac{\partial r_s / \sigma_{1,s}}{\partial \sigma_{1,j}} = \frac{\partial r_s}{\partial \sigma_{1,j}} \frac{1}{\sigma_{1,s}} - \delta_{s=j} \frac{r_j}{\sigma_{1,j}^2}.$$

Then

$$\begin{aligned}
\frac{\partial w_j}{\partial \sigma_{1,j}} &= \frac{\partial w_j^c}{\partial \sigma_{1,j}} w_r + w_j^c \frac{\partial w_r}{\partial \sigma_{1,j}} \\
&= w_r \sigma_{1,j} w_j^{tc} \frac{\partial r_j / \sigma_{1,j}}{\partial \sigma_{1,j}} + \frac{w_j^c w^r}{2pt} \sum_{s=1}^p \left[\delta_{s=j} 2\sigma_{1,j} \rho_1 \left(\frac{r_j}{\sigma_{1,j}} \right) + \sigma_{1,s} r_s w_s^c \frac{\partial r_s / \sigma_{1,s}}{\partial \sigma_{1,j}} \right].
\end{aligned}$$

Moreover,

$$-\frac{\partial}{\partial \sigma_2} \mathbb{E}_{H_0} [w_j(x_j - \mathbf{v}_j^T \mathbf{u}_x) u_{x,k}] = -\mathbb{E}_{H_0} \left[\frac{\partial w_j}{\partial \sigma_2} r_j u_{x,k} + w_j \frac{\partial r_j}{\partial \sigma_2} u_{x,k} + w_j r_j \frac{\partial u_{x,k}}{\partial \sigma_2} \right]$$

where

$$\frac{\partial r_j}{\partial \sigma_2} = -\mathbf{v}_j^T \frac{\partial \mathbf{u}_x}{\partial \sigma_2}.$$

Then

$$\begin{aligned}
\frac{\partial w_j^c}{\partial \sigma_2} &= \left(\psi_1'(r_j / \sigma_{1,j}) \frac{\partial r_j}{\partial \sigma_2} \frac{r_j}{\sigma_{1,j}^2} - \frac{\psi_1(r_j / \sigma_{1,j})}{\sigma_{1,j}} \frac{\partial r_j}{\partial \sigma_2} \right) / \frac{r_j^2}{\sigma_{1,j}^2} \\
&= \left(\frac{\psi_1'(r_j / \sigma_{1,j})}{r_j} \frac{\partial r_j}{\partial \sigma_2} - \sigma_{1,j} \frac{\psi_1(r_j / \sigma_{1,j})}{r_j^2} \frac{\partial r_j}{\partial \sigma_2} \right) \\
&= w_j^{tc} \frac{\partial r_j}{\partial \sigma_2}.
\end{aligned}$$

Moreover,

$$\begin{aligned}
\frac{\partial w^r}{\partial \sigma_2} &= \left(\psi_2'(t/\sigma_2) \frac{\partial t/\sigma_2}{\partial \sigma_2} \frac{t}{\sigma_2} - \psi_2(t/\sigma_2) \frac{\partial t/\sigma_2}{\partial \sigma_2} \right) / \frac{t^2}{\sigma_2^2} \\
&= \left(\sigma_2 \frac{\psi_2'(t/\sigma_2)}{t} - \sigma_2^2 \frac{\psi_2(t/\sigma_2)}{t^2} \right) \frac{\partial t/\sigma_2}{\partial \sigma_2} \\
&= \sigma_2 w'^r \frac{\partial t/\sigma_2}{\partial \sigma_2}
\end{aligned}$$

where

$$\frac{\partial t/\sigma_2}{\partial \sigma_2} = \frac{\partial t}{\partial \sigma_2} \frac{1}{\sigma_2} - \frac{t}{\sigma_2^2}$$

and

$$\begin{aligned}
\frac{\partial t}{\partial \sigma_2} &= \frac{1}{2pt} \sum_{s=1}^p \sigma_{1,s} \psi_1 \left(\frac{r_j}{\sigma_{1,s}} \right) \frac{\partial r_s}{\partial \sigma_2} \\
&= \frac{1}{2pt} \sum_{s=1}^p \sigma_{1,s} r_s w_s^c \frac{\partial r_s}{\partial \sigma_2}.
\end{aligned}$$

Then

$$\begin{aligned}
\frac{\partial w_j}{\partial \sigma_2} &= \frac{\partial w_j^c}{\partial \sigma_2} w_r + w_j^c \frac{\partial w_r}{\partial \sigma_2} \\
&= w_r w_j^c \frac{\partial r_j}{\partial \sigma_2} + w_j^c \sigma_2 w'^r \left(\frac{1}{2pt} \sum_{s=1}^p \sigma_{1,s} r_s w_s^c \frac{\partial r_s}{\partial \sigma_2} \frac{1}{\sigma_2} - \frac{t}{\sigma_2^2} \right).
\end{aligned}$$

Here $\frac{\partial \mathbf{u}_x}{\partial \sigma_{1,j}}$ and $\frac{\partial \mathbf{u}_x}{\partial \sigma_2}$ do not have not a closed form either, so they must be computed numerically as well.

G Additional simulation results

Figure 13 shows the median angle and MSE for the A09 covariance model in the presence of either cellwise outliers, rowwise outliers, or both, without NA's, this time for $p = 20$. Figure 14 shows the corresponding results when 20% of randomly selected cells were made NA. All of these curves look a lot like those for $p = 200$ in Section 6 of the paper.

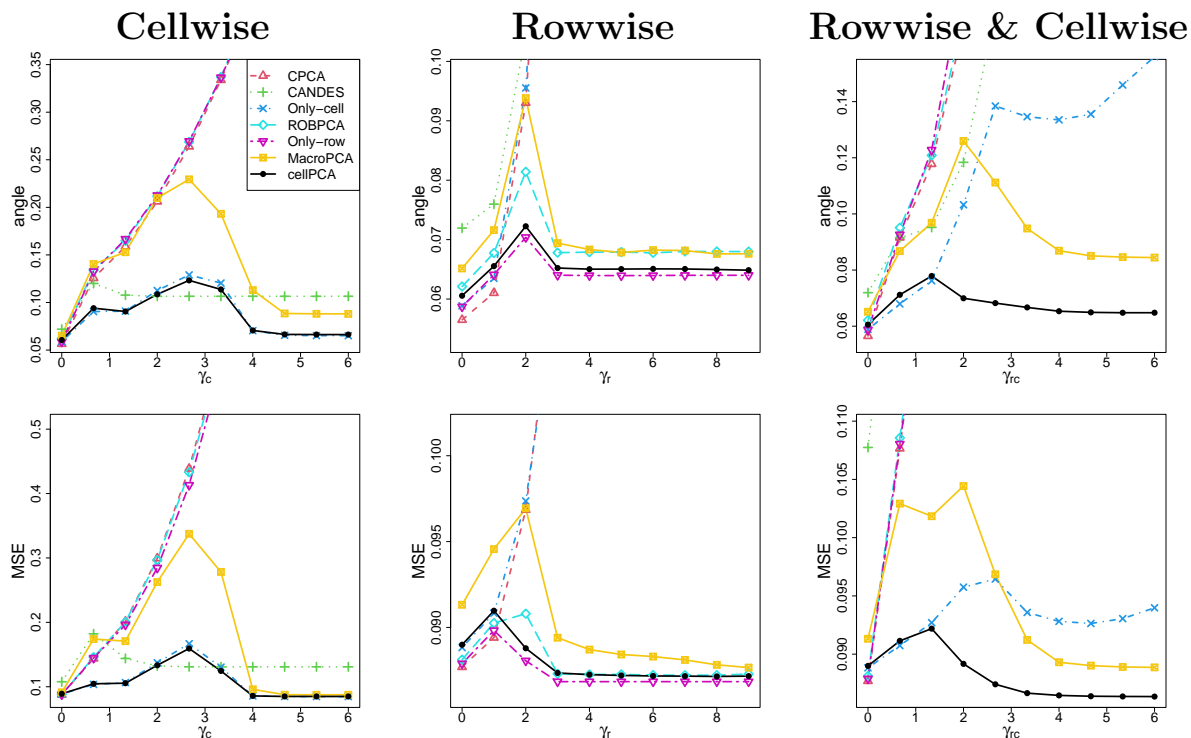


Figure 13: Median angle (top) and MSE (bottom) attained by CPCA, CANDES, Only-cell, ROBPCA, Only-row, MacroPCA, and cellPCA in the presence of either cellwise outliers, rowwise outliers, or both. The covariance model was A09 with $n = 100$ and $p = 20$, without NA's.

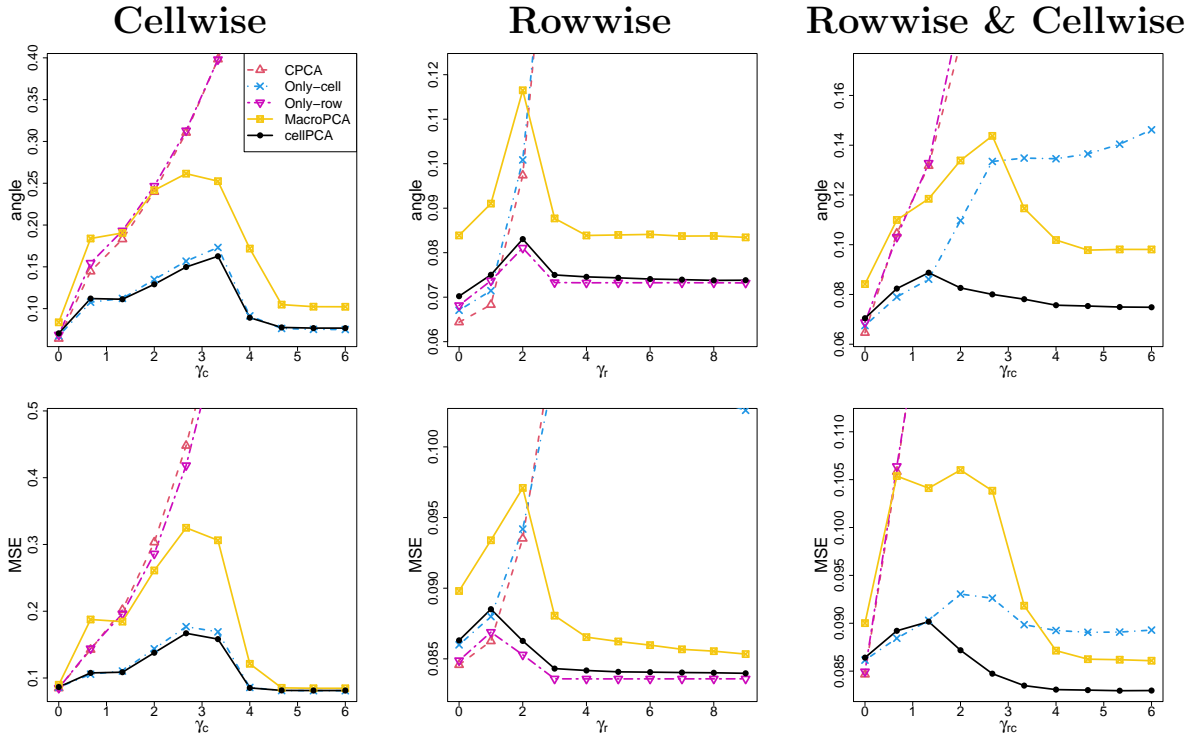


Figure 14: Median angle (top) and MSE (bottom) attained by CPCA, Only-cell, Only-row, MacroPCA, and cellPCA in the presence of either cellwise outliers, rowwise outliers, or both. The covariance model was A09 with $n = 100$ and $p = 20$, and 20% of randomly selected cells were set to NA.

The second type of covariance matrix is based on the random correlation matrices of Agostinelli et al. (2015) and will be called ALYZ. These correlation matrices are turned into covariance matrices with other eigenvalues. More specifically, the matrix \mathbf{L} in the spectral decomposition \mathbf{OLO}^T of the correlation matrix is replaced by $\text{diag}(9.57, 6.70, 0.11, 0.10, \dots, 0.10)$ for $p = 20$ and by $\text{diag}(104.88, 73.42, 0.11, 0.10, \dots, 0.10)$ for $p = 200$. These are the same eigenvalues as in A09, but now the directions of the eigenvectors vary a lot. Therefore two components explain 90% of the variance, and we set $q = 2$ in the simulation.

Again three contamination types are considered. In the cellwise outlier scenario we randomly select 20% of the cells x_{ij} and add $\gamma_c \sigma_j$ to them, where γ_c varies from 0 to 6 and σ_j^2 is the j th diagonal element of $\mathbf{\Sigma}$. Note that the diagonal entries of this $\mathbf{\Sigma}$ are no longer 1 as in A09. In the rowwise outlier setting 20% of the rows are generated from $N(\gamma_r(\mathbf{e}_1 + \mathbf{e}_{q+1}), \mathbf{\Sigma}/1.5)$, where \mathbf{e}_1 and \mathbf{e}_{q+1} are the first and $(q + 1)$ -th eigenvectors of $\mathbf{\Sigma}$, and γ_r varies from 0 to 9 when $p = 20$, and from 0 to 24 when $p = 200$. In the third scenario, the data is contaminated by 10% of cellwise outliers as well as 10% of rowwise outliers. Here $\gamma_r = 1.5\gamma_c$ when $p = 20$ and $\gamma_r = 4\gamma_c$ when $p = 200$, where γ_c again varies from 0 to 6. The data are clean when $\gamma_c = \gamma_r = 0$.

Repeating the entire simulation with the ALYZ covariance model instead of A09 yields Figure 15 for $p = 20$ without NA's, Figure 16 for $p = 200$ without NA's, Figure 17 for $p = 20$ with NA's, and Figure 18 for $p = 200$ with NA's. These figures are qualitatively similar to those for A09, and yield the same conclusions.

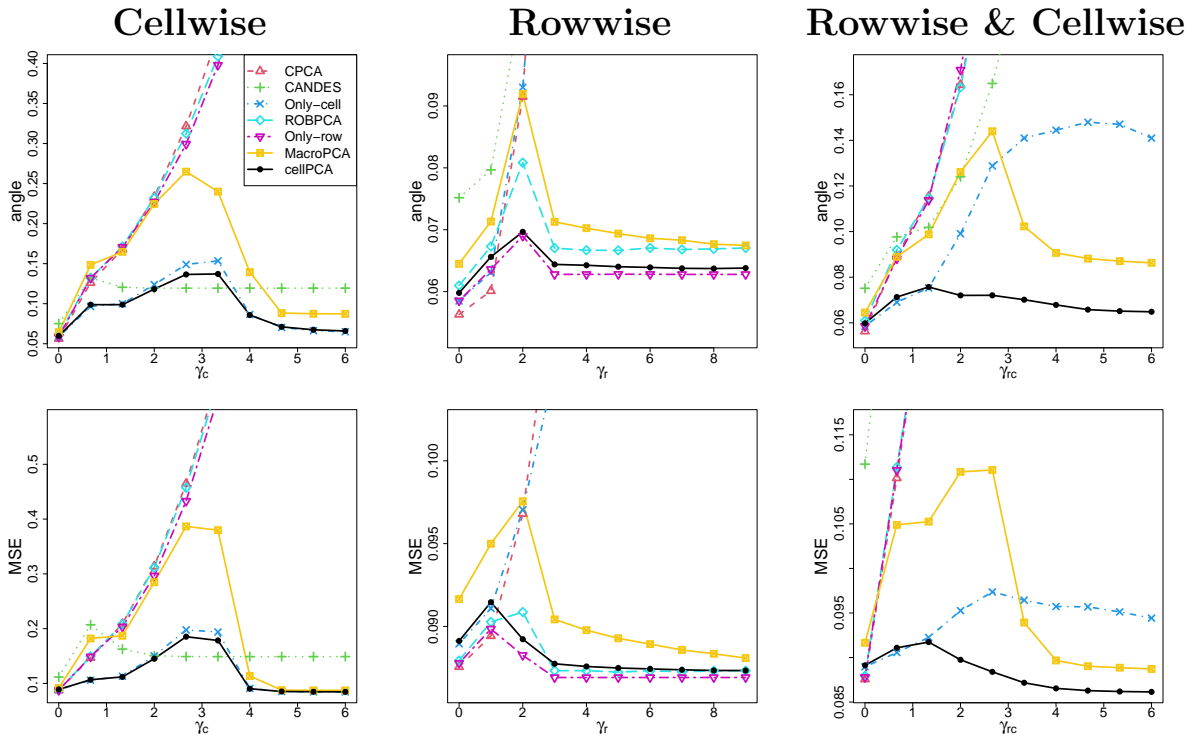


Figure 15: Median angle (top) and MSE (bottom) attained by CPCA, CANDES, Only-cell, ROBPCA, Only-row, MacroPCA, and cellPCA in the presence of either cellwise outliers, rowwise outliers, or both. The covariance model was ALYZ with $n = 100$ and $p = 20$, without NA's.

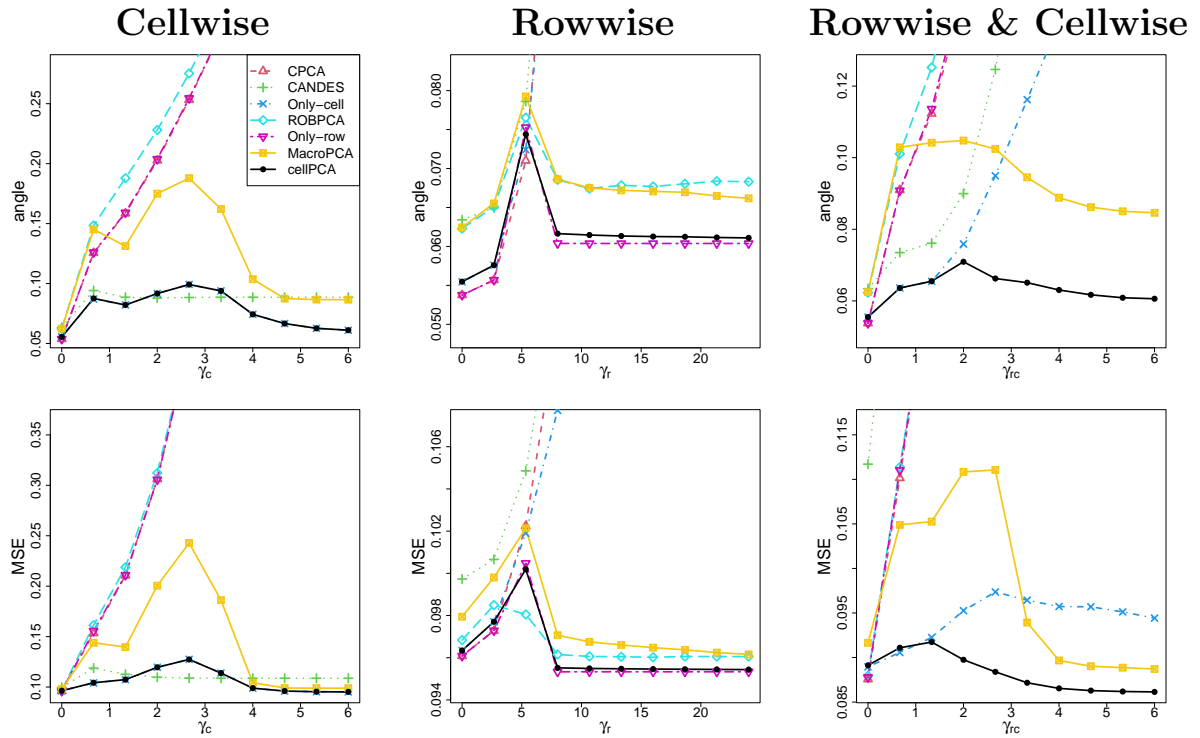


Figure 16: Median angle (top) and MSE (bottom) attained by CPCA, CANDES, Only-cell, ROBPCA, Only-row, MacroPCA, and cellPCA in the presence of either cellwise outliers, rowwise outliers, or both. The covariance model was ALYZ with $n = 100$ and $p = 200$, without NA's.

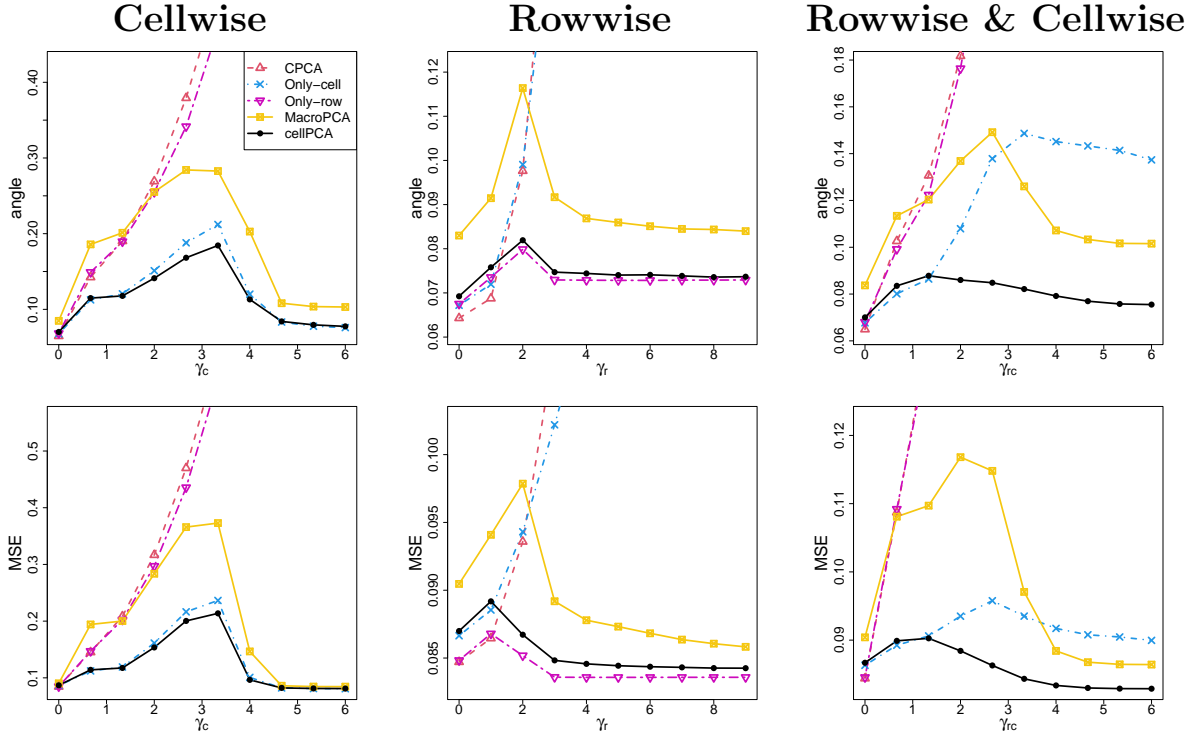


Figure 17: Median angle (top) and MSE (bottom) attained by CPCA, Only-cell, Only-row, MacroPCA, and cellPCA in the presence of either cellwise outliers, rowwise outliers, or both. The covariance model was ALYZ with $n = 100$ and $p = 20$, and 20% of randomly selected cells were set to NA.

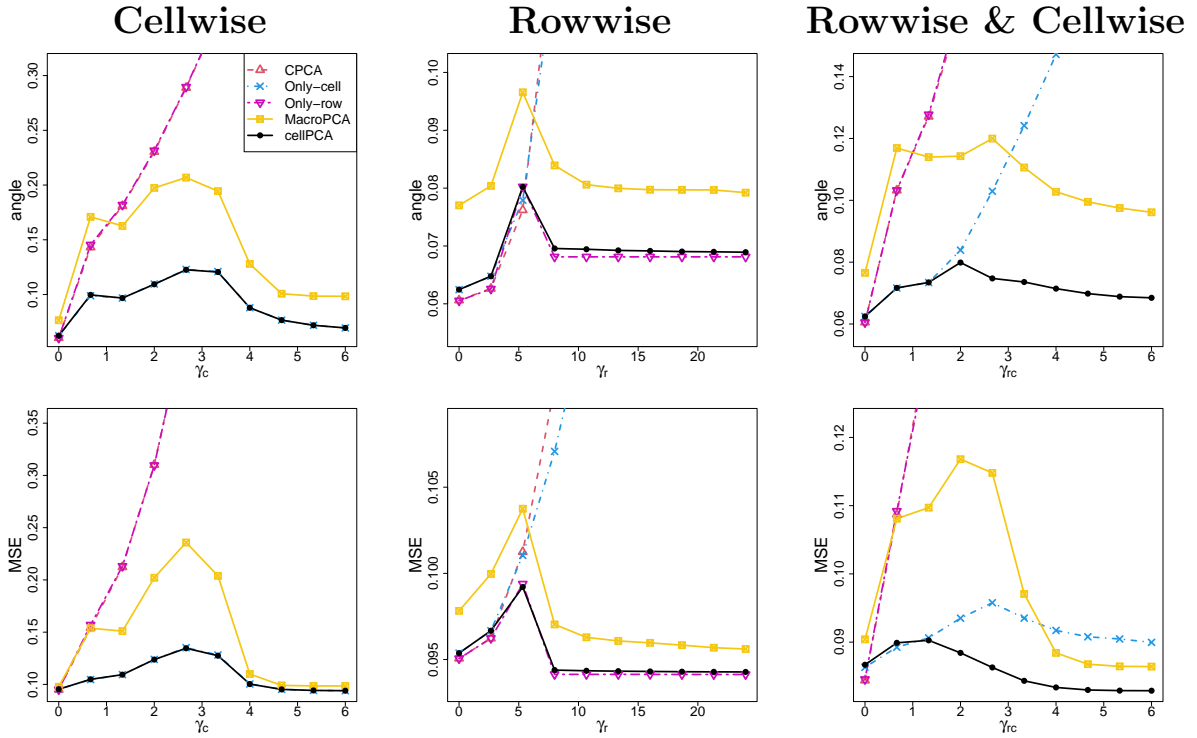


Figure 18: Median angle (top) and MSE (bottom) attained by CPCA, Only-cell, Only-row, MacroPCA, and cellPCA in the presence of either cellwise outliers, rowwise outliers, or both. The covariance model was ALYZ with $n = 100$ and $p = 200$, and 20% of randomly selected cells were set to NA.

H Additional Results for the Ionosphere Data

For cases 119 and 156 of the ionosphere data, Figure 19 illustrates that each cell of the imputed x_i^{imp} can be seen as a weighted average of the observed x_{ij} and the fitted \hat{x}_{ij} . Only a subset of the variables are shown. The plot also displays the cellwise weights w_{ij}^c . The smaller the weight, the more the imputed value becomes close to the fitted value. For $w_{ij}^c = 1$ the imputed cell is the observed value, and for $w_{ij}^c = 0$ the imputed cell becomes the fitted value.

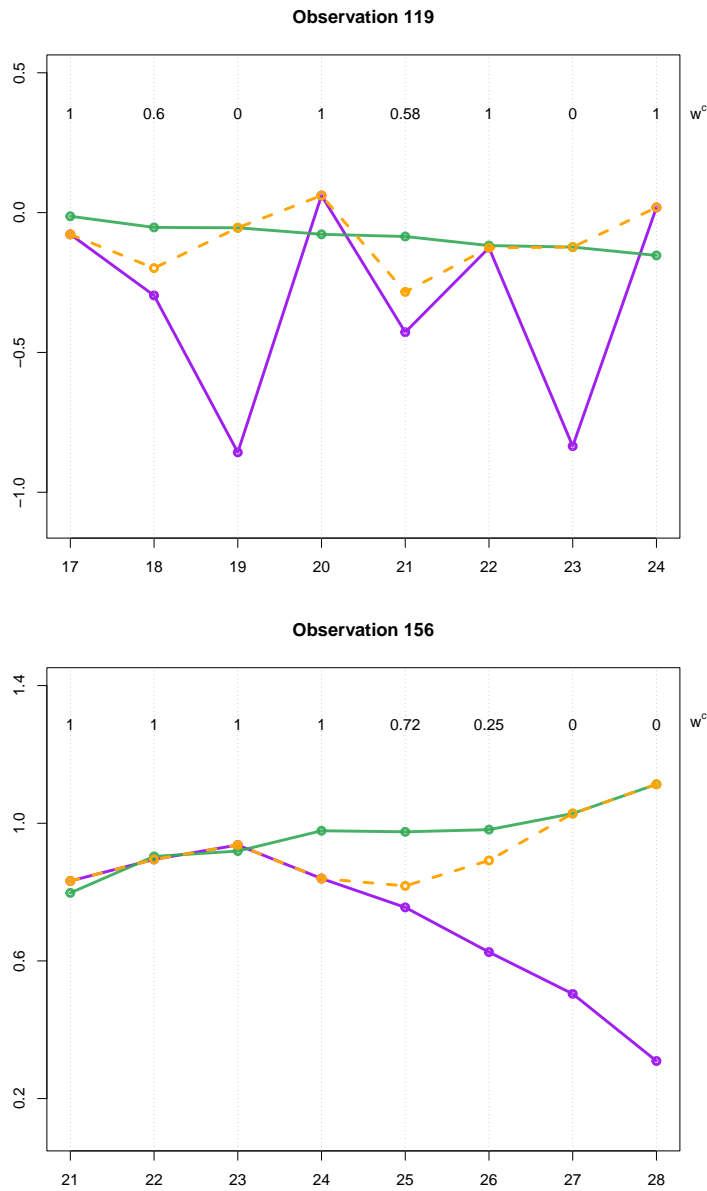


Figure 19: Observed (purple), fitted (green) and imputed (orange dashed) curves of cases 119 and 156 of the Ionosphere dataset. Above each cell we see its cellwise weight.

I More on the Solfatara Data

Figure 20 shows frame 203 of the Solfatara data, taken in the Fall. The interpretation is similar to that in Section 7.2 for frame 14 taken in the Spring, only the shape of the condensation cloud is a bit different.

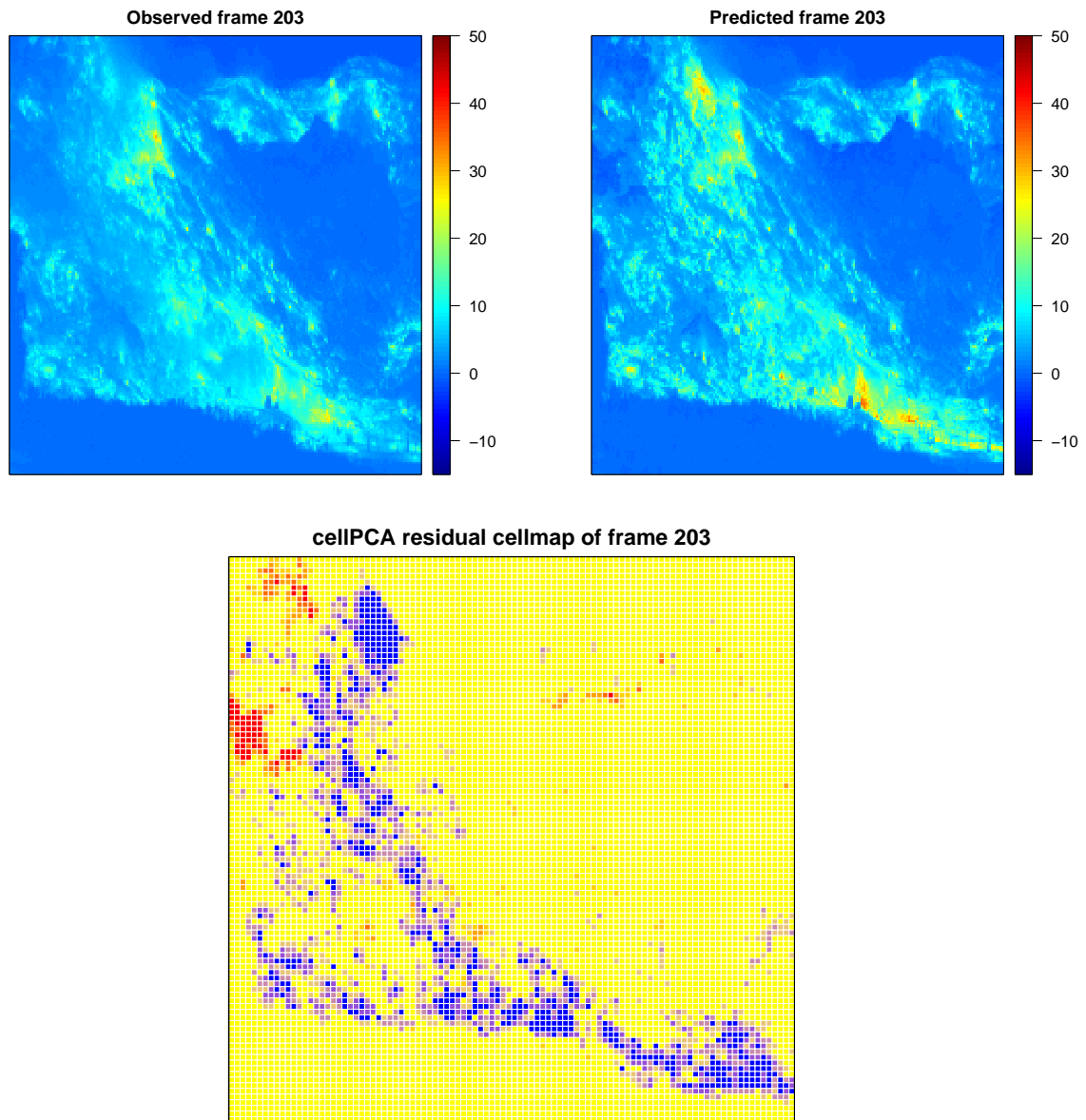


Figure 20: Solfatara data: observed frame 203, its prediction, and its residual cellmap.

Additional References

Casella, G. and R. L. Berger (2002). *Statistical Inference*, Volume 2. Duxbury Pacific Grove, CA.

Magnus, J. R. and H. Neudecker (2019). *Matrix Differential Calculus with Applications in Statistics and Econometrics, Third Edition*. Wiley.

Rio Branco de Oliveira, O. (2012). The implicit and the inverse function theorems: easy proofs, arXiv preprint 1212.2066.